TECHNICAL REPORT

Extent and Persistence of Secondary Water Quality Impacts after Enhanced Reductive Bioremediation

SERDP Project ER-2131

SEPTEMBER 2015

Robert C. Borden
Jason M. Tillotson
North Carolina State University

Gene-Hua Crystal Ng
Barbara A. Bekins
Douglas B. Kent
Gary P. Curtis
U.S. Geological Survey

SERDP
DOD ▪ EPA ▪ DOE

REPORT DOCUMENTATION PAGE

Form Approved
OMB No. 0704-0188

1. REPORT DATE *(DD-MM-YYYY)*: 15-08-2015

2. REPORT TYPE: Technical Report

3. DATES COVERED *(From - To)*: March 2011 – March 2015

4. TITLE AND SUBTITLE

Extent and Persistence of Secondary Water Quality Impacts after Enhanced Reductive Bioremediation

5a. CONTRACT NUMBER: W912HW-11-C-0058

5b. GRANT NUMBER: ER-2131

5c. PROGRAM ELEMENT NUMBER

6. AUTHOR(S)

Borden, Robert C.
Tillotson, Jason M.
Ng, Gene-Hua Crystal
Bekins, Barbara A.
Kent, Douglas B.
Curtis, Gary P.

5d. PROJECT NUMBER

5e. TASK NUMBER

5f. WORK UNIT NUMBER

7. PERFORMING ORGANIZATION NAME(S) AND ADDRESS(ES)

North Carolina State Univ.
2711 Founders Dr.
Raleigh, NC 27695

U. S. Geological Survey
345 Middlefield Rd
Menlo Park, CA 94025

8. PERFORMING ORGANIZATION REPORT NUMBER

9. SPONSORING / MONITORING AGENCY NAME(S) AND ADDRESS(ES)

Strategic Environmental Research and Development Program
4800 Mark Center Drive, Suite 17D08, Alexandria, VA 22350

10. SPONSOR/MONITOR'S ACRONYM(S): SERDP

11. SPONSOR/MONITOR'S REPORT NUMBER(S)

12. DISTRIBUTION / AVAILABILITY STATEMENT

Unlimited Distribution

13. SUPPLEMENTARY NOTES

14. ABSTRACT

Electron donor (ED) addition can be very effective in stimulating enhanced reductive bioremediation (ERB) of a wide variety of groundwater contaminants. However, ERB can result Secondary Water Quality Impacts (SWQI) including decreased levels of dissolved oxygen (O_2), nitrate (NO_3^-), and sulfate (SO_4^{2-}), and elevated levels of dissolved manganese (Mn^{2+}), dissolved iron (Fe^{2+}), methane (CH_4), organic carbon, and naturally occurring hazardous compounds (e.g., As). This report summarizes available information on processes controlling the production and natural attenuation of SWQI parameters and can be used as a guide in understanding the magnitude, areal extent and duration of SWQI in ERB treatment zones and the natural attenuation of SWQI parameters as the dissolved solutes migrate downgradient with ambient groundwater flow. This information was compiled from a wide variety of sources including a survey and statistical analysis of SWQI from 47 ERB sites, geochemical model simulations, field studies at sites where organic-rich materials have entered the subsurface (e.g., wastewater, landfill leachate and hydrocarbon plumes), and basic information on physical, chemical and biological processes in the subsurface. This information is then integrated to provide a general conceptual model of the major processes controlling the production and attenuation of SWQI production and attenuation.

15. SUBJECT TERMS

secondary water quality impacts; anaerobic bioremediation; enhanced reductive dechlorination; methane; iron; manganese; arsenic

16. SECURITY CLASSIFICATION OF:			**17. LIMITATION OF ABSTRACT**	**18. NUMBER OF PAGES**	**19a. NAME OF RESPONSIBLE PERSON**
a. REPORT	**b. ABSTRACT**	**c. THIS PAGE**			Robert C. Borden
unclassified	unclassified	unclassified	UU		**19b. TELEPHONE NUMBER** *(include area code)*: 919-873-1060

Standard Form 298 (Rev. 8-98)
Prescribed by ANSI Std. Z39.18

This Page Intentionally Left Blank

TABLE OF CONTENTS

LIST OF FIGURES

Page

LIST OF FIGURES (Continued)

Page

LIST OF TABLES

Page

ACRONYMS AND ABBREVIATIONS

°C	degrees Celsius
µg/L	micrograms per liter
g	grams
g/kg	gram per kilogram
kg	kilogram
M	moles per liter
m	meter
m/day	meter per day
mg	milligram
mg/L	milligrams per liter
ml	milliliter(s)
mV	millivolts
mmol	millimoles
mM	milliMolar = mmol/L
AB	Anaerobic bioremediation
AFCEE	Air Force Center for Environmental Excellence
AFCEC	Air Force Civil Engineering Center
AOM	Anaerobic Oxidation of Methane
bgs	below ground surface
CE	Chlorinated ethene
CEC	Cation Exchange Capacity
CoC	Contaminants of Concern
DAFB	Dover Air Force Base
DFE	Denatured Fuel Ethanol
DNAPL	Dense Non-aqueous Phase Liquid
DO	Dissolved Oxygen
DOC	Dissolved Organic Carbon
DNRA	Dissimilatory Nitrate Reduction to Ammonium
e^-	electron
ED	Electron Donor
Eh	Measure of oxidation-reduction potential
ERD	Enhanced Reductive Dechlorination
ERB	Enhanced Reductive Bioremediation
ESTCP	Environmental Security Technology Certification Program
EVO	Emulsified Vegetable Oil
HRC™	Hydrogen Release Compound

IRB	Iron-Reducing Bacteria
ISB	*In Situ* Bioremediation
ISCR	*In Situ* Chemical Reduction
LCFA	Long-chain Fatty Acid
LEL	Lower Explosive Limit
MCL	Maximum Contamination Level
MNA	Monitored Natural Attenuation
MS	Magnetic Susceptibility
NAPL	Non-Aqueous Phase Liquid
NCSU	North Carolina State University
ND	Non-detect
NFESC	Naval Facilities Engineering Service Center
ORP	Oxidation-Reduction Potential
PE	Partial Equilibrium
pK(a)	Acid Disassociation Constant (also, pK)
pK_{SP}	Solubility Product Constant
PLA	Polylactide
PRB	Permeable Reactive Barrier
SERDP	Strategic Environmental Research and Development Program
SWQI	Secondary Water Quality Impact
SU	Standard Units (for pH)
TEA(s)	Terminal Electron Acceptor(s)
TOC	Total Organic Carbon
USAF	U.S Air Force
USEPA	U.S. Environmental Protection Agency
USGS	U.S. Geological Survey
VFA(s)	Volatile Fatty Acid(s)
VOC(s)	Volatile Organic Compound(s)
XRD	X-ray Diffraction
ZVI	Zero Valent Iron

ABBREVIATIONS FOR COMPOUNDS AND ELEMENTS

Al	Aluminum
As	Arsenic
As(III)	Arsenite
AS(V)	Arsenate
ATP	Adenosine Triphosphate
Ca	Calcium
CH_4	Methane
Cl^-	Chloride Ion
CO_2	Carbon Dioxide
Cr(VI)	Hexavalent Chromium
cis-DCE	*cis*-1,2-Dichloroethene
Fe	Iron
Fe(II)	Ferrous Iron
Fe(III)	Ferric Iron
α-Fe_2O_3	Hematite
$Fe_{(1-x)}S$	Pyrrhotite
Fe_3O_4	Magnetite
$FeCO_3$	Siderite
FeS	Mackinawite
FeS_2	Pyrite / Marcasite
FeOOH	Goethite
H_2	Hydrogen
H_2O	Water
H_2S	Hydrogen Sulfide
HCO_3^-	Bicarbonate Ion
HAHCl	Hydroxylamine Hydrochloride in HCl
HCl	Hydrochloric Acid
HCO_3^-	Bicarbonate
HMX	High Melting Explosive; octahydro-1,3,5,7-tetranitro-1,3,5,7 tetrazocine
K	Potassium
KOH	Potassium Hydroxide
Mg	Magnesium
Mn	Manganese

Na	Sodium
NaOH	Sodium Hydroxide
N_2	Nitrogen
NH_3	Ammonia
NO_2^-	Nitrite ion
NO_3^-	Nitrate ion
O_2	Oxygen
PCE	Tetrachloroethene
RDX	Research Department Explosive; Hexahydro-1,3,5-trinitro-1,3,5 triazine
S^{2-}	Sulfide
$S_2O_3^{2-}$	Thiosulfate
S_8	Elemental Sulfur
S_n^{2-}	Polysulfides
SO_3^{2-}	Sulfites
SO_4^{2-}	Sulfate
TCE	Trichloroethene
TNT	Trinitrotoluene
U(VI)	Uranium
VC	Vinyl Chloride

ACKNOWLEDGEMENTS

The research described in this report was conducted by a team comprised of Jason Tillotson and Robert C. Borden at North Carolina State University and Gene-Hua Crystal Ng, Barbara A. Bekins, Douglas B. Kent, and Gary P. Curtis at the U.S. Geological Survey (USGS). Isabelle Cozzarelli (USGS), Mary Jo Baedecker (USGS), Philip Bennett (University of Texas), and Richard Amos (University of Waterloo) are gratefully acknowledged for their contribution of data on the Bemidji oil spill site. Denis LeBlanc and Richard Smith are gratefully acknowledged for their contribution of data and process-insight from the Cape Cod wastewater disposal site. The research described in this final project report was supported by the U.S. Department of Defense, through the Strategic Environmental Research and Development Program (SERDP). Dr. Andrea Leeson and other SERDP staff are gratefully acknowledged for their assistance and support.

The authors wish to thank the following site managers for providing groundwater data for the Secondary Water Quality Impact (SWQI) database: Dave Adamson (GSI); Hunter Anderson (Air Force Civil Engineering Center [AFCEC]); Paul Hatzinger (CB&I); Bruce Henry (Army Corps of Engineers); Dan Leigh (FMC, formerly of CB&I); Chris Lutes (ARCADIS); Travis McGuire (GSI); Gene Ng (CH2M Hill); Matt Schnobrich (ARCADIS); and Laurie Stenberg (URS Corporation). In addition, the work of Leonor Sanchez in entering data into the database is gratefully acknowledged.

Jo Anne Deramo (United States Air Force [USAF]), Angie Frizzell (ARCADIS), Valerie Harris (NAVFAC), Neil Hey (CB&I), Brian Riha (Savannah River National Laboratory), and Rich Zambito (ATK) are thanked for their help in providing site access to collect additional soil and groundwater samples. The laboratory contributions of Della Shaw and David Black at North Carolina State University's Environmental Engineering Laboratory are also gratefully acknowledged.

ABSTRACT

Electron donor (ED) addition can be very effective in stimulating enhanced reductive bioremediation (ERB) of a wide variety of groundwater contaminants. However, ERB can result in Secondary Water Quality Impacts (SWQIs) including decreased levels of dissolved oxygen (O_2), nitrate (NO_3^-), and sulfate (SO_4^{2-}), and elevated levels of dissolved manganese (Mn^{2+}), dissolved iron (Fe^{2+}), methane (CH_4), sulfide (S^{2-}), organic carbon, and naturally occurring hazardous compounds (e.g., arsenic). Fortunately, this 'plume' of impacted groundwater is usually confined within the original contaminant plume and is unlikely to adversely impact potable water supplies. This report summarizes available information on processes controlling the production and natural attenuation of SWQI parameters and can be used as a guide in understanding the magnitude, areal extent, and duration of SWQIs in ERB treatment zones and the natural attenuation of SWQI parameters as the dissolved solutes migrate downgradient with ambient groundwater flow. This information was compiled from a wide variety of sources including a survey and statistical analysis of SWQIs from 47 ERB sites, geochemical model simulations, field studies at sites where organic-rich materials have entered the subsurface (e.g., wastewater, landfill leachate, and hydrocarbon plumes), and basic information on physical, chemical, and biological processes in the subsurface. This information is then integrated to provide a general conceptual model of the major processes controlling SWQI production and attenuation.

EXECUTIVE SUMMARY & CONCEPTUAL MODEL OF SWQI PRODUCTION AND ATTENUATION

Electron donor (ED) addition can be very effective in stimulating enhanced reductive bioremediation (ERB) of a wide variety of groundwater contaminants. However, ERB can result in Secondary Water Quality Impacts (SWQIs) including decreased levels of dissolved oxygen (O_2), nitrate (NO_3^-), and sulfate (SO_4^{2-}), and elevated levels of dissolved manganese (Mn^{2+}), dissolved iron (Fe^{2+}), methane (CH_4), sulfide (S^{2-}), organic carbon, and naturally occurring hazardous compounds (e.g., arsenic [As]). Fortunately, this 'plume' of impacted groundwater is usually confined within the original contaminant plume and is unlikely to adversely impact potable water supplies.

This report summarizes available information on processes controlling the production and natural attenuation of SWQI parameters compiled as part of project ER-2131 "Numerical Modeling of Post-Remediation Impacts of Anaerobic Bioremediation on Groundwater Quality" supported by the Strategic Environmental Research and Development Program (SERDP). The information presented in this report can be used as a guide in understanding the magnitude, areal extent, and duration of SWQIs in ERB treatment zones and the natural attenuation of SWQI parameters as the dissolved solutes migrate downgradient with ambient groundwater flow.

Information presented in this report were compiled from a wide variety of sources including a survey and statistical analysis of SWQI from 47 ERB sites (Tillotson and Borden, 2015), geochemical model simulations (Ng et al. 2014), field studies at sites where organic-rich materials have entered the subsurface (e.g., wastewater, landfill leachate, and hydrocarbon plumes), and basic information on physical, chemical, and biological processes in the subsurface. This information is then integrated to provide a general conceptual model of the major processes controlling SWQI production and attenuation.

Conceptual Model of SWQI Production and Attenuation

During ERB, large amounts of easily fermented organic substrates are added to the target treatment area to degrade or immobilize the contaminants of concern (CoC). These substrates are fermented to hydrogen (H_2), acetate, and other volatile fatty acids that are then used as electron donors by microbes to mediate oxidation-reduction (redox) reactions that reduce dissolved oxygen, nitrate, and sulfate as well as Ferric Iron (Fe[III]) and Mn(III/IV) containing minerals and the CoC. **Figure ES.1** shows a typical pattern of SWQI parameters with time in the: 1) injection area; 2) near plume (25 m downgradient); 3) medium-distance plume (50 m downgradient); and 4) far plume (100 m downgradient). Readers should note that the trends shown in **Figure ES.1** may not occur at all sites and broad ranges of Secondary Water Quality Impact (SWQI) parameter concentrations have been observed. The time period for production and attenuation of SWQIs can vary from 10 to over 100 years, depending on the amount and duration of substrate addition, groundwater transport velocity, and concentrations of background electron acceptors.

Organic substrate addition results in a rapid increase in total organic carbon (TOC) in injection area monitoring wells with maximum TOC concentrations typically ranging from 50 to 500 mg/L.

However, much higher TOC concentrations were observed at some sites. TOC concentrations often remain high for several years in the injection area due to the use of slow release electron donors (e.g., emulsified vegetable oil or Emulsified Vegetable Oil [EVO]) and/or repeated substrate injections, and then decline once substrate addition ends. However, low levels of TOC may continue to be released from endogenous decay of accumulated biomass. Increases in carbon loading are expected to result in greater SWQI formation. However, these SWQIs will attenuate with time and distance downgradient. Reducing the carbon loading to reduce SWQIs production may reduce treatment efficiency, possibly resulting in greater exposure to chlorinated solvents and other contaminants.

Maximum TOC concentrations in downgradient wells are generally much lower than in the injection area, indicating TOC in the aqueous phase is rapidly consumed and does not migrate long distances downgradient. The rapid consumption of TOC in the injection area is due to reactions with background electron acceptors (e.g. O_2, NO_3^-, Mn[IV], Fe[III], SO_4^{2-}), the target contaminants, and fermentation to CH_4. Since TOC is largely restricted to the injection area, these redox reactions are also largely restricted to the same area. Thermodynamic calculations indicate that reduction reactions should proceed in the order of O_2, NO_3^-, Mn(IV), Fe(III), SO_4^{2-}, and carbon dioxide (CO_2). However, these processes often overlap (e.g., methane production occurring before complete sulfate reduction) due to spatial variability, energy limitations from low reactant concentrations, slow reaction kinetics, and addition of excess electron donor.

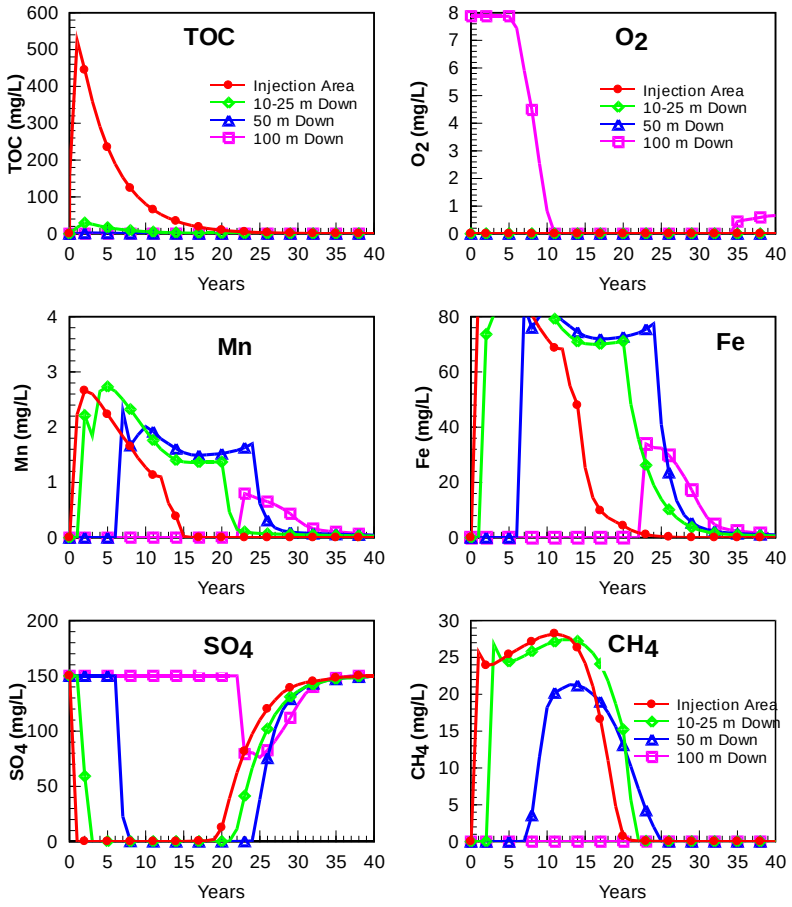

Figure ES.1. Typical Variation in SWQI Parameters over Time with Distance from Injection.
Graphs compare concentrations in injection area, 25 m, 50 m and 100 m downgradient for 40 years post-injection.

In the injection area, O_2 and NO_3^- decline rapidly following substrate addition and often remain low for years after TOC declines due to reduction of O_2 and NO_3^- by sediment organic carbon and/or reduced minerals. Concentrations of O_2 and NO_3^- in downgradient wells decline with the arrival of anaerobic, oxygen- and nitrate-depleted water. In most cases, there is little or no increase in O_2 or NO_3^- with distance downgradient due to the very limited mixing between the anaerobic plume and background aerobic groundwater.

SO_4^{2-} concentrations follow the same general pattern as O_2 and NO_3^-, with an initial decline in the injection area following substrate addition. However, biodegradation coupled to sulfate reduction is less energetically favorable than biodegradation coupled to O_2, NO_3^-, Mn(IV), and Fe(III) reduction. As a result, SO_4^{2-} is depleted more slowly than these other terminal electron acceptors (TEAs) and substantial amounts of SO_4^{2-} may persist in the injection area if background SO_4^{2-} levels are high. In downgradient wells, SO_4^{2-} concentrations decline with the arrival of anaerobic, low SO_4^{2-} groundwater. In most cases, there is little increase in SO_4^{2-} with distance downgradient due to the very limited mixing between the anaerobic low SO_4^{2-} plume and background higher SO_4^{2-} groundwater. The amount of dissolved S^{2-} produced from SO_4^{2-} reduction depends on the SO_4^{2-} concentration, extent of SO_4^{2-} reduction, as well as the amount of Fe^{2+} and Mn^{2+} in groundwater. If S^{2-} is in excess (Saturation Index of FeS>1), then S^{2-} will persist and limit the extent of Fe^{2+} released to solution. In practice, at most sites, sufficient sediment-bound Mn and Fe are present to react with S^{2-} and precipitate as sulfide minerals. As a result, aqueous sulfide concentrations are low in the injection area and downgradient aquifer. In uncommon cases where SO_4^{2-} concentrations are high and solid phase Fe is low, some dissolved sulfide may migrate a short distance downgradient before reacting or precipitating. Once injection area TOC declines, SO_4^{2-} is expected to recover somewhat more rapidly than O_2 or NO_3^-.

Excess TOC in the injection area will stimulate reduction of solid phase Mn(IV) and Fe(III), causing a gradual increase in Mn^{2+} and Fe^{2+} in injection area wells. Much of the reduced Mn(II) and Ferrous Iron (Fe[II]) produced in these reactions will be retained on the aquifer material within the injection area. However, a portion of the reduced Mn and Fe will be in the aqueous phase and will migrate downgradient with natural groundwater flow. Sorption reactions will diminish the rate of transport of Fe and Mn compared to the groundwater flow rate as well as the maximum concentrations observed in downgradient wells. However, significant increases in Mn and Fe have been observed in monitoring wells at significant distances downgradient. In some aquifers, Mn and Fe concentrations have been observed to decline before TOC is depleted, presumably due to depletion of bioavailable Mn(IV) and Fe(III) in the injection-area aquifer material. Once TOC levels decline in the injection area, production of additional Mn(II) and Fe(II) will slow, and dissolved Mn and Fe concentrations in monitoring wells should start to decline.

In some aquifers, arsenic (As) is naturally present as As(V) sorbed or coprecipitated with Fe(III) or other minerals. The general term sorption is used to encompass all binding mechanisms of As to Fe(III) phases. If arsenic is present in these forms, the addition of TOC to remediate contaminants could release dissolved arsenic to groundwater by both reduction of Fe(III) to Fe(II) and reduction of As(V) to As(III). As Fe-rich groundwater migrates downgradient, Fe(II) sorbs to the sediment or precipitates as Fe-bearing minerals (FeS, carbonates, magnetite) and aqueous Fe concentrations decline. The available monitoring data suggest that arsenic follows a similar pattern and aqueous arsenic concentrations decline as the anaerobic plume migrates downgradient

and encounters Fe(III)-rich sediments. Once TOC concentrations in the injection area decline, Fe(III) and As(V) reduction is expected to decline with a concurrent decline in arsenic release. At sites where concentrations of sediment-bound As(V) are low, minimal arsenic will be released.

TOC fermentation products (H_2 and acetate) in the injection area that are not consumed in microbially mediated reactions with contaminants or background electron acceptors will be fermented to CH_4, which can result in high CH_4 concentrations in the injection area and downgradient aquifer. If the sum of gas partial pressures (mainly $N_2 + CO_2 + CH_4$) exceeds the hydrostatic pressure, these gases will come out of solution and form bubbles. This occurs primarily near the water table due to the lower hydrostatic pressure there compared to deeper in the aquifer. At greater depths, groundwater can appear to be supersaturated with CH_4 due to the higher pressure. In relatively homogeneous, coarse grained sediments, gas bubbles can migrate upward into the vadose zone, removing CH_4 from the aquifer. However, in finer grained sediments, upward migration of gas bubbles will be more limited. If the gas bubbles are not released to the vadose zone, they may eventually dissolve, releasing CH_4 back into groundwater. Dissolved CH_4 produced in the injection area will migrate downgradient with groundwater flow. Since mixing between the anaerobic plume and aerobic background groundwater is low, aerobic methane oxidation will be limited. Recent research suggests that CH_4 plume migration may be limited by anaerobic oxidation of methane (AOM) using NO_3^{2-}, Mn(III/IV), Fe(III), or SO_4^{2-} as terminal electron acceptors. However, this reaction may be slow or may not occur at some sites. As a result, dissolved CH_4 can migrate long distances in some aquifers. Once TOC in the injection area declines, CH_4 production will stop and dissolved CH_4 should be transported downgradient by groundwater flow.

1.0 INTRODUCTION

Electron donor (ED) addition can be very effective in stimulating enhanced reductive bioremediation (ERB) of chlorinated solvents, explosives and propellants (Trinitrotoluene [TNT], research department explosive; Hexahydro-1,3,5-trinitro-1,3,5 triazine [RDX], high melting explosive; octahydro-1,3,5,7-tetranitro-1,3,5,7 tetrazocine [HMX], ClO_4^-), selected metals and radionuclides (Cr[VI], TcO_4^-, UO_2^{2+}), and other groundwater contaminants. In the published literature, this process is sometimes referred to as *in situ* bioremediation (ISB), anaerobic bioremediation (AB), or enhanced reductive dechlorination (ERD). In this report, we use the term ERB to cover the broad range of reductive processes for treating both chlorinated and non-chlorinated compounds that may permanently destroy these compounds or immobilize them on the aquifer material. Much of the data summarized in this document are from sites where ERB was used for chlorinated solvents. For more information on the reaction mechanisms and effectiveness of ERB for metals and radionuclides see Wielinga et al. (2000), Yurovsky et al. (2009), and Vanbroekhoven et al. (2009).

In the anaerobic treatment zone and downgradient aquifer, ERB can result in decreased levels of dissolved oxygen (O_2), nitrate (NO_3^-), and sulfate (SO_4^{2-}), and elevated levels of dissolved manganese (Mn^{2+}), dissolved iron (Fe^{2+}), methane (CH_4), sulfide (S^{2-}), organic carbon, and naturally occurring hazardous compounds (e.g., arsenic [As]). There is growing concern about these 'secondary impacts' of ERB. In most cases, the groundwater within or downgradient of ERB treatment zones is not acutely toxic, but may have impaired taste, odor, and aesthetic quality, possibly making it unsuitable as a potable water source. In a few cases, regulators have required documentation of the expected or potential impacts prior to issuing required permits. While secondary impacts are monitored at many ERB sites, little of this data has been compiled in a usable form that can be shared with regulators. Fortunately, there is a wealth of information on the natural attenuation of these same parameters at sites where organic-rich materials have entered the subsurface (e.g., wastewater, landfill leachate, and hydrocarbon plumes).

For the purposes of this report, we define secondary water quality impacts (SWQIs) as changes in groundwater quality resulting from ERB that could potentially have adverse impacts on the beneficial use of the groundwater resource. SWQIs may be temporary or long-lived, expected or unexpected, have significant health consequences or only result in a mild change in the palatability of the water supply. As defined in this report, SWQIs do not include degradation products produced from the primary contaminant, but are limited to those constituents produced by or mobilized due to conditions caused by ERB. The following groups of parameters may be impacted by ERB (i.e., SWQIs).

- Organic substrates
- Geochemical indicators (Oxidation-Reduction Potential [ORP]/ Measure of oxidation-reduction potential [Eh] and pH)
- Oxygen and nitrate
- Sulfate and sulfide
- Iron, manganese, and arsenic
- Methane

1.1 MONITORED NATURAL ATTENUATION

The U.S. Environmental Protection Agency (USEPA) defines Monitored Natural Attenuation (MNA) as a "knowledge-based" remedy that relies upon natural processes of contaminant attenuation to achieve site-specific remediation requirements within a reasonable timeframe as compared to other more active methods (USEPA, 1999). These natural processes include a variety of physical, chemical, and biological methods, such as biodegradation, dilution, sorption, and volatilization that under favorable conditions reduce the mass, toxicity, mobility, volume, or concentration of contaminants without human intervention (USEPA, 1999).

Field data and modeling results developed as part of the project "Numerical Modeling of Post-Remediation Impacts of Anaerobic Bioremediation on Groundwater Quality (ER-2131)" supported by the Strategic Environmental Research and Development Program (SERDP), indicate that most SWQIs decline with time since substrate addition and with distance downgradient from the ERB injection area. This suggests that MNA may be an effective approach for management of SWQIs from ERB. However, the rate and extent of SWQI attenuation depends on a variety of site-specific factors.

1.2 REPORT OVERVIEW

The purpose of this report is to provide a compilation of information needed to understand the formation, mobilization, and attenuation of SWQIs at ERB sites. This report summarizes available information on typical characteristics of ERB systems (Section 2), SWQI generation and attenuation processes (Section 3), and modeling SWQI production and attenuation (Section 4). This information was obtained from prior research on fate and transport of organic and inorganic contaminants in the subsurface, results from a compilation of monitoring data from 47 ERB sites (Tillotson and Borden, 2015), and biogeochemical modeling of SWQIs conducted as part of SERDP Project ER-2131.

Readers of this document are expected to possess a general understanding of the ERB process, design, implementation, and monitoring procedures. For general background information on ERB, readers should consult the following documents.

- Principles and Practices of Enhanced Anaerobic Bioremediation of Chlorinated Solvents, (Air Force Center for Environmental Excellence [AFCEE], Naval Facilities Engineering Service Center [NFESC], and Environmental Security Technology Certification Program [ESTCP], 2004).
- Protocol for Enhanced *In Situ* Bioremediation Using Emulsified Edible Oil (ESTCP, 2006)

2.0 ENHANCED REDUCTIVE BIOREMEDIATION

2.1 INTRODUCTION

ERB technologies examined in this report typically involve the addition of fermentable organic substrate to the aquifer which will: 1) deplete O_2, NO_3^-, and reactive sediment-bound Mn(III/IV), Ferric Iron (Fe[III]), and SO_4^{2-}; and 2) stimulate the biological and/or chemical reduction of the contaminants of concern (CoCs). ERB is commonly employed to treat a broad range of contaminants including chloroethenes, chloroethanes, chloromethanes, chlorinated cyclic hydrocarbons, various energetics (e.g., perchlorate, RDX, TNT), and nitrate (AFCEE, NFESC, ESTCP, 2004). Hexavalent chromium (Cr[VI]) and uranium (U[VI]) can be reduced to less mobile and/or less toxic forms (e.g., Cr[III], U[IV]) (Wielinga et al., 2000; Yurovsky et al., 2009). Similarly, reduction of sulfate to sulfide (sulfidogenesis) can be used to precipitate certain metals (e.g., zinc, cadmium, and cobalt) (Vanbroekhoven et al., 2009).

The choice of substrate and the method of injection depend on the contaminant type and distribution in the aquifer, hydrogeology, and remediation objectives. Substrate can be added using conventional well installations, by direct-push technology, or by excavation and backfill such as permeable reactive barriers (PRB). Slow-release products composed of edible oils or solid substrates tend to stay in place for an extended treatment period. Soluble substrates or soluble fermentation products of slow-release substrates can potentially migrate via advection and diffusion, providing broader but shorter-lived treatment zones. The added organic substrates are first fermented to hydrogen (H_2) and volatile fatty acids (VFAs). The VFAs, including acetate, lactate, propionate and butyrate, provide carbon and energy for bacterial metabolism. In the design and operation of ERB treatment systems, the amount of ED added is a critical factor in the extent of SWQI.

Many *in situ* remediation technologies are implemented by injecting an organic substrate into the subsurface via injection wells (AFCEE, NFESC, and ESTCP 2004; ESTCP 2006). Common injection system designs include area treatment and barriers (**Figure 2.1**). Grids of injection wells are commonly used to treat source areas. Downgradient of the source area, injection wells may be aligned in rows, generally perpendicular to groundwater flow, to form a biologically active barrier and intercept a plume.

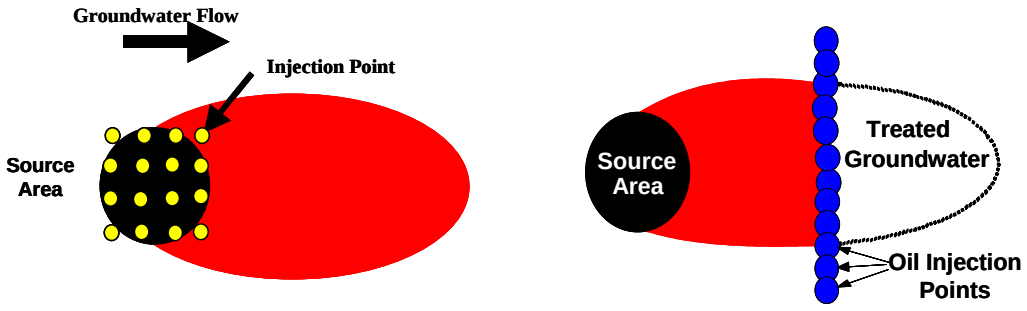

Area Injection System Design Barrier Injection System Design

Figure 2.1. Common Injection System Designs.

2.2 REMEDIATION SYSTEM CHARACTERISTICS

As part of ER-2131, a survey of ERB sites was conducted to identify typical operating characteristics and the range of SWQIs commonly observed at these projects. A total of 47 sites were surveyed (**Table A-1** in Appendix A). Results of this survey are presented in Tillotson and Borden (2015). Organic substrates included soluble substrates (14 sites), low solubility liquid substrates (21 sites), solid substrates (2 sites), and mixed or multiple substrates (10 sites). The injected substrates were introduced into the subsurface as source area point injections (32 times), PRBs (16 times), recirculation systems (7 times), biowalls (mulch or mulch and soybean oil) (4 times), or horizontal wells (1 time). The sum of these is greater than 47 because some sites used multiple injections designs.

In addition to the primary substrates, some ERB sites were amended with pH buffering reagents (e.g., bicarbonate, carbonate) (10 sites); bioaugmentation cultures (e.g., KB-1®, SDC-9) (9 sites); *in situ* chemical reduction (ISCR) reagents (e.g., ferrous sulfate) (5 sites); and nutrients to aid biological growth (e.g., diammonium phosphate, vitamin B_{12}) (5 sites). Available monitoring data ranged from 5 months to 11 years post-injection.

Figure 2.2 shows the range of remediation site characteristics including estimated groundwater velocity at the site, vertical injection interval, width of barrier or area treatment perpendicular to flow, and length of treatment zone parallel to flow. Estimated groundwater velocity varied greatly from 2 to 350 m/yr. Many of the remediation systems were relatively small and served as pilot systems to evaluate system performance before moving to full-scale remediation. The median length of the injection area parallel to flow was small since many of the remediation systems were designed to operate as PRBs to limit contaminant migration.

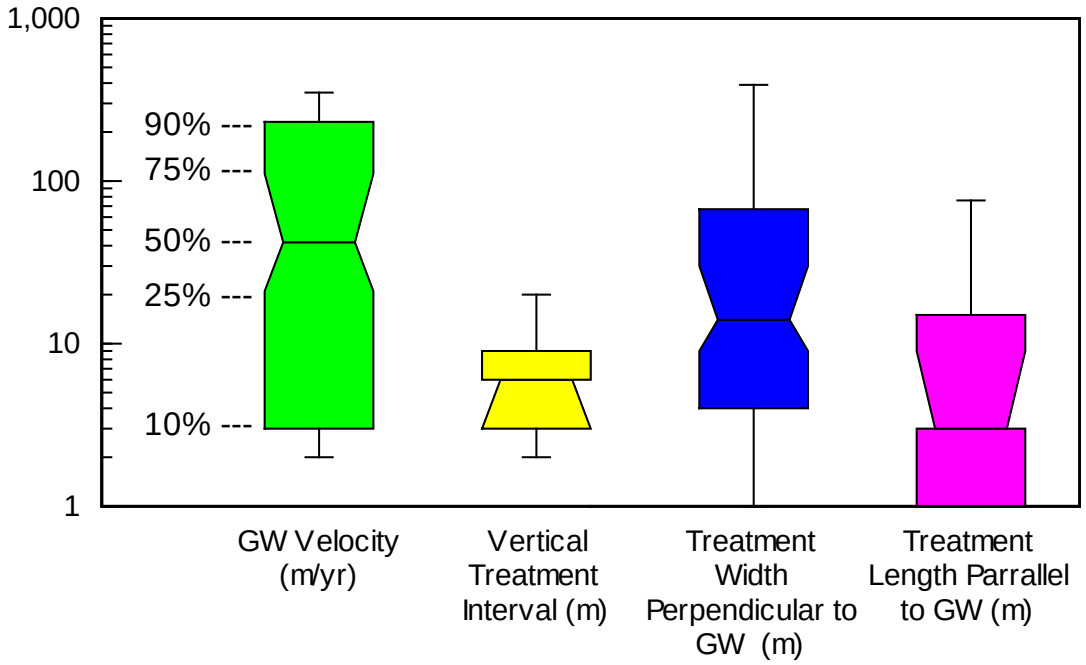

Figure 2.2. Summary of Database Treatment System Characteristics.
Data compiled show minimum, 10th, 25th, 50th, 75th, 90th percentile and maximum values.

There were large differences in the amount of carbon added to the different treatment systems, even when normalized for the barrier cross-sectional area or source area treatment volume. **Figure 2.3** shows the total carbon added to the different treatment systems and the carbon load in kg/m^2 perpendicular to flow for barriers and kg/m^3 of treatment volume for source area treatments. Carbon loadings in barriers and source area treatments injected with liquid substrates varied by over an order of magnitude. The carbon loading for the two mulch-only biowalls included in the database is similar to the median value for injected substrates. However, most of the organic carbon in mulch is not readily fermented so the amount of bioavailable, fermentable carbon in the biowalls will be lower than in injected barriers. These large differences in carbon loading may influence the severity and longevity of SWQIs.

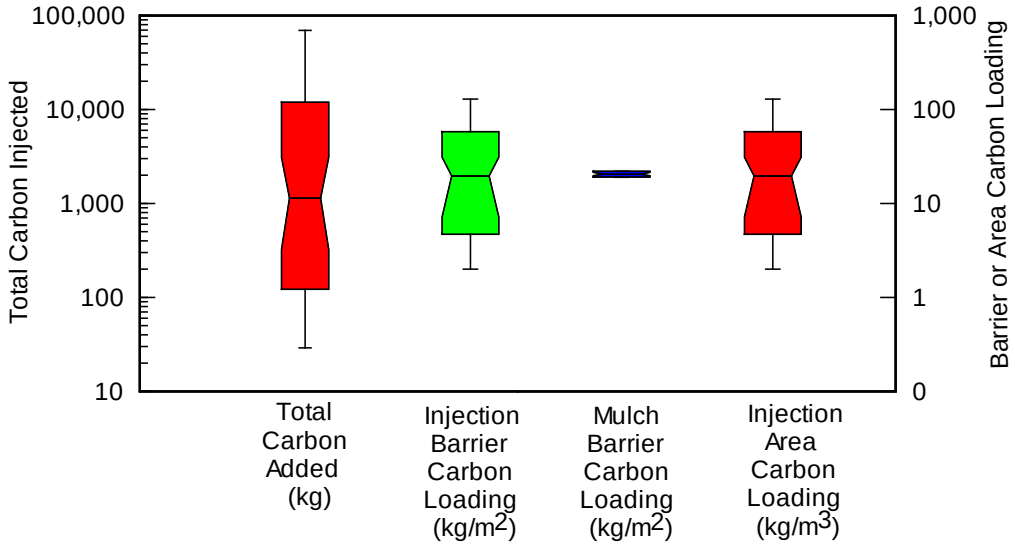

Figure 2.3. Summary of Carbon Addition to Different Treatment Systems.
Data compiled show minimum, 10th, 25th, 50th, 75th, 90th percentile and maximum values. Barrier loadings are per unit area perpendicular to groundwater flow. Area loadings are per unit volume treated aquifer.

2.3 ORGANIC SUBSTRATES

Common substrates added to aquifers for ERB include soluble substrates, low solubility liquid substrates, solid substrates, and mixtures of these materials.

2.3.1 Soluble Substrates

Common soluble substrates include sugars (molasses, high fructose corn syrup), alcohols (methanol, ethanol, glycerol), VFAs such as acetate and their salts (citric acid, lactic acid, sodium lactate), and complex materials containing a combination of substrates (cheese whey, ethyl lactate). All of these materials are readily fermented, releasing H_2, acetate (CH_3COO^-), bicarbonate (HCO_3^-), and H^+. The ratio of C to H to O in the parent substrate controls the amount of each product ultimately produced. Since these materials are soluble, they are easily accessed by microorganisms and rapidly consumed in the aquifer.

2.3.2 Low Solubility Liquid Substrates

Low solubility liquid substrates include Hydrogen Release Compound (HRC™), neat vegetable oil, and emulsified vegetable oil (EVO). HRC™ is a neat viscous liquid composed of glycerol and polylactide (PLA), a form of biodegradable plastic. In water, the PLA hydrolyzes releasing lactic acid which is then fermented, as described above. Commercially available EVOs are mixtures of vegetable oils, soluble substrates, biodegradable surfactants, and/or bacterial nutrients.

All vegetable oils and natural fats are triglycerides composed of three long-chain fatty acids (LCFAs) esterified to a glycerol core. Anaerobic fermentation of triglycerides is believed to occur through a two-step process where the ester linkages between the glycerol and the fatty acids are hydrolyzed releasing free fatty acids and glycerol to solution. Glycerol is miscible with water and can be rapidly fermented, releasing 1,3-propanediol and subsequently acetate (Papanikolaou et al., 2000). The LCFAs are less soluble and may precipitate with Ca, Mg, or Fe (Tang et al., 2013) forming 'soap scum' or sorb to positively charged porous media surfaces. Precipitated organics are generally less bioavailable, so fermentation rates are expected to be slower. However, a fraction of the LCFAs will remain in the aqueous phase. This fraction will undergo further breakdown by *beta*-oxidation releasing H_2, one molecule of acetate, and a new acid derivative of the original molecule with two fewer carbon atoms (Sawyer et al., 1994).

$$C_nH_{2n}O_2 + 2H_2O \rightarrow 2H_2 + C_2H_3O_2^- + H^+ + C_{n-2}H_{2n-4}O_2$$

By successive oxidation at the *beta* carbon atom, LCFAs are whittled into progressively shorter fatty acids and acetic acid. Two molecules of H_2 and one proton are produced for each acetic acid unit produced (Sawyer et al., 1994). Unsaturated fatty acids undergo the same general process, but release two atoms of hydrogen for each acetic acid unit.

2.3.3 Solid Substrates

Solid substrates include wood mulch, compost, fibrous biomass, and mixtures of these materials. In most cases, the solid substrates are blended with sand or gravel to increase the biowall permeability and reduce compaction over time. At some sites, zero valent iron (ZVI) is added to the organic substrates to further enhance pollutant removal. ZVI enhances reduction by several mechanisms. Corrosion of the ZVI produces H_2 and Fe^{2+}, which act as EDs, and OH^-, which limits the pH decrease.

The large majority of the solid organic material used in ERB consists of cellulose, hemicellulose, and lignin. Cellulose is a glucose polymer with the chemical formula $(C_6H_{10}O_5)_n$, where *n* ranges from several hundred to several thousand. Hemicellulose is a short, highly branched polymer of five-carbon and six-carbon sugars that is more readily hydrolyzed compared to cellulose. Lignin is a polyphenolic structural constituent of plants that provides structural rigidity and binds plant cells together.

Cellulose and hemicellulose can be hydrolyzed and fermented to Methane (CH_4) and carbon dioxide (CO_2) under anaerobic conditions. However, lignin is resistant to anaerobic biodegradation (Colberg, 1988). Wood is composed of approximately 40-50% cellulose, 20-30% hemicellulose, and 25-30% lignin (Wang et al., 2011), so the large majority of wood mulch should be fermentable.

However, in nature, hemicellulose, cellulose, and lignin form a three-dimensional polymeric composite structure referred to as lignocellulose. The resistance of lignin to anaerobic biodegradation can reduce the bioavailability of hemicellulose and cellulose, greatly reducing the fraction of organic carbon that is bioavailable under anaerobic conditions. In laboratory reactors designed to maximize anaerobic decomposition, less than 2% of the added carbon was converted to CH_4 and CO_2 for seven out of nine wood products tested (Wang et al., 2011).

2.3.4 Mixed Reagents

Mixtures or combinations of substrates are used at many sites, including mixtures of soluble substrates and vegetable oil, ZVI and vegetable oil, or ZVI and solid organic substrate (EHC®). In addition, pH buffering reagents (e.g., bicarbonate, carbonate), bioaugmentation cultures (e.g., KB-1®, SDC-9), ISCR reagents (e.g., ferrous sulfate, gypsum), and nutrients to aid biological growth (e.g., diammonium phosphate, yeast extract, vitamin B_{12}) are added at some sites to aid degradation of the CoCs.

2.3.5 Substrate Fermentation

The different organic substrates contain different levels of carbon, oxygen, and hydrogen, so the ultimate fermentation products can vary. As a consequence, one substrate may produce more H_2 per C atom. This effect is illustrated by the reaction,

$$C_\alpha H_\beta O_\gamma + (3\alpha - \gamma)\, H_2O \rightarrow \alpha\, HCO_3^- + \alpha\, H^+ + (2\alpha + \beta/2 - \gamma)\, H_2$$

where: α is the number of carbon atoms per mole of substrate
β is the number of hydrogen atoms per mole of substrate
γ is the number of oxygen atoms per mole of substrate

This formula assumes that any organic intermediates (e.g., acetate) produced during substrate fermentation will eventually be fermented to hydrogen (H_2), bicarbonate (HCO_3^-), and H^+. All carbon is assumed to be converted to CO_2 which reacts with water releasing one mole of HCO_3^- and H^+ for each mole of C. The amount of H_2 released varies from 2.0 H_2/C for lactic acid and sucrose, to 2.3 H_2/C for glycerol and ethyl lactate, and 2.8 H_2/C for vegetable oils. The reaction stoichiometry may be useful for predicting the flux of SWQIs from the treatment zone and the longevity of the ERB source. The upper limit of the flux of reducing equivalents will be the number of moles of C added times the number of H_2 produced times two.

This Page Intentionally Left Blank

3.0 SWQI GENERATION AND ATTENUATION

3.1 INTRODUCTION

This section reviews the major physical, chemical, and microbiological processes controlling the formation and attenuation of the important SWQI parameters. The sections on each parameter begin with basic information on formation and attenuation mechanisms followed by a summary and interpretation of field results from the database. **Table A-2** in Appendix A provides summary statistics for post-injection monitoring data for all upgradient, injection area, and downgradient wells at the 47 sites contained in the SWQI database. Downgradient wells include monitoring points outside of the target treatment zone and up to 760 m downgradient. Most site data comes from sites where the duration of monitoring is longer than the estimated travel time to the downgradient wells. A few sites had extremely low listed groundwater velocities, so theoretically the travel time may have been longer than the time monitored; however, in most cases SWQIs showed up sooner than expected based on the available velocity estimates, indicating actual groundwater velocity is likely much higher. In order to counteract the effect of sampling results skewing to pre-treatment conditions, most parameters (with the exception of pH and ΔpH) looked at the minimum or maximum concentration (depending on how reducing conditions affected the particular parameter).

Because of the broad range of concentrations observed, monitoring results are presented as frequency distributions. For parameters that generally increase following ERB (total organic carbon [TOC], iron [Fe], manganese [Mn], As, S^{2-}, CH_4), maximum values are shown, while minimum values are shown for parameters that generally decrease (oxidation-reduction potential [ORP], O_2, NO_3^-, SO_4). For parameters that may increase or decrease (pH), median values are shown. To examine changes in concentration resulting from ERB, cumulative frequency distributions are plotted for change in measured values for these same parameters. Delta (Δ) concentration is the maximum or minimum value (C) minus the pre-injection value (C_o). Thus negative values represent loss and positive values are gains. In some cases, C/C_o is plotted to better illustrate the results. These cases are noted in the figure captions.

3.2 ORGANIC CARBON, ORP / EH, PH, AND OXYGEN

ERB systems are intended to alter the geochemical environment to generate conditions favorable for biodegradation or sequestration of the target contaminants. Reductions in the aquifer ORP/Eh and pH following various *in situ* bioremediation techniques are well documented (Perkins and Chui, 2008; Freedman et al., 2003; Vanbroekhoven et al., 2009; Kelly et al., 2009; LaPat-Polasko et al., 2009).

3.2.1 Organic Carbon

Figure 3.1 shows the maximum observed TOC concentrations and the ratio of maximum TOC to the pre-injection value in each well. Maximum values are reported because average values may be biased by measurements collected before the organic substrate reached the well or after it was depleted. As expected, following organic substrate addition, injection area concentrations were substantially elevated compared to upgradient concentrations. For instance, the median injection area TOC concentration is nearly two orders of magnitude higher than the median upgradient TOC concentration.

However, TOC concentrations decline rapidly with distance, dropping almost an order of magnitude in the 0-10 m wells and with median concentrations of 10 mg/L or less for wells more than 10 m downgradient, similar to that of upgradient wells. In the upgradient wells, the ratio of maximum to pre-injection concentration was greater than 1 in some wells due to random variations in concentration and/or upgradient migration of some TOC during injection.

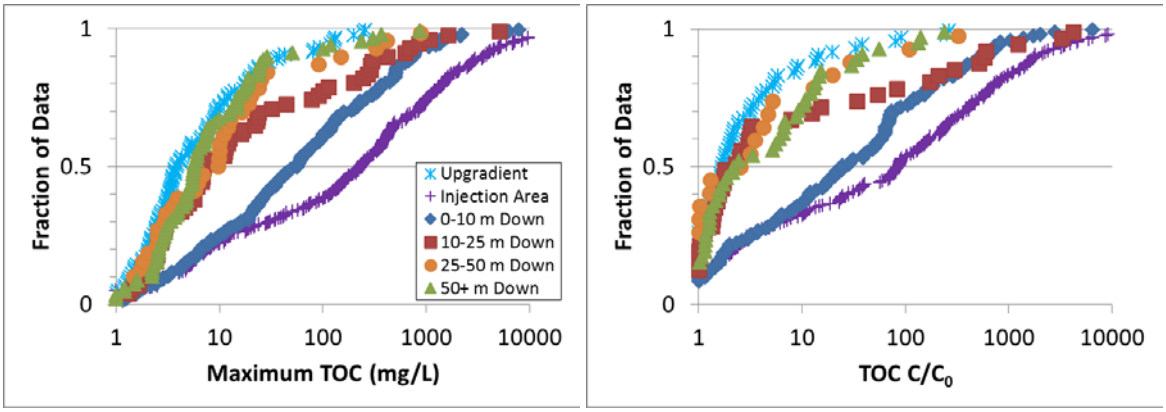

Figure 3.1. Total Organic Carbon (TOC) Concentrations Reported in Upgradient, Injection Area, and Downgradient Monitoring Wells.

Compiled data show cumulative frequency distributions for maximum TOC concentrations and ratio of maximum and pre-injection value (TOC C/C$_o$) observed in each well.

When organic substrates are added to the subsurface, naturally occurring bacteria ferment them to VFAs including acetic, propionic, butyric, pyruvic, lactic, n-pentanoic (valeric), i-pentanoic, n-hexanoic, and i-hexanoic acids (AFCEE, NFESC, ESTCP, 2004). Elevated VFA levels give groundwater in the treatment zone a noxious odor. However, VFAs are expected to rapidly biodegrade. As a result, VFAs are not expected to migrate far from the treatment zone and the taste and odor of groundwater further downgradient may not be impacted.

Acetone, butanol, and other ketones can be produced during anaerobic fermentation by the bacterium *Clostridium acetobutylicum* and a variety of related organisms during anaerobic fermentation of a wide variety of organic materials (potatoes, corn, rye, millet, cheese whey, apple pomace, algal biomass, and any wood product containing lignocellulose) (Jones and Woods, 1986; Woods, 1995). As a result, these ketones are sometimes observed in strongly reducing ERB treatment zones (Jacob et al., 2005). These materials are readily biodegradable under both aerobic and anaerobic conditions (Tabak et al., 1981; Boyd et al., 1983; Shelton and Tiedje, 1983) and are not expected to migrate significant distances from the ERB treatment zone.

3.2.2 ORP / Eh

ORP provides a qualitative indication of the relative oxidizing or reducing condition of groundwater and is typically monitored using a handheld voltage meter that measures the electrical potential between a platinum electrode and a reference electrode. In most cases, the platinum electrode and reference electrode are combined into a single probe that is inserted into the solution. In theory, ORP values measured with a platinum electrode can be converted to the standard redox potential (Eh) by correcting for the electrode potential of the reference electrode (E_{ref}).

E_{ref} values for common Ag/AgCl reference electrodes vary from +236 mV for 1 M KCl to +197 mV for saturated KCl solutions (Nordstrom and Wilde, 2005). For example, assume ORP was measured in the field with a platinum - Ag/AgCl electrode containing 1 M KCl and the meter reading was 200 mV. The Eh of the solution would be:

Eh = 200 mV + 236 mV = 436 mV = 0.436 V

However in practice, a variety of factors plague ORP measurements including effects of solution temperature and pH, irreversible and slow reactions, multiple redox couples, and electrode poisoning. In addition, in the case of the iron or manganese couples, one of the critical members of the redox couple is on the aquifer sediments rather than in the groundwater sample where the measurement is made. As a result, field measured ORP values likely underestimate the Eh change and should be considered as a rough qualitative indicator of the system Eh.

ERB processes influence, and are influenced by, redox conditions with biotransformation of different contaminants considered to be optimal at different Eh values. Microbial reduction with different terminal electron acceptors is commonly described as following a sequence where O_2 is reduced first followed by NO_3^-, Mn(IV), Fe(III), SO_4^{2-}, and CO_2 reduction. In this approach, biodegradation is assumed to occur with a sequence of TEAs dictated by the standard electrode potentials of the half reaction. **Figure 3.2** shows Eh at pH 7 for various TEAs. ORP values (as measured by an Ag/AgCl reference electrode) will be roughly 0.2 V lower.

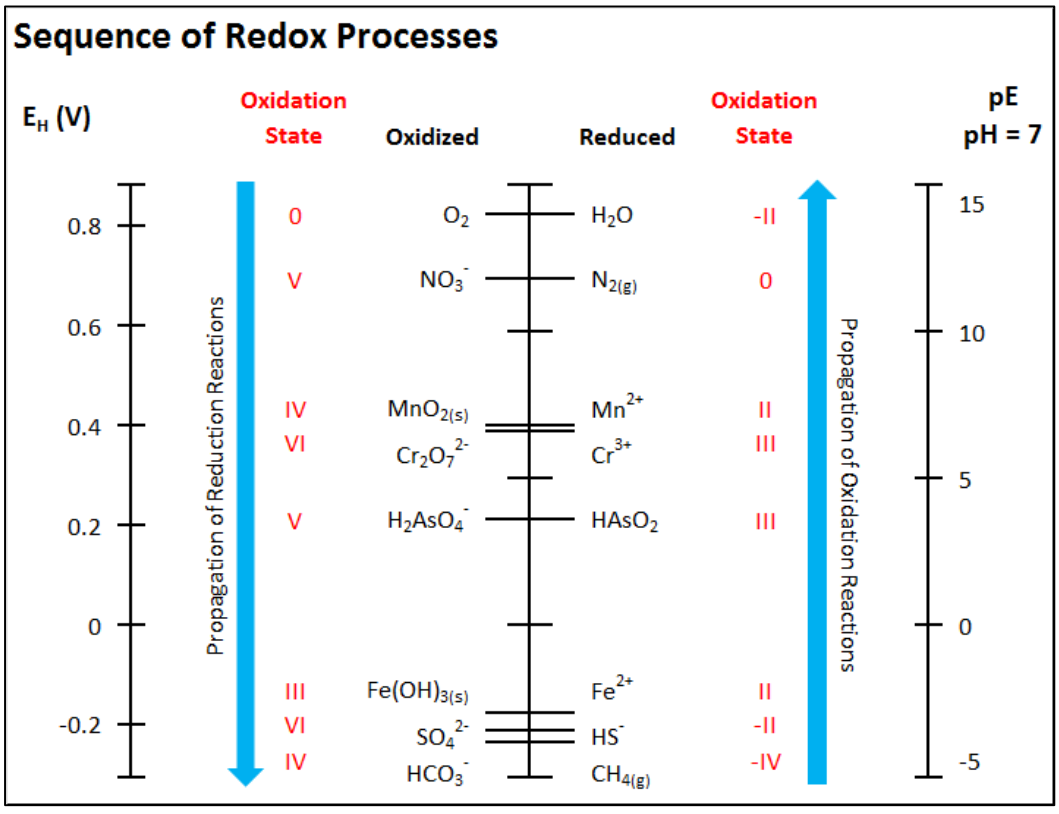

Figure 3.2. Redox Ladder for Various Terminal Electron Acceptor Parameters.
Voltages are calculated from a specific set of chemical conditions, including pH 7, temperature, and unit concentration of oxidized and reduced species. Reference values from Snoeyink and Jenkins (1980) and Vanysek (2014)

Further analysis of the role of microorganisms in driving redox processes in aquifers leads to different sequences of reactions (Bethke et al., 2011). This analysis differs from the simple redox ladder in **Figure 3.2** in several ways. First, rather than considering the free energy of a particular TEA with respect to the electron, the free energy is considered with respect to an electron donor such as acetate or hydrogen (H_2). Consideration of the electron donor puts an additional reaction stoichiometry into play:

$$CH_3COO^- + 4H_2O = 2HCO_3^- + 9H^+ + 8e^- \text{ or,}$$
$$H_2(aq) = 2H^+ + 4e^- .$$

Second, instead of using standard condition concentrations (e.g., one mole per liter of solution or kg water for dissolved species), actual aqueous phase environmental concentrations are considered. Based on these two considerations, the potential energy available to microbial communities in the groundwater environment can be calculated. Third, microbial physiological requirements are taken into account. These include the energy stored in the cell from production of adenosine triphosphate (ATP) and the stoichiometric coefficient for constituents involved in the rate-determining step of the governing metabolic process. When these factors are considered, the thermodynamically most favorable microbial metabolic processes are different than those suggested by the sequence in **Figure 3.2**. For example, Fe(III) reducers are favored at acidic pH values but sulfate reducers or methanogens are favored at alkaline pH values. Consideration of a solubility control on ferrous iron (Fe[II]) and S(-II) concentration can account for the co-occurrence of Fe(III) and sulfate reduction, as has been observed in some aquifers (Jakobsen et al., 1998). At alkaline pH values, whether conditions are thermodynamically favorable for sulfate reducers or methanogens depends on sulfate and methane concentrations. Thus, ORP measurements should not be relied upon to predict the dominant TEA likely to be operating in a given region of an aquifer.

Minimum ORP values and changes in the minimum ORP from pre-injection conditions in the SWQI database wells are shown in **Figure 3.3**. In upgradient wells, measured ORP varies widely from +200 mV to -400 mV indicating background geochemical conditions vary from mildly oxidizing to strongly reducing. Electron donor addition results in a median drop in ORP to approximately -180 mV, and then ORP begins to rebound at 10-25 m downgradient. ORP values at 50+ m downgradient appear to exceed background (upgradient) values. However, this difference is an artifact of differences in sample populations. The difference between the initial ORP and minimum observed ORP in the 50+ m wells is similar to the upgradient wells, indicating ORP is not strongly impacted in the most downgradient wells.

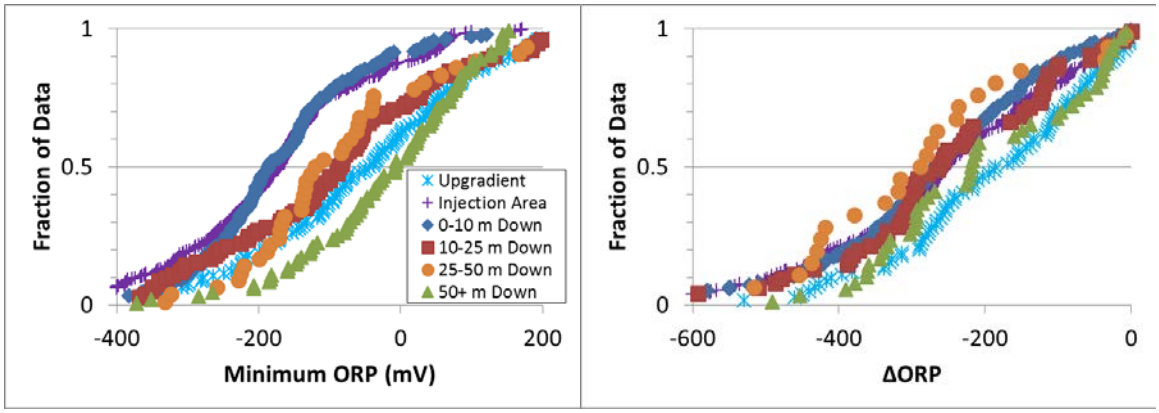

Figure 3.3. Oxidation-Reduction Potential (ORP) Observed in Upgradient, Injection Area, and Downgradient Monitoring Wells.

Compiled data show frequency distributions for minimum ORP values and difference between minimum and pre-injection values (ΔORP) in each well.

3.2.3 pH

pH is the negative logarithm (base 10) of the hydrogen ion or proton (H^+) activity. In dilute solutions, activity is approximately equal to the molar concentration of H^+, so a solution with pH = 7 standard units (SU) contains approximately 10^{-7} moles of H^+ per liter. The pH is typically measured in the field using an ion selective electrode calibrated against standard buffer solutions. Reactions that affect pH in natural waters are discussed by Hem (1985). The term buffered refers to a solution in which the pH is not altered much by adding moderate quantities of acid or base. Important aquifer solid phases that buffer pH include carbonate minerals and surface exchange reactions of H^+ with clays and iron oxy-hydroxides.

As with most biological processes, a pH close to neutral is optimum for microbial growth and contaminant biodegradation. However, this may be especially important when stimulating reductive dechlorination since dechlorinating bacteria appear to be more sensitive to pH than other common microorganisms. Dechlorination of tetrachloroethene (PCE) and trichloroethene (TCE) to dichloroethene (DCE) can occur at pH down to 5.5 SU, while reduction of DCE and vinyl chloride (VC) is more sensitive, with little or no ethene production observed below a pH of six SU (Vainberg et al., 2009; Eaddy, 2008).

Changes in pH can also influence sorption reactions, and, therefore the mobility of inorganic contaminants (Kent et al., 2000, 2007; Parkhurst et al., 2003). Clay minerals and Fe and aluminum (Al) oxyhydroxides are the dominant sorbents in soils and sediments (Serrano et al., 2013), even when not present at high enough abundance to be detected by X-ray diffraction (XRD) on bulk samples (Zhang et al., 2011). For the purpose of describing contaminant sorption, sorption reactions are divided into two types of reactions, ion exchange and surface complexation (Davis and Kent, 1990; Davis et al., 1998; Baeyans and Bradbury, 1997). Ion exchange reactions are reactions between cations on sites whose concentration is mostly independent of groundwater chemical conditions:

$$2Na^+ + X_2Ca = 2XNa + Ca^{2+}$$

where X represents a cation exchange site. The total concentration of exchange sites is independent of groundwater chemical conditions because it is controlled by heteroionic, isomorphic substitutions or cation vacancies in the crystal lattice. All cationic solutes, including H^+, participate in cation exchange reactions in proportion to their concentration in solution, charge, and affinity for the exchange sites. Cation exchange shows only a weak dependence on pH because, in most cases, H^+ is a minor component of the cation charge balance in solution. Thus, the extent of sodium (Na^+), potassium (K^+), magnesium (Mg^{2+}), and calcium (Ca^{2+}) sorption on aquifer sediments is not expected to vary with pH. Sorption of the cation NH_4^+ is pH-dependent but observations show that NH_4^+ concentrations are low at most ERD sites.

Surface complexation involves coordination of a solute with a site that is fixed on the solid phase. For example,

$$Mn^{2+} + >SOH = >SOMn^+ + H^+$$

$$PO_4^{3-} + 2H^+ + >SOH = >SOPO_3H^- + H_2O$$

where >SOH represents a surface complexation site (examples from Bradbury and Baeyans, 1997 and Parkhurst et al., 2003, respectively). Surface complexation sites occur at surfaces of Fe and Al oxyhydroxides as well as on aluminosilicates, such as the edges of clay minerals. H^+ sorbs strongly to surface complexation sites, so surface complexation reactions can strongly buffer pH, taking up large amounts of H^+ as the solution pH declines and releasing H^+ to solution as the pH rises.

Binding of cation and anion solutes to surface complexation sites often exhibit a strong dependence on pH (Davis and Kent, 1990; Davis et al., 1998). At low pH, Mn^{2+} and Fe^{2+} will sorb primarily to cation exchange sites. Consequently, the extent of Mn^{2+} and Fe^{2+} sorption is not expected to vary with pH under mildly acidic conditions. However, as the pH rises both cation exchange and surface complexation reactions will contribute to Mn^{2+} and Fe^{2+} sorption (Bradbury and Baeyans, 1997; Liger et al., 1999; Dixit and Hering, 2006). Surface complexation of oxyanions like phosphate and As[V] exhibit a complex dependence on pH owing to changes in solution speciation with pH, but generally decreases with increasing pH at alkaline pH values (Davis and Kent, 1990; Stollenwerk, 2003; Dixit and Hering, 2003).

pH can decline during ERB due to release of VFAs and carbonic acid (H_2CO_3) from substrate fermentation and hydrochloric acid (HCl) from dechlorination reactions. In some cases, pH declines are limited by alkalinity released during reduction of nitrate, manganese and iron oxides, and by CO_2 degassing. Dissolution of carbonate minerals can prevent extreme drops in pH. However, at near neutral pH CO_2 production can cause the groundwater to become supersaturated with $CaCO_3$ (Robinson et al., 2009) and $CaCO_3$ is not an effective buffer.

At many sites, alkaline materials are added to the aquifer to increase the pH and/or neutralize acidity produced dsodium hydroxidepotassium hydroxideHarkness and Fisher (2013) reported that up to 71.4 mM (6.0 g/L) of sodium bicarbonate was required to neutralize the acidity produced during dechlorination of ~ 5 mM TCE.

Figure 3.4 shows median pH and ΔpH values for wells at sites with and without buffer addition. ΔpH is the difference between the median pH and the value prior to injection in the treatment zone. At non-buffered sites, the background pH is slightly below neutral. The largest pH declines occur in wells closest to the injection area and lessen with distance downgradient. At buffered sites, the upgradient/background pH values are low, which is likely why buffer is added. At buffered sites, the largest pH increases (positive ΔpH) occurs in wells close to the injection area, with smaller increases farther downgradient.

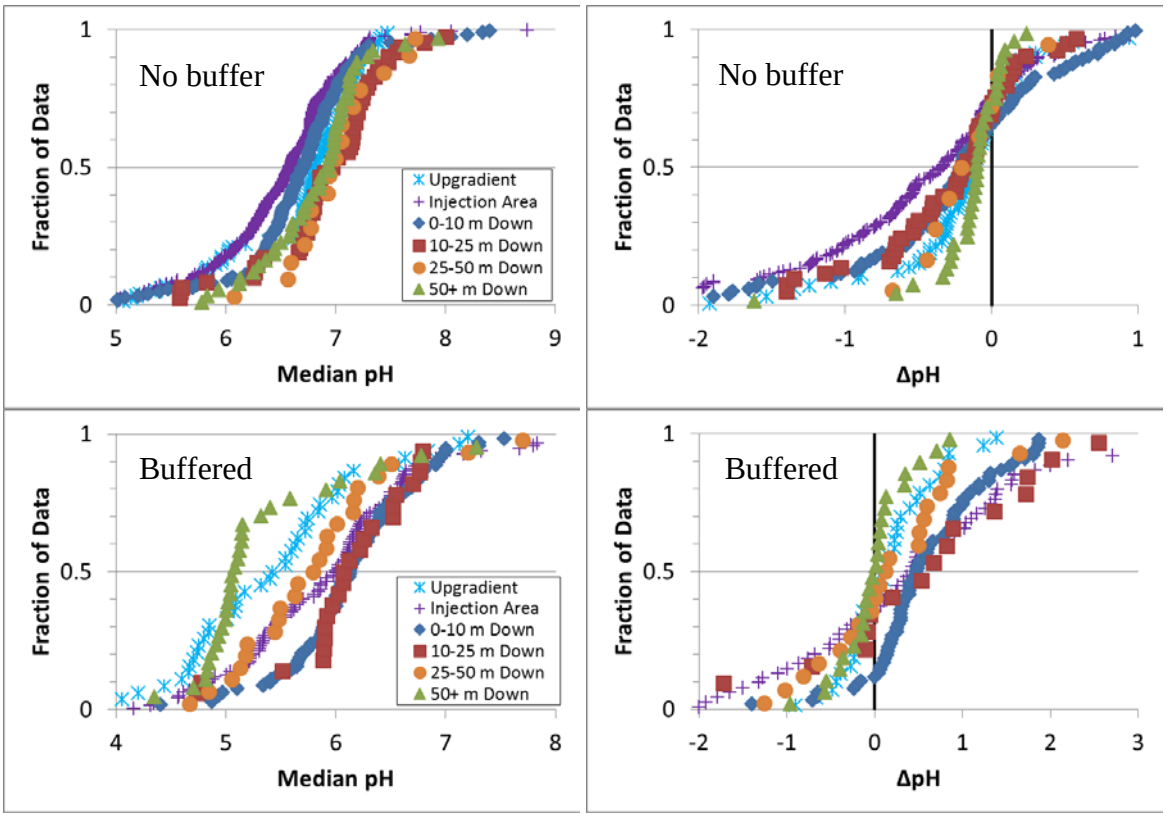

Figure 3.4. pH Measurements in Buffered and Non-Buffered Systems Observed in Upgradient, Injection Area, and Downgradient Monitoring Wells.

Compiled data show cumulative frequency distributions for median pH and difference between median and pre-injection value (ΔpH) at sites without added alkaline material (Non-Buffered) and with added alkaline material (Buffered). Note that different scales were used on the graphs to allow better visualization of changes with distance.

Figure 3.5 shows the median ΔpH values in injection area wells at non-buffered sites for the substrate groups: oils; soluble substrates; mulch biowalls; and EHC®, which is a combination organic substrate and ZVI. The range of pH changes indicates that oils and soluble substrates behaved in very similar ways, with no significant difference between the two types of substrates. Declines in median pH were observed for approximately 75% of injection area wells, with a median pH change of about -0.4 pH units for both substrate types. Mulch biowalls induced the smallest range of pH changes, with a median change of -0.2 pH units and a maximum pH change of -0.4 pH units. The small change in pH may be due to slow or limited degradation of the mulch. The median pH change for EHC was approximately +0.1 pH units, with the range of pH changes from -0.9 pH units to +1.4 pH units. The increased range in ΔpH is likely due to corrosion of ZVI,

which can release OH^- and thus mitigate some of the acidity produced from the fermentation of the organic substrate.

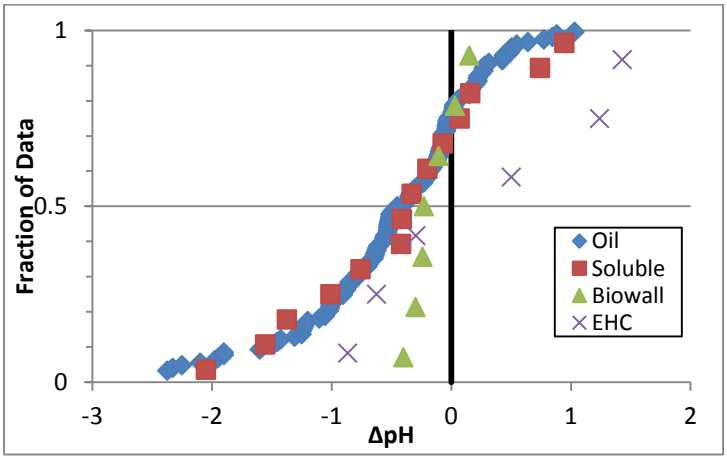

Figure 3.5. Effect of Substrate Type on Difference between Median and Pre-injection pH (ΔpH) in Injection Area Wells at Non-Buffered Sites.

3.2.4 Oxygen

A variety of microorganisms using organic carbon as an ED utilize O_2 as the preferred electron acceptor. As a result, O_2 is rapidly depleted following ED addition. Water in equilibrium with the atmosphere will have dissolved O_2 levels between 7 and 12 mg/L, depending on temperature. **Figure 3.6** shows dissolved O_2 concentrations in upgradient, injection area, and downgradient wells. Much of this data was obtained using membrane-covered polarographic electrodes with hand-held meters, which may not be reliable for oxygen concentrations less than 1 mg/L (Wilkin et al., 2001).

Observed upgradient O_2 concentrations in groundwater at these sites are often lower than water in equilibrium with the atmosphere (**Figure 3.6**). Upgradient O_2 concentrations were greater than injection area and downgradient concentrations at corresponding percentiles, reflecting the rapid depletion of O_2 following ED addition. Further downgradient, the difference between minimum O_2 and pre-injection O_2 is smaller. Numerical model simulations indicate O_2 recovery will be slow due to limited mixing with unimpacted groundwater and O_2 consumption by reactions with Mn(II), Fe(II), sulfide, and methane. The apparent recovery in O_2 concentrations in monitoring wells could be due to mixing of aerobic and anaerobic groundwater in long screen wells, position of wells at the edge or beyond the front of the plume, or difficulties in accurately measuring dissolved oxygen in groundwater (Wilkin et al., 2001).

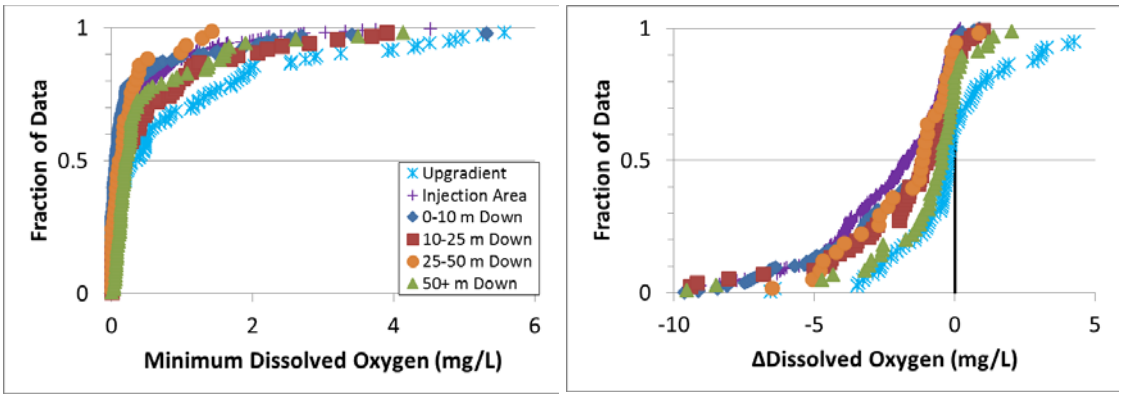

Figure 3.6. Dissolved Oxygen (O_2) Concentrations Reported in Upgradient, Injection Area, and Downgradient Monitoring Wells.

Compiled data show cumulative frequency distributions for minimum O_2 concentrations and difference between minimum and pre-injection values (ΔO_2) in each well.

3.2.5 Nitrate

NO_3^- is commonly present in background groundwater from atmospheric deposition, fertilizer application, septic tanks, and other sources. NO_3^- is not strongly sorbed by aquifer material under typical pH conditions. Under anaerobic conditions denitrifying microorganisms reduce NO_3^- through a series of intermediates to nitrogen (N_2) gas coupled to organic carbon or Fe(II) oxidation. Under some conditions, particularly where there are large concentration of metabolizable organic carbon, microorganisms can reduce NO_3^- to ammonia (NH_3) through a process called dissimilatory nitrate reduction to ammonium (DNRA).

Nitrate was only monitored at 44% of the wells at ERB sites, so there is little data to judge changes in nitrate concentration. At sites where nitrate was monitored, NO_3^- was below the applicable detection limit in 40% of the upgradient wells indicating native groundwater at many of the sites was anoxic (data not shown). Numerical model simulations suggest the return to pretreatment NO_3^- concentrations will be slow due to limited mixing with background water and the potential for nitrate reduction coupled to organic carbon or sediment-bound Fe(II) oxidation. This slow timescale for NO_3^- replenishment may be an advantage at sites with elevated NO_3^-.

3.3 SULFATE AND SULFIDE

Sulfur can occur in a range of oxidation states varying from -2 to +6. Under aerobic conditions, the dominant form is SO_4^{2-} with a +6 oxidation state. Under anaerobic conditions, SO_4^{2-} can be reduced to S^{2-} with a -2 oxidation state. However, sulfur can also be present in intermediate oxidation states including sulfite (SO_3^{2-}), thiosulfate ($S_2O_3^{2-}$), elemental sulfur (S_8), and polysulfides (S_n^{2-}).

Sulfate present in groundwater originates from a variety of sources including atmospheric deposition, weathering processes, oxidation of sulfide minerals, gypsum (calcium sulfate) dissolution, and anthropogenic releases. Since sulfate is relatively soluble in water, it is naturally flushed through aquifers with flowing groundwater. However, in areas with naturally occurring gypsum, sulfate concentrations can reach 2,000 mg/L as SO_4^{2-}, reflecting equilibrium with gypsum in the aquifer material. Sulfate concentrations may also be high in arid climates where evapotranspiration can concentrate salts.

Sulfate can be reduced to hydrogen sulfide (H_2S) using low molecular weight fatty acids (acetate, butyrate, propionate, lactate), alcohols, and H_2 as electron donors. H_2S is a weak acid, dissociating to H^+ and HS^- with an acid dissociation constant (pKa) of 7.0. At neutral pH, the concentration of HS^- is approximately equal to H_2S, while at pH 6 about 90% of the sulfide occurs as H_2S. H_2S is a colorless, poisonous, inflammable gas with the characteristic 'rotten egg' smell which is detectable at 0.01 ppm (USEPA, 2009). H_2S exposure can also result in eye irritation, sore throat and cough, nausea, shortness of breath, and fluid in the lungs.

High concentrations of H_2S can also inhibit reductive dechlorination, reducing remediation efficiency. Hoelen and Reinhard (2004) reported that 5 mM Na_2S inhibited TCE, DCE, and VC degradation. Sung (2005) found that 2 mM total sulfide inhibited growth of *Desulfuromonas michiganensis strain BB1, Sulfurospirillum multivorans, Desulfitobacterium sp. strain Viet1*, and *Dehalococcoides sp. strain FL2* and *strain BAV1*. However, at low concentrations (< 0.5 mM), sulfide does not inhibit dechlorinators (Löffler et al., 2005).

In most aquifers, substantial amounts of naturally occurring iron are present and H_2S will rapidly precipitate as insoluble iron sulfide minerals (Cozzarelli et al., 1999). Known reactions include S^{2-} precipitating with Fe^{2+} as FeS and also S^{2-} reacting with Fe(III) to produce Fe^{2+} and elemental S, followed by Fe^{2+} precipitation as FeS. H_2S production can also enhance precipitation of metals (Edwards et al., 1992; Vanbroekhoven et al., 2009). In most aquifers, sulfide attenuates rapidly downgradient of the anaerobic treatment zone and rarely persists as the substrate is depleted. However when iron concentrations are low and background sulfate concentrations are high, substantial amounts of sulfide can be produced, inhibiting reductive dechlorination and making the water unsuitable for other uses.

Figure 3.7 shows the minimum observed sulfate concentrations in upgradient, injection area and downgradient wells. There is a broad range of upgradient (background) sulfate concentrations varying from < 1 mg/L to near the gypsum solubility limit. Median injection area concentrations were about one order of magnitude lower than upgradient concentrations indicating significant depletion during ERB.

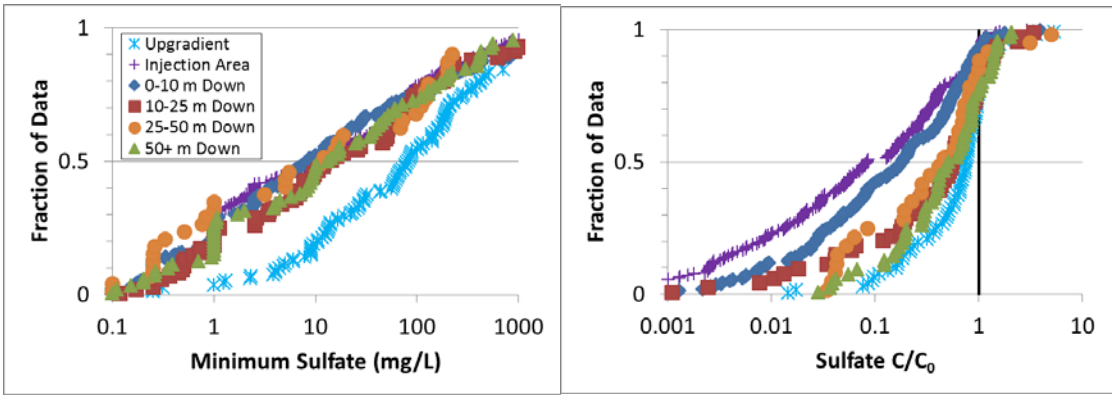

Figure 3.7. Sulfate (SO_4^{2-}) Concentrations Reported in Upgradient, Injection Area, and Downgradient Monitoring Wells.

Compiled data show cumulative frequency distributions for minimum sulfate concentrations and ratio of minimum and pre-injection values (SO_4^{2-} C/C_o) in each well.

Figure 3.8 shows the maximum observed sulfide (S^{2-}) and the difference between maximum and pre-injection values in upgradient, injection area, and downgradient wells. Only about 340 wells or 35% of the database reported values for sulfide, so care should be taken in extrapolating these results to other sites. Sulfate reduction did result in detectable concentrations of sulfide in injection area and downgradient wells. In those wells where sulfide was monitored, the increase in sulfide was typically less than 1 mg/L, although sulfide increased by more than 10 mg/L in a few injection area wells. There was little difference between the change in sulfide (Δsulfide) distribution in upgradient and downgradient wells, indicating sulfide migration is not an issue at most sites.

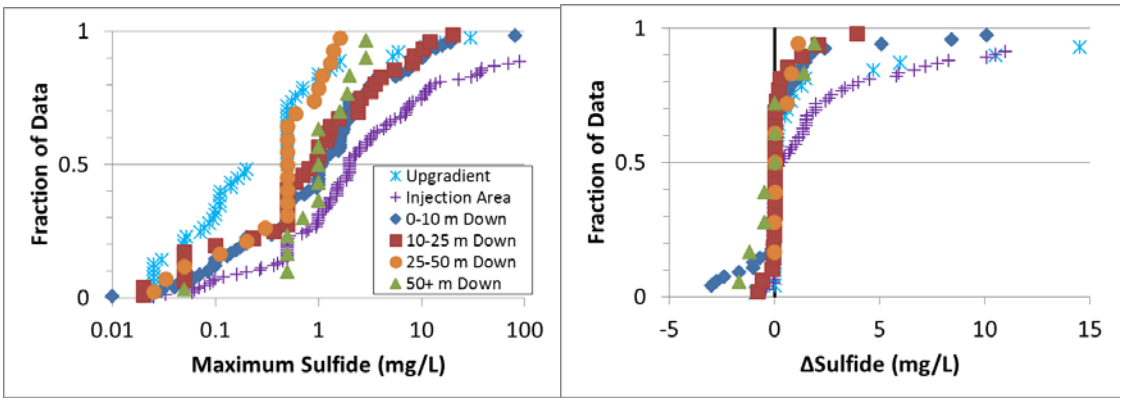

Figure 3.8. Sulfide (S^{2-}) Concentrations Reported in Upgradient, Injection Area, and Downgradient Monitoring Wells.

Compiled data show cumulative frequency distributions for maximum S^{2-} and difference between maximum and pre-injection values (ΔS^{2-}) in each well.

3.4 IRON, MANGANESE, AND ARSENIC

Iron, manganese, and arsenic can undergo redox reactions that can increase their mobility in the subsurface following ERB. In upper crustal rocks that are source material for soils and aquifer sediment, Fe occurs primarily as Fe(II) in ferro- and aluminosilicate minerals, manganese occurs as Mn(II) substituted for Fe(II) in these minerals, and arsenic occurs as reduced forms (e.g., As[0] and As[III]) in pyrite and other sulfide minerals. The average abundance of these elements in upper crustal rocks is estimated to be 4% for Fe, 0.08% for Mn, and 5 µg/g for arsenic. Over time, weathering reactions generate Fe(III) and Mn(III/IV) oxyhydroxides as a result of prolonged exposure to oxic groundwater. These oxides often occur as grain coatings on both reduced phases and on other minerals. The grain coatings have high reactive surface area and shield the underlying minerals from reactions. Oxidation of sulfide minerals generates Fe(III) oxyhydroxides and sulfate, which gets transported away. Arsenic is oxidized to As(V), which sorbs strongly to surfaces of a variety of minerals, including Fe(III) oxyhydroxides and aluminosilicate minerals (Ford, 2002, 2005; Dixit and Hering, 2003; Stollenwerk, 2003). For each of these elements, only a fraction of the total concentration in aquifer sediments is likely to be reactive.

During ERB, increased levels of H_2 and VFAs produced from substrate fermentation lead to reduction of Fe(III) and Mn(III/IV) oxyhydroxides and release of dissolved Fe(II) and Mn(II). Mn(II) is produced through direct microbial reduction of Mn(IV) and also indirectly when Mn(IV) reacts with Fe(II) produced by dissimilatory Fe reducers. Where present, sorbed As(V) is released to solution when As(V) is reduced to As(III) and also when Fe(III) hydroxides are reductively dissolved

(Kent and Fox, 2004; Höhn et al., 2006; Hering et al., 2009; He et al., 2010). Dissolved Fe, Mn, and arsenic in the aqueous phase can subsequently sorb or precipitate through a variety of processes.

3.4.1 Iron

In natural soils and aquifers, iron is present in the +2 or +3 valence states, which has a major impact on solubility. Iron minerals commonly present in soils and aquifers include poorly crystalline forms of ferric hydroxide (am-$Fe[OH]_3$) and ferrihydrite ($(Fe^{3+})_2O_3 \cdot 0.5(H_2O)$) subsequently referred to in this document as amorphous Fe(III) oxy-hydroxides. Common forms of more crystalline iron oxides include goethite (FeOOH), hematite (α-Fe_2O_3), siderite ($FeCO_3$), magnetite (Fe_3O_4), mackinawite (FeS), pyrite / marcasite (FeS_2), and pyrrhotite ($Fe_{(1-x)}S$). Fe solubility in water depends on redox conditions, pH, and presence of other solutes.

Reduction of Fe(III) oxyhydroxide minerals in aquifers by organic carbon is primarily carried out by iron-reducing bacteria (IRB). Subsurface sediments are thought to contain a mixture of poorly crystalline amorphous Fe(III) oxy-hydroxides and more crystalline forms. Characterization of sediments from a quartz-sand aquifer showed that nano-crystalline, Al-substituted goethite was the dominant reactive Fe(III) mineral except where cyclical Fe(III) reduction and Fe(II) oxidation had occurred, where ferrihydrite was also observed (Zhang et al., 2011). Likewise, nano-crystalline goethite was found to be the dominant Fe(III) oxyhydroxide mineral identified in a variety of lacustrine sediments, which had minimal amounts of ferrihydrite and amorphous Fe(III) oxyhydroxides (van der Zee et al., 2003). Early research suggested that the poorly crystalline forms of Fe(III) (e.g., ferrihydrite) could be rapidly and completed reduced (Lovley and Phillips, 1986) while reduction of more crystalline forms (e.g., goethite and hematite) was more limited (Lovley and Phillips, 1987). However, more recent work has shown that a variety of crystalline Fe-oxides can be reduced by IRB (Roden and Zachara, 1996; Roden et al., 2000; Roden and Urrutia, 2002). In addition Fe[III] oxides and silicates may be reduced by sulfide (e.g. Li et al., 2009; Komlos et al., 2007).

Figure 3.9 shows cumulative frequency distributions of bioavailable and total iron in sediment samples at 20 sites. Bioavailable and total iron are based on soil extractions in 0.5 N HCl and 5 N HCl, respectively. These sites include 16 ERB sites, three petroleum release sites, and one landfill leachate release site. Data were gathered from samples collected at the seven sites shown in **Figure 3.10** (described below), from unpublished data shared by site project managers, and from the literature (Albrechtsen et al., 1995; Hunt 1997; ESS, 2004; Kota et al., 2004; Whiting et al., 2008). Concentrations of bioavailable Fe varied approximately three orders of magnitude from 0.01 g/kg to over 17 g/kg. Total iron varied from 0.2 to 110 g/kg and was typically five to ten times bioavailable iron.

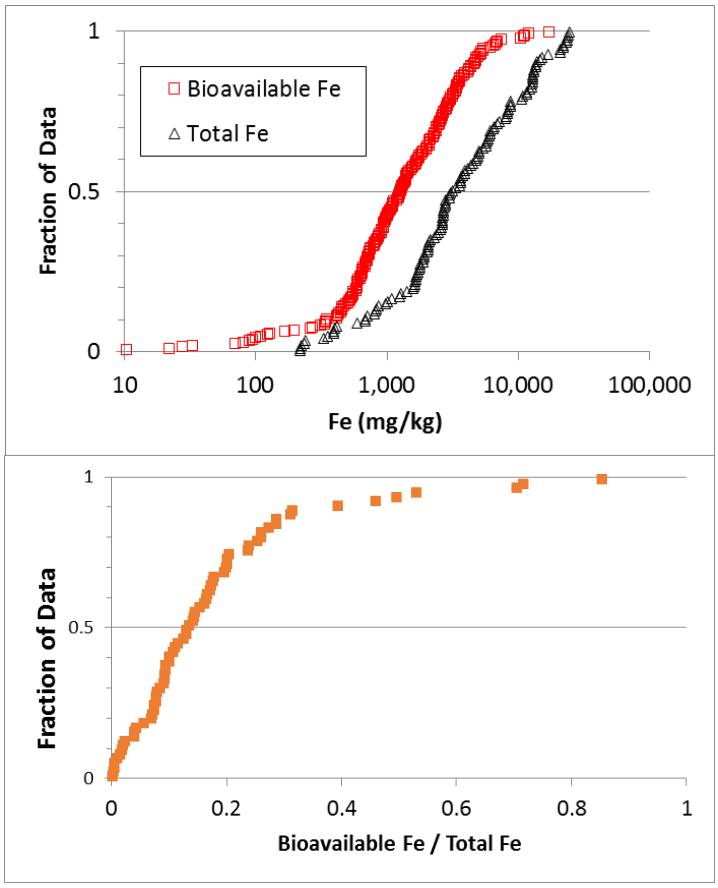

Figure 3.9. Bioavailable and Total Iron Concentrations in Aquifer Material from 20 Sites.

Migration of Fe(II) will be influenced by sorption reactions which will decrease the rate of downgradient migration of dissolved Fe^{2+} and increase the concentration of sediment-bound Fe(II). Concentrations of sediment-bound Fe(II) can be further increased by formation of pure Fe(II) phases like siderite and mixed Fe(II)-Fe(III) phases such as magnetite and green rust, which can form by reactions between Fe(II) and Fe(III) oxyhydroxide minerals (Frederickson et al., 1998; Hansel et al., 2005; Qafoku et al., 2009). Sorbed Fe(II) will be a sink for dissolved oxygen, and therefore delay the re-establishment of oxic conditions following ERB treatment. The extent to which mixed Fe(II)-Fe(III) phases and siderite react with dissolved oxygen requires further investigation.

Recent results suggest that CH_4 can be used as an electron donor to reduce Fe(III) and Mn(IV) oxides (Beal et al., 2009; Crowe et al., 2011). Evidence for this process has been documented at the Bemidji, MN crude oil site (Amos et al., 2012). It is not known how common this process is or at what rate it typically occurs. Methane represents a mobile form of reduced carbon that is transported away from the treatment zone. Reaction of methane with Fe(III) oxides represents a mechanism for producing aqueous Fe(II) at significant distances downgradient from the injection area. However, sorption of Fe(II) to the solids appears to be the fate of 95-99% of the aqueous Fe(II) at both the Bemidji (Ng et al., 2014) and Cape Cod sites [Smith et al., *in revision*].

Reduced iron and sulfide bearing minerals (e.g., mackinawite, amorphous FeS, and magnetite) formed following the addition of electron donors to aquifers can serve as electron donors for continued chlorinated ethene (CE) reduction after the end of active treatment (AFCEE, 2008). As such, the presence of these minerals in aquifers could lead to long-term treatment of CEs slowly released from clays, silts, or dead-end fractures and pore spaces following active remediation, thereby serving as a means to mitigate contaminant rebound emanating from source areas. He et al. (2009) reviewed the abiotic reactivity of these minerals, including iron sulfides, mixed Fe(II)-Fe(III) oxides (e.g., magnetite and green rusts), and iron in phyllosilicate clays. Mackinawite was the most reactive of the minerals encountered under reducing conditions, with magnetite an order of magnitude less reactive, and green rust another order of magnitude less reactive than magnetite. He et al. (2009) showed that sediments with higher magnetic susceptibility (MS) associated with magnetite abiotically dechlorinated *cis*-1,2- and 1,1-DCE. Several factors have been shown to affect the kinetic reactivity of soils containing these minerals, including their specific mineralogy, their surface area, and the prevailing groundwater chemistry. For example, Butler and Hayes (1998) showed the pH of groundwater affected the rate of abiotic degradation with degradation increasing as the pH increased from 7.1 to 9.5. Ferry et al. (2004) observed abiotic DCE degradation in an aquifer occurring at rates comparable to biodegradation rates observed at other sites, and suggested that these abiotic processes can continue to occur for many years following cessation of active biological treatment.

Lee and Batchelor (2003) observed that the reductive capacity of several minerals, defined by the maximum amount of oxidant that can be reduced, was proportional to the bulk Fe(II) content of the minerals. Interestingly, it was observed that only approximately 1% of Fe(II) was able to reduce PCE, suggesting that not all Fe(II) is available for CE reduction.

Another factor that likely influences the reactivity of reduced iron bearing soils as they oxidize is the transformation from one mineral form to another. For example, the transformation of metastable mackinawite (FeS) to more stable, and less reactive, pyrite (FeS_2) can affect *in situ* CE transformation rates. The rate of this transformation in environmental settings is not well known, but could significantly affect the abiotic degradation of CEs (He et al., 2010). Another example is provided by the work of Lee and Batchelor (2002) who observed that the surface area normalized pseudo first-order decay rates for CEs by green rust, which is a mixed oxidation state iron mineral, was 3.4 to 8.2 times greater than that of pyrite.

Figure 3.10 shows the distribution of bioavailable iron and manganese mineral forms in aquifer material at seven ERB sites: five EVO sites (Dover Air Force Base [DAFB] Areas 5 and 6; Elkton; and Moffett Field Intermediate [Inter] and Deep); and two mulch biowall sites (DAFB Biowalls 1 and 2). Manganese data will be discussed in Section 3.4.2. Bioavailable Fe(II) and Fe(III) are based on 96-hr extractions of homogenized core samples with 0.25 N HCl and 0.25 N hydroxylamine hydrochloride in 0.25 N HCl (HAHCl), respectively (Fuller et al., 1996). Magnetite is not extractable by this method and was estimated from magnetitic susceptibility by the following formula taken from He et al. (2009):

$$\log(Magnetite) = 1.0803 * \log(MS) + 9.7038$$

where magnetite is in mg/kg and MS is mass magnetic susceptibility (m^3/kg).

Upgradient of the injection areas at most of the sites, the aquifer material is a mixture of Fe(II) and Fe(III) minerals. At three of the five EVO sites described above, Fe(III) has been depleted in and around the injection area, while at four of the five EVO sites the aquifer is enriched in Fe(II) and/or magnetite either in the treatment zone or downgradient.

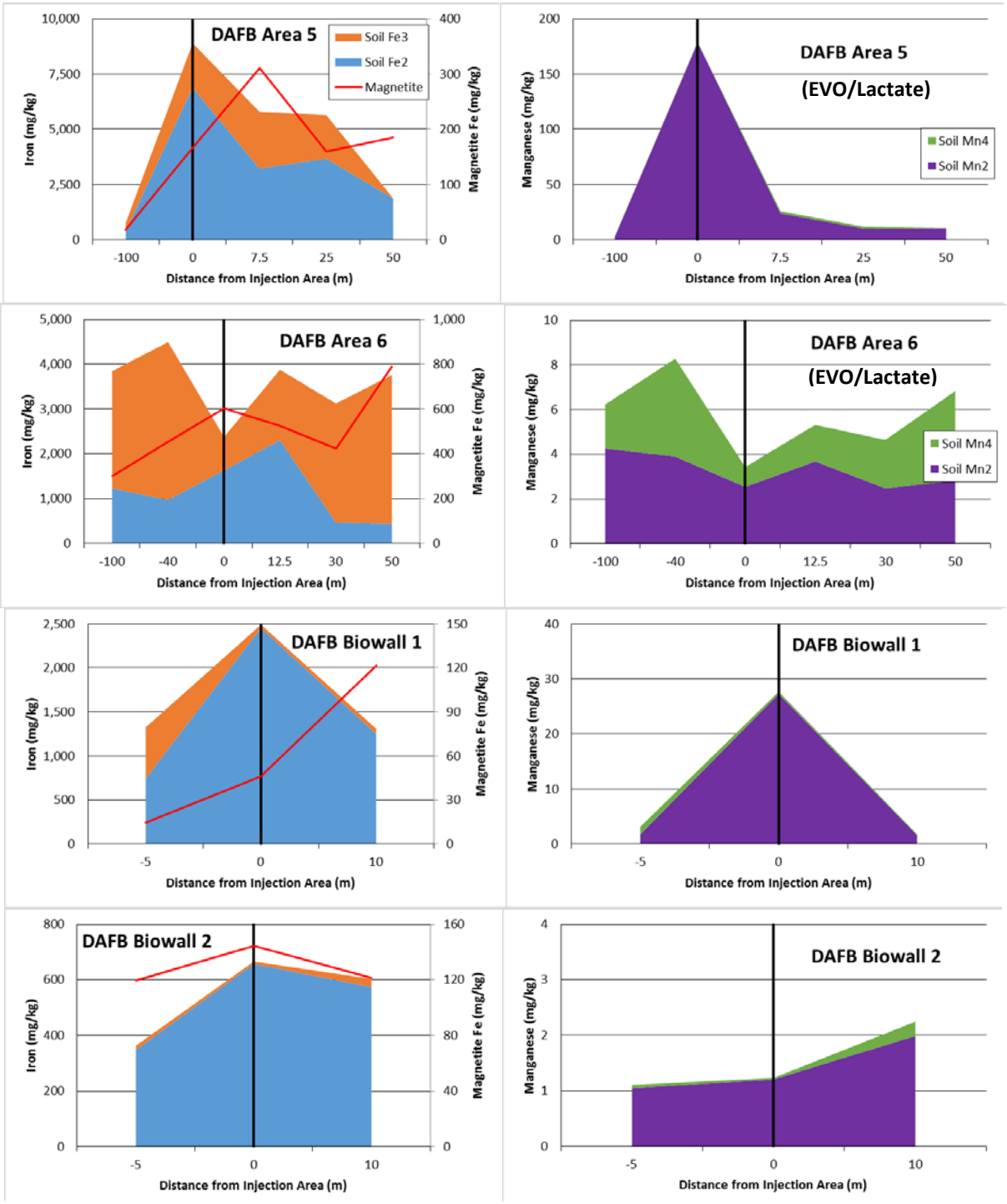

Figure 3.10. Bioavailable Iron and Manganese Concentrations in Sediment at Seven ERB Sites.
Iron mineral concentrations shown on left and manganese forms shown on right. Concentrations are represented by the vertical heights of the color bands.

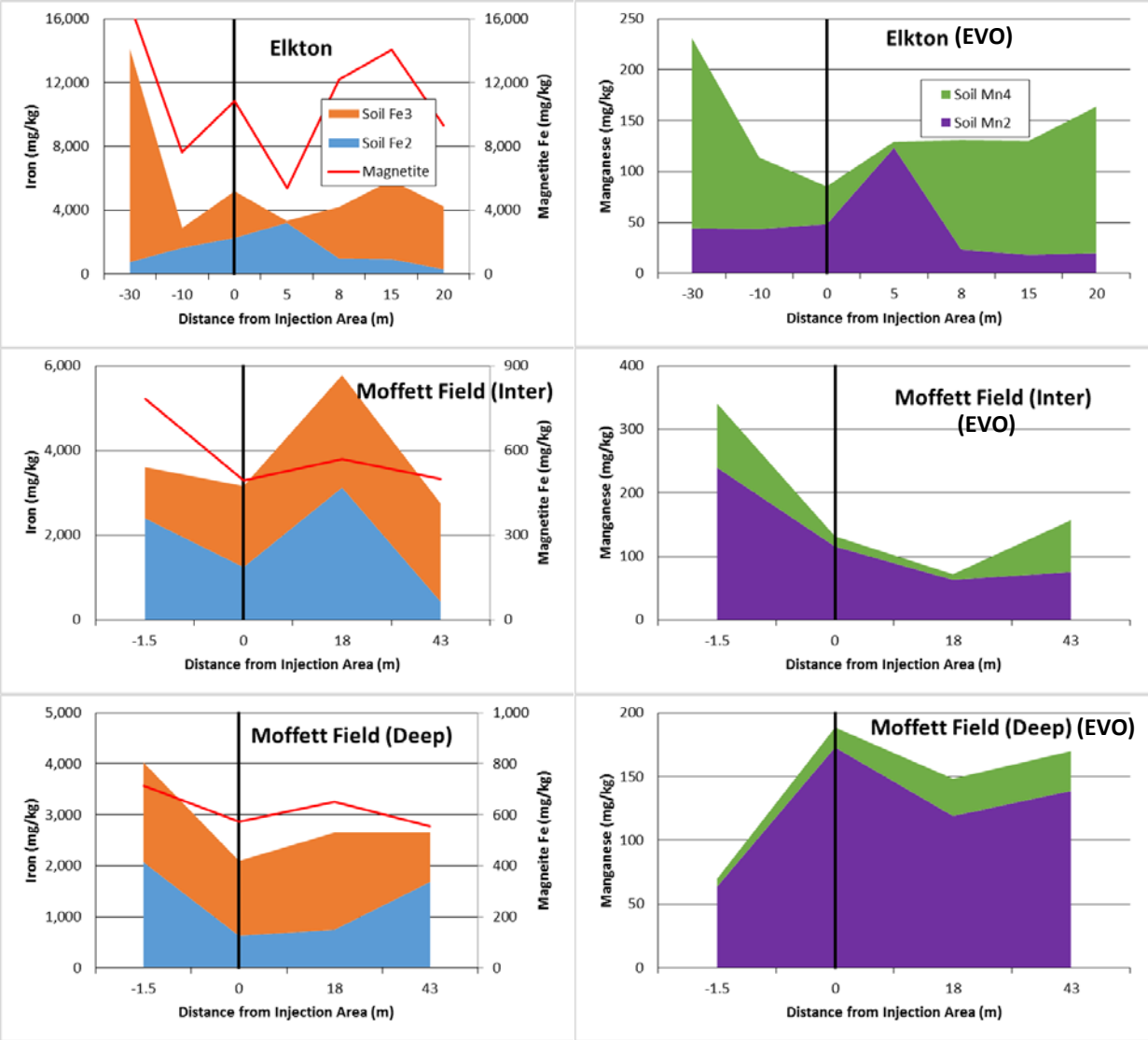

Figure 3.10 (continued). Bioavailable Iron and Manganese Concentrations in Sediment at Seven ERB Sites.
Iron mineral forms shown on left and manganese forms shown on right.

Maximum dissolved iron concentrations observed in upgradient, injection area, and downgradient wells are shown in **Figure 3.11**. All dissolved iron data were from samples collected with a 0.45 µm filter and are presumed to be Fe(II). For reference, the USEPA secondary maximum contaminant level (MCL) of 0.3 mg/L is also shown. Substrate addition during ERB results in large increases in Fe concentrations in injection area wells. The iron concentration ranges for wells 0-10 m downgradient, 10-25 m downgradient, and 25-50 m downgradient are slightly less than the range for injection area wells, and are relatively similar to each other. At 50+ m downgradient, the median increase in dissolved iron (ΔFe) is less than 1 mg/L. This indicates that iron is migrating at rates below the groundwater flow rates because of attenuation reactions with the solids and not being rapidly generated by dissimilatory iron reduction at travel distances over 50 m.

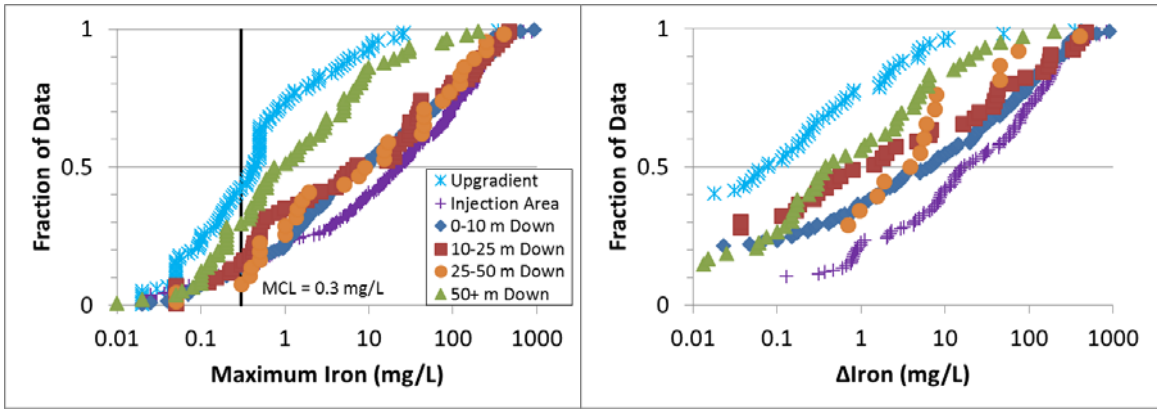

Figure 3.11. Dissolved Iron (Fe) Concentrations Reported in Upgradient, Injection Area, and Downgradient Monitoring Wells.

Compiled data show cumulative frequency distributions for maximum dissolved Fe and difference between maximum and pre-injection value (ΔFe) concentrations in each well.

3.4.2 Manganese

In soils and aquifer sediments, the predominant form of solid-phase Mn is likely Mn(II) in detrital ferrosilicate minerals (Hem, 1985). Based on thermodynamic considerations, weathering reactions in oxic aquifers should produce the Mn(IV) mineral pyrolusite. However, the most commonly observed weathering products are metastable Mn(IV) and Mn(III) hydrous oxides. These minerals are often poorly ordered and characterized by structural defects, domain intergrowths, cation vacancies, and solid solutions (Villalobos et al., 2003). Although present at low concentrations in soils and aquifer sediments (median = 19 mg/kg as Mn; Chen et al., 1999), these minerals are important because they can exist as grain coatings with high reactive surface area despite low bulk concentration. In addition, they can participate in cation exchange reactions and promote abiotic and microbial redox reactions under anaerobic conditions generated during ERB (Villalobos et al., 2003; Tebo et al., 2004).

Dissolved Mn in groundwater can occur at concentrations exceeding 50 mg/L (**Figure 3.12**). Manganese in groundwater is typically assumed to be present as Mn(II), although elevated concentrations of organically complexed Mn(III) have been reported in sediment pore waters (Madison et al., 2013). Dissolved Mn can occur at elevated concentrations even in oxic groundwater, where it would be thermodynamically unstable either as Mn(II) or Mn(III). For example, Mn concentrations exceeding 3 mg/L can persist in groundwater with dissolved oxygen concentrations exceeding 5 mg/L (Savoie et al., 2012).

Manganese in groundwater can be mobilized or immobilized by abiotic and microbial redox reactions and Mn migration is influenced by sorption reactions. For example, Mn(II) can be generated by dissimilatory reduction of Mn(III/IV) hydrous oxides on sediments by microorganisms (Tebo et al., 2004) or by abiotic reduction of these oxides by Fe(II) (Postma and Appelo, 2000). Current thinking is that dissimilatory Mn(IV) reduction is very similar to dissimilatory Fe(III) reduction (Lovley, 1991; 1993). Most microorganisms that reduce Mn(IV) also reduce Fe(III) and *vice versa*. In natural environments, Mn(IV) could be directly reduced by microorganisms.

However, Fe(III) and Mn(IV) reduction could also be coupled where Fe(III) is enzymatically reduced to Fe(II). Mn(IV) would then reoxidize Fe(II) to Fe(III) providing a source of highly reactive electron acceptor for further reduction. Abiotic oxidation of Mn(II) by dissolved oxygen is slow and not likely to be important in groundwater (Morgan, 2005). Both bacteria and fungi can catalyze the oxidation of Mn(II) by dissolved oxygen (Tebo et al., 2004) but whether this occurs in groundwater is unknown. Low concentrations of dissolved salts and alkaline pH values favor sorption of Mn(II) (Bradbury and Baeyans, 1997). Conversely, sorbed Mn(II) can be mobilized by decreases in pH, increases in dissolved salt concentrations, and increases in concentrations of dissolved organic carbon that can complex Mn(II) or Mn(III) (Kent et al., 2002).

Figure 3.10 showed the distribution of bioavailable iron and manganese mineral forms in aquifer material at five EVO sites and two mulch biowall sites. Bioavailable Mn(II) and Mn(III/IV) are based on 96-hr extractions of homogenized core samples with 0.25 N HCl and 0.25 N HAHCl, respectively. Manganese in sediments was present at concentrations 1 to 3 orders of magnitude lower than iron. Trends in manganese concentrations generally mirrored those of iron, with Mn[II] concentrations increasing in or immediately downgradient of the injection area. Three sites (DAFB Area 5, DAFB Biowall 1, DAFB Biowall 2) did not contain Mn(IV) in either upgradient or injection area samples and so there was minimal impact on Mn(II/IV) distribution.

Maximum manganese concentrations at each well in the database are shown in **Figure 3.12**. For reference, the USEPA secondary MCL of 0.05 mg/L is also shown. Manganese concentrations exceeded the secondary MCL at 80% (48 of 61) of upgradient wells, 94% (118 of 125) of injection area wells, and 76% (152 of 201) of downgradient wells. This indicates that native groundwater at many sites prior to ERB already had elevated concentrations of Mn, and, from a regulatory standpoint, ED addition did not greatly alter the number of exceedances downgradient.

Manganese concentrations in injection area wells were significantly elevated compared to upgradient concentrations. At the 10^{th} through 90^{th} percentiles, the injection area concentration was at least one order of magnitude higher than the corresponding upgradient concentration. The range of manganese concentrations generally lessens with increasing distance downgradient, indicating some attenuation of manganese concentrations with transport distance. Although at some sites Mn(II) concentrations at >50 m are nearly as high as the 0-10 m and 10-25 m wells, while the 25-50 m wells only reach values of 1-2 mg/L, this observation is likely an artifact of pooling data from many sites with sparse well coverage. Attenuation in Mn concentrations could occur as a result of sorption reactions or by Mn(II) precipitation with carbonate or oxidation and precipitation as oxides, although the latter process has yet to be demonstrated to occur in groundwater. Moreover, oxidation of Mn(II) back to Mn(III/IV) is very slow unless microbially catalyzed in oxic conditions. The highest downgradient manganese concentrations (e.g., top quintile) were fairly similar to the highest injection area manganese concentrations, even at distances greater than 50 m downgradient implying little attenuation at some sites.

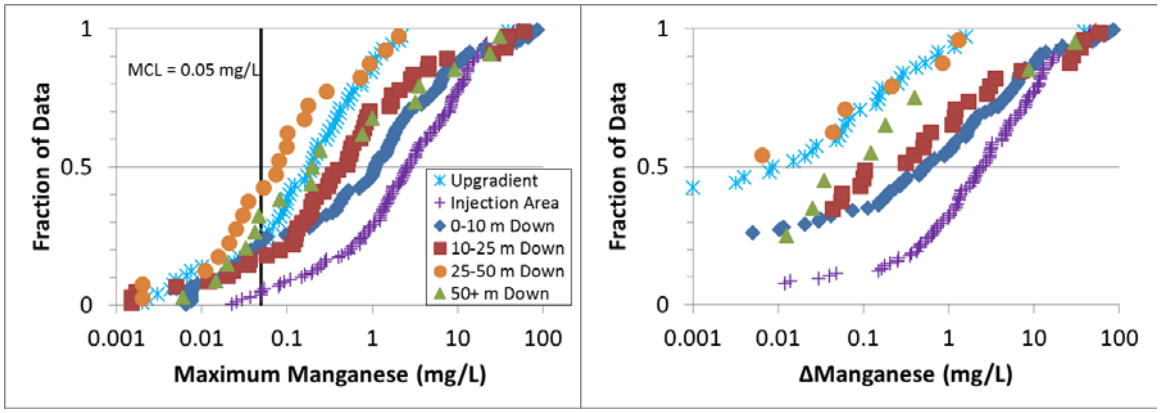

Figure 3.12. Dissolved Manganese (Mn) Concentrations Reported in Upgradient, Injection Area, and Downgradient Monitoring Wells.

Compiled data show cumulative frequency distributions for maximum dissolved Mn and difference between maximum and pre-injection value (ΔMn) concentrations in each well.

3.4.3 Arsenic

Arsenic is naturally present in many aquifers and can result in significant health impacts including skin damage, problems with circulatory systems, and an increased risk of cancer (ATSDR, 2007). Deleterious arsenic effects are not usually acute, but prolonged exposure can result in organ damage, changes in skin pigmentation, hair loss, and cancer or tumors in the lungs, bladder, kidney, and liver.

Increased arsenic levels may be associated with disposal of arsenic wastes including wood preserving chemicals, pesticides, and mining wastes (USEPA, 1997; Korte and Fernando, 1991; Smedley and Kinniburgh, 2002). However, arsenic is naturally present in many aquifers, often sorbed to iron and aluminosilicate minerals (Bose and Sharma, 2002; Kent and Fox, 2004; Pierce and Moore, 1982; Raven et al., 1998; Smedley and Kinniburgh, 2002), including ferric oxyhydroxides. **Figure 3.13** shows regions where the USGS has detected arsenic in at least 25% of the wells or springs sampled. Arsenic is naturally present above the USEPA MCL of 10 µg/L in a number of locations throughout the United States, particularly in the West, Midwest, and northern New England.

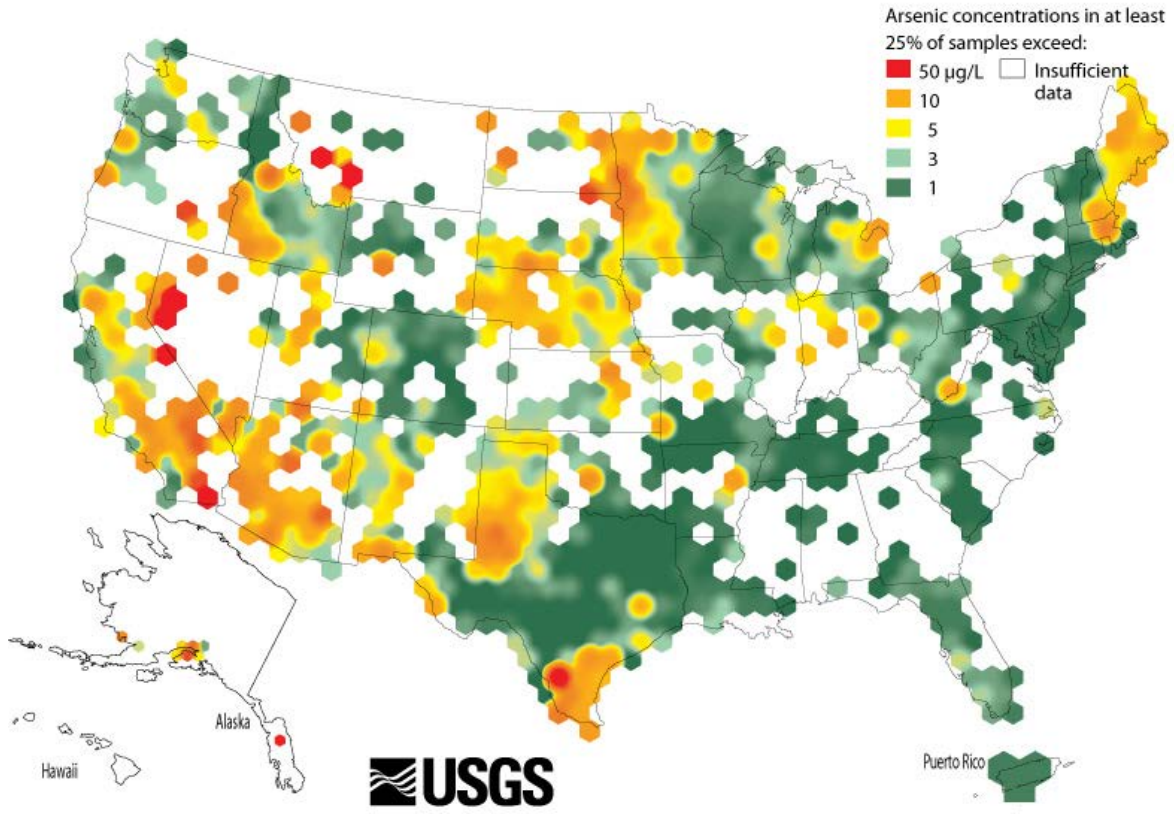

Figure 3.13. Arsenic Concentrations Found in at least 25% of Groundwater Samples within a Moving 50 km Radius.

Data from 31,000 wells and springs sampled by the USGS between 1973 and 2000 (Ryker, 2001).

Figure 3.14 shows the Eh-pH diagram for arsenic for typical conditions that might occur in groundwater. Arsenic is typically present in oxidizing groundwater as arsenate (As[V]) in either the $H_2AsO_4^-$ or $HAsO_4^{2-}$ form, depending on pH. Under mildly reducing conditions, arsenite (As[III]) is present as an uncharged ion ($As(OH)_{3\ (aq)}$). In general, As(III) sorbs less strongly than As(V) on all minerals except Fe(III) oxides and oxyhydroxides (Dzombak and Morel, 1990; Dixit and Hering, 2003), so the arsenic oxidation state can influence mobility. Once reduced, oxidation of aqueous arsenic is a kinetically slow process. However, heterogeneous arsenic oxidation (i.e., oxidation at an iron or manganese mineral surface) is much more rapid. Amorphous Fe(III) oxy-hydroxides have high surface area and high affinity for both arsenic oxidation states (Pierce and Moore, 1982; Smedley and Kinniburgh, 2002). Amorphous ferrihydrite is generally assumed to be the first Fe(III) form to precipitate following oxidation. Thus, if more oxidative conditions are encountered, iron will oxidize and precipitate; arsenic can be removed from the aqueous phase by sorption and/or co-precipitation.

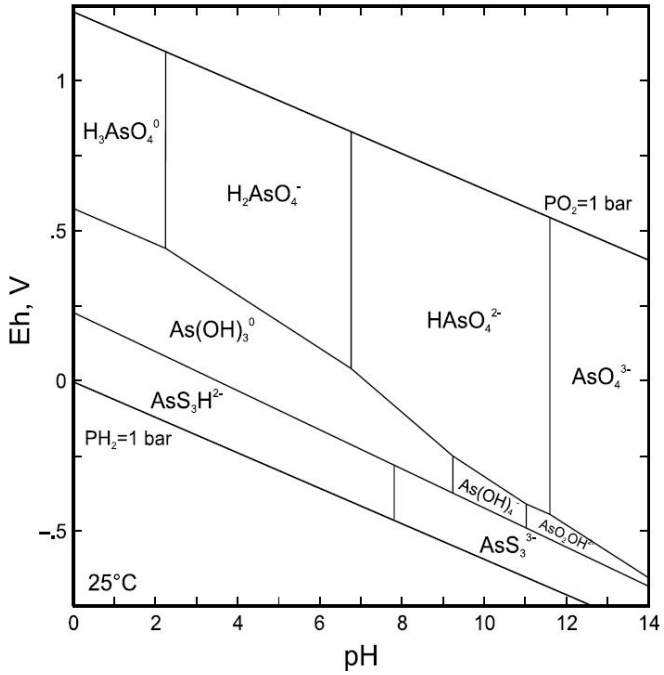

Figure 3.14. Eh-pH Diagrams for Arsenic at 25°C for Coupled Iron- and Sulfate-Reducing Systems.

$\Sigma As=10^{-5}$ and $\Sigma S=10^{-3}$; all solids suppressed to show stability fields for the aqueous species (Ford et al., 2007).

A simple calculation illustrates the potential for groundwater contamination by naturally occurring arsenic. Using a conservative estimate for the average crustal abundance of arsenic in aquifer sediments of 1 mg As/kg sediment and a solid/liquid ratio of 3 kg/L, the concentration of arsenic that would occur upon instantaneous release of all arsenic would be 3000 µg/L. Thus, if only 0.3% of the total arsenic were present as sorbed As(V), and that arsenic were to be mobilized, the groundwater would exceed the drinking water standard. This estimate is likely an upper limit, because the arsenic is not necessarily on the sediment surfaces and available to be mobilized. For comparison, Kent and Fox (2004) found that 25 to 50% of the arsenic in sediments in quartz-dominated sand and gravel aquifer was present as sorbed As(V).

Inputs of elevated concentrations of metabolizable organic compounds promote reduction of As(V) to As(III) and reductive dissolution of Fe(III) oxyhydroxides, resulting in mobilization of arsenic (Harvey et al., 2002; Swartz et al., 2004; Polizzotto et al., 2006). Mobilization of naturally occurring arsenic was also observed to result from input of organic carbon from landfill leachate (Hounslow, 1980). Inputs of organic carbon from land disposal of wastewater on Cape Cod, MA mobilized arsenic in the anoxic, iron-reducing zone by reductive dissolution of aluminum-substituted goethite, dissimilatory reduction of As(V) to As(III), and sorptive competition with wastewater-derived phosphate (Kent and Fox, 2004; Höhn et al., 2006). However, downgradient of the iron-reducing zone, As(III) is oxidized to As(V) by Mn oxides on the sediments, decreasing arsenic concentrations from greater than 10 µg/L to 5 µg/L or lower (Amirbahman et al., 2006).

Maximum arsenic concentrations at each well in the database are shown in **Figure 3.15**. Only about 270 wells or 28% of the database reported values for arsenic, so care should be taken in extrapolating these results to other sites. For reference, the USEPA MCL of 0.01 mg/L is also shown.

Arsenic concentrations at injection area wells were significantly elevated compared to upgradient concentrations. This indicates that electron donor addition often results in an increase in injection area arsenic concentrations. There is also evidence of a decline in arsenic concentrations with distance downgradient from the injection area, indicating either attenuation of arsenic concentrations or diminution in arsenic mobilization processes with transport of the added electron donor downgradient. The arsenic concentration ranges for wells 0-10 m downgradient, 10-25 m downgradient, 25-50 m downgradient, and greater than 50 m downgradient are slightly less than the range for injection area wells, though still substantially elevated compared to upgradient wells. The concentration ranges for the downgradient divisions are fairly similar to each other, though slightly decreasing with distance. For instance, the 50th percentile concentration is 0.014 mg/L for wells 0-10 m downgradient; 0.011 mg/L for wells 10-25 m downgradient; 0.0056 mg/L for wells 25-50 m downgradient; and 0.0056 mg/L for wells greater than 50 m downgradient. Two of six (33%) wells 25-50 m downgradient and 4 of 10 (40%) wells greater than 50 m downgradient contained maximum arsenic concentrations greater than MCLs, compared to 1 of 38 (3%) upgradient wells.

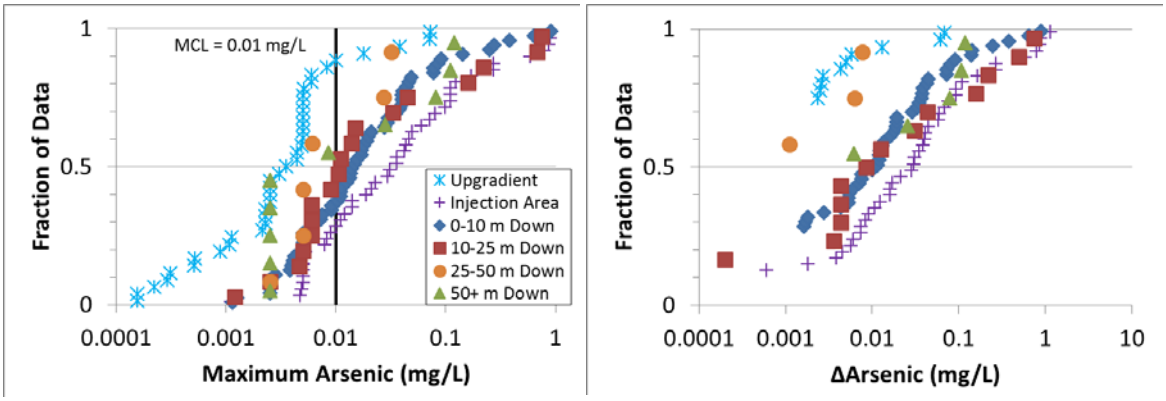

Figure 3.15. Dissolved Arsenic (As) Concentrations Reported in Upgradient, Injection Area, and Downgradient Monitoring Wells.

Compiled data show cumulative frequency distributions for maximum dissolved As and difference between maximum and pre-injection values (ΔAs) in each well.

These data indicate that arsenic mobilization could be a problem at distances greater than 50 m downgradient. However, it should be cautioned that there are very few monitoring points greater than 25 m downgradient (16 in total). In addition, all wells greater than 50 m downgradient are from a single site (Ft Devens, MA). Data from other sites would help verify if arsenic mobilization is an important concern. It should be noted that there is likely some selection bias in sites with arsenic data; that is, arsenic is most often monitored at sites where naturally occurring arsenic is known or expected to be a problem.

3.4.4 Correlation between Dissolved Iron and Arsenic

Figure 3.16 shows dissolved arsenic and dissolved iron concentrations in the same samples collected from injection area (**Figure 3.16a**) and downgradient (**Figure 3.16b**) monitoring wells. Increasing dissolved arsenic concentrations were highly correlated with increasing Fe concentrations ($p<0.01$), consistent with arsenic release during reduction of Fe oxides and/or arsenic removal as Fe is immobilized. It should be noted that Fe(II), As(V), and As(III) participate in sorption reactions, the extent of which depend on chemical conditions. This limits the usefulness of the data compilation for drawing conclusions about specific reactions controlling immobilization of As and Fe(II).

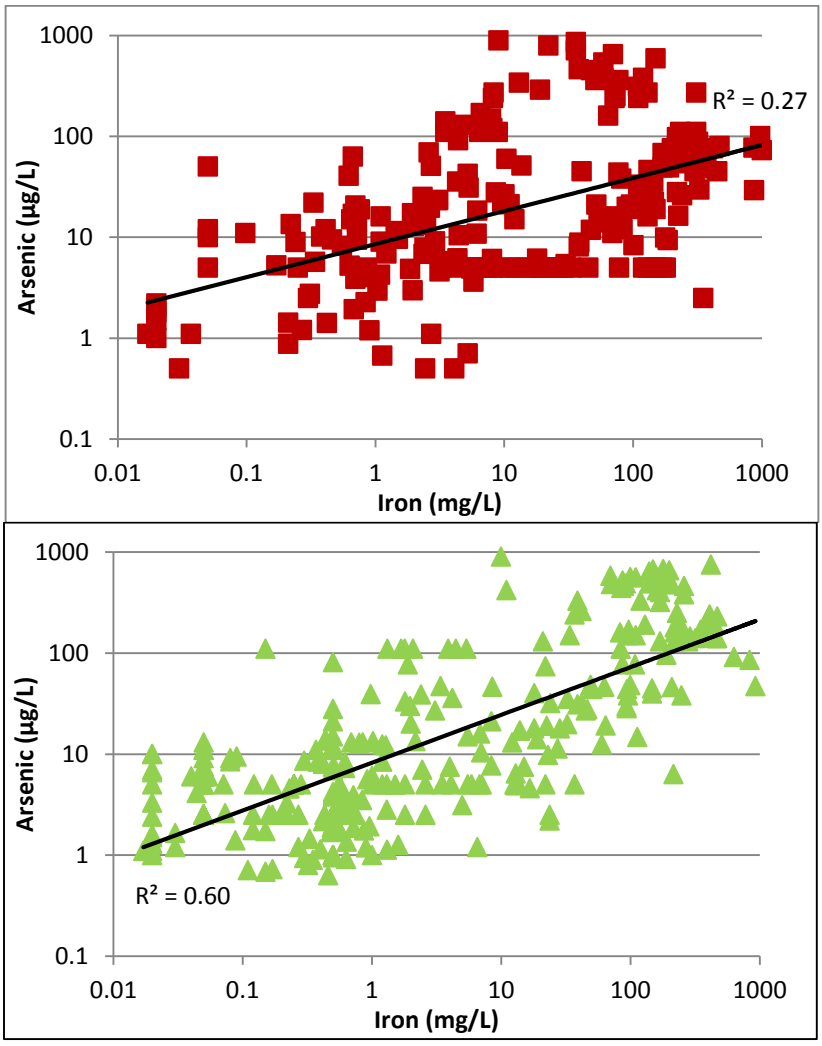

Figure 3.16. Dissolved Arsenic Concentrations vs. Dissolved Iron Concentrations for (a) Injection Area and (b) Downgradient Monitoring Wells.

3.5 METHANE

Methane is a colorless, odorless, non-toxic gas. However, high concentrations of CH_4 can displace oxygen leading to asphyxiation (HSDB, 2012) and can result in an explosion hazard at concentrations above 5% by volume (Coward and Jones, 1931).

CH_4 is produced by bacterial breakdown of organic matter under anaerobic, strongly reducing conditions. Vegetable oil, lactate, acetate, molasses, and other substrates used during ERB can increase CH_4 production (Jacob et al., 2005; Yurovsky et al., 2009; Riis et al., 2007). Methane accumulation in aquifers has been correlated directly to the amount of substrate injected (Molin et al., 2009; Gnabasik et al., 2009; Kruczek and Timmins, 2009). CH_4 is produced from complex organics in a multi-step process where the complex organics are hydrolyzed to simpler organic compounds. These simpler compounds are then fermented to H_2 and acetate, which are then used by methanogens to produce CH_4.

Maximum methane concentrations at each well in the database are shown in **Figure 3.17**. Upgradient methane concentrations were substantially lower than injection area and downgradient concentrations at most percentiles due to methane production following organic carbon addition. Methane concentrations in wells located 0-10 m downgradient were similar to injection area wells. Maximum CH_4 concentrations generally decreased with increasing distance downgradient, with methane concentrations returning to near background levels in wells greater than 100 m downgradient (data not shown). However, there were a significant number of wells at greater than 25 m downgradient with high CH_4 levels (> 10 mg/L), indicating the potential for downgradient migration of dissolved CH_4.

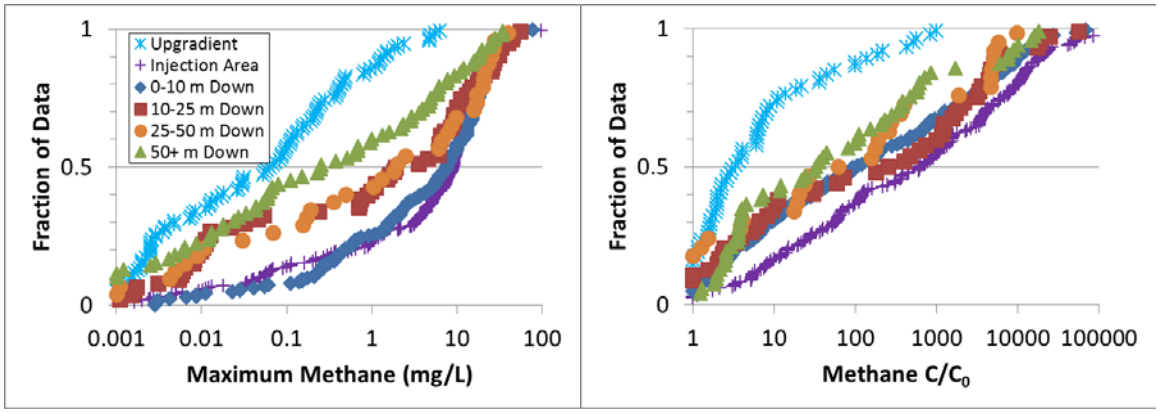

Figure 3.17. Methane (CH_4) Concentrations Reported in Upgradient, Injection Area, and Downgradient Monitoring Wells.

Compiled data show cumulative frequency distributions for maximum CH_4 concentrations and ratio of maximum and pre-injection values (CH_4 C/C_0) in each well.

3.5.1 Methane in the Saturated Zone

Under aerobic conditions, methane can be oxidized to CO_2 and H_2O by methanotrophic microorganisms by the following reaction:

$$CH_4 + 2O_2 \rightarrow CO_2 + 2H_2O$$

However at many ERB sites, aerobic degradation of CH_4 will be limited by an interface that develops between the strongly reducing conditions in water containing methane and the oxygenated background groundwater. The reactive area on the fringes of the plume depends on the cross-sectional area of the treatment zone. Smaller treatment zones provide for greater mixing along the edges of the methane plume. At the Bemidji crude oil site, methane biodegradation occurs within 120 m of the crude oil source by aerobic oxidation at the upper fringe of the plume near the water table.

Anaerobic oxidation of methane (AOM) has been documented using NO_2^- and NO_3^- (Islas-Lima et al. 2004, Raghoebarsing et al., 2006), Mn and Fe oxides (Beal et al., 2009; Crowe et al. 2012) and SO_4^{2-} (Caldwell et al., 2008; Grossman et al., 2002) in sediments from marine-seeps, fresh and brackish wetlands, lakes, drainage ditches, and canals (Boetius et al., 2000; Iversen et al., 1987; Oremland et al., 1987; Reeburgh, 2007, Ettwig et al. 2009). In groundwater, AOM has been linked to denitrification (Smith et al., 1991; Bjerg, 1995; van Breukelen et al., 2003), iron reduction (Amos et al., 2012), and sulfate reduction (Grossman et al. 2002; Williams et al., 1992; van Breukelen & Griffioen, 2004).

While the occurrence of AOM has been extensively documented, the factors controlling the rate and extent of CH_4 attenuation are still poorly understood. The energy yield from AOM using SO_4^{2-} as the terminal electron acceptor is near the threshold required for ATP synthesis (Caldwell et al., 2008). However, energy yields from NO_2^-, NO_3^-, MnO_2 (birnessite), and $Fe(OH)_3$ are much greater (Caldwell et al., 2008; Segarra et al. 2013), potentially supporting larger populations of anaerobic methane oxidizers when these electron acceptors are available.

At present, the significance of AOM in limiting downgradient migration of CH_4 from ERB sites is not well understood. Data from the Bemidji site suggest that AOM using Fe(III) oxyhydroxides is limiting downgradient migration of CH_4 (Amos et al., 2012). Similarly, data from the Norman landfill site indicate that methane oxidation occurs in the anaerobic plume where SO_4^{2-} is the dominant electron acceptor (Grossman et al., 2002). However at some of the sites in the database (**Figure 3.17**), relatively high concentrations of CH_4 were observed over 50 m downgradient of the injection area, suggesting that rates of AOM may not always be sufficient to limit downgradient migration.

3.5.2 Methane in the Unsaturated Zone

Below the water table, CH_4 may form bubbles and degas to the vadose zone when the sum of the partial pressures of N_2, CH_4, CO_2, and other gases exceed the absolute pressure in the aquifer. As a result, methane degassing can be significant, even when methane concentrations are well below concentrations in equilibrium with one atmosphere of CH_4. CH_4 degassing is expected to be less important deeper below the water table due to the increase in water pressure with depth.

Field monitoring at ERB sites has shown that CH_4 levels can be elevated in the headspace of injection area wells. However, CH_4 levels in soil gas measurements collected just below the land surface are typically lower. This is due to diffusive transport of O_2 from the land surface and subsequent oxidation by methanotrophs (Amos et al., 2005). Ma et al. (2012) studied the release and subsequent oxidation of methane in a large sand tank experiment where a 10% ethanol solution was continuously injected 22.5 cm below the water table. Methane concentrations in groundwater reached 20 – 23 mg/L which could release gas with over 80% methane by volume to the vadose zone. However, slow mass transfer of methane through the capillary fringe combined with rapid oxygen transport through the 1.5 m thick vadose zone resulted in rapid oxygen consumption by methanotrophs near the capillary fringe. The maximum methane concentration observed in flux chambers at the land surface was only 21 parts per million by volume (ppmv), a 5-log unit reduction from concentrations observed just below the water table.

Field studies of methane release from petroleum spills also show rapid attenuation in the vadose zone due to aerobic biodegradation. In a study of potential vapor intrusion into a slab-on-grade house overlying a residual petroleum non-aqueous phase liquid (NAPL), Lundegard et al. (2008) observed methane concentrations of 14% at 6 feet below the slab, immediately adjoining the NAPL source area. However, methane concentrations were reduced to below detection at 1.6 feet below the slab. In a study of methane concentrations below a slab-on-grade building at a gasoline service station, Fischer et al. (1996) found that methane concentrations declined from 5.2% at 2 feet to below detection (<0.15%) at 0.7 feet. At an intensively monitored crude oil spill in Bemidji, Minnesota, methane released to the vadose zone migrates upward and is oxidized in a methanotrophic zone midway between the water table and the land surface (Amos et al., 2005).

In an early field demonstration evaluating the use of EVO for ERB at Dover AFB, methane accumulated above the lower explosive limit (LEL) in the headspace of injection wells (TSI and Solutions-IES, 2003). However, methane was reduced to less than 1% of the LEL in three different gas monitoring points located 0.6 to 1.2 feet below ground surface (bgs).

Methane can be released to the land surface or subsurface structures when methane production rates are high and oxygen transport through the vadose zone is restricted. Sihota et al. (2013) observed methane release directly to the land surface from soil impacted by a ~25,000 gallon release of denatured fuel ethanol (DFE) from a multi-railcar derailment. Soils consisted of silty loam and the water table was shallow (< 1 m) with standing water observed over portions of the site. The saturated soil conditions greatly reduced oxygen transfer, limiting methane oxidation. In contrast, there was minimal methane release to the land surface from a large DFE release when the water table was over 2 m bgs in a silty sand aquifer. Based on their field observations and computer modeling, Sihota et al. (2013) concluded that "although the possibility exists for accumulation of CH_4 in confined spaces at concentrations exceeding the LEL of 5 v/v %, a unique set of conditions is required, such as the large DFE release … into low permeability soils with a shallow water table. It is expected that a more typical case would involve the partial or complete oxidation of CH_4 before it is released at the ground surface".

3.6 POTABLE WATER IMPACTS

While SWQIs were detected in downgradient wells, the large majority of these wells were within the primary contaminant plume. At chlorinated ethene sites, only 31 of 380 downgradient wells (8%) did not contain at least one chlorinated ethene (PCE, TCE, cis-1,2-DCE, trans-1,2-DCE, 1,1-DCE , or vinyl chloride) above applicable MCLs. **Figure 3.18** shows the maximum concentrations of TOC, dissolved Mn, dissolved Fe, S^{2-}, and CH_4 at these wells; arsenic was not monitored at any of the wells. The concentrations of these SWQIs were generally within background levels. Where concentrations were much higher than background (e.g., TOC greater than 10 mg/L, CH_4 greater than 0.1 mg/L), these wells were generally located less than 10 m from the injection zone. The production of SWQIs is therefore unlikely to adversely impact potable water supplies.

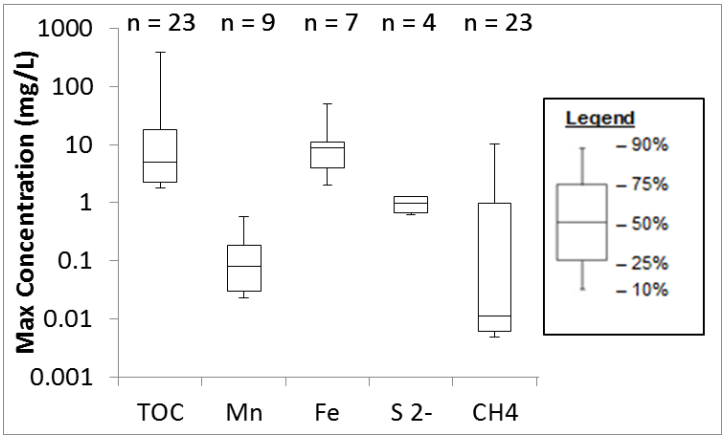

Figure 3.18. Box Plots of Maximum TOC, Dissolved Mn, Dissolved Fe, Dissolved S^{2-}, and Dissolved CH_4 in Wells without a Chlorinated Ethene Above Applicable MCLs.

Concentrations of SWQIs at these wells were generally within background ranges, indicating SWQIs will not further degrade potable water supplies.

4.0 NUMERICAL MODEL OF SWQI PRODUCTION AND ATTENUATION

In this section, the formation and natural attenuation of SWQIs at ERB sites is illustrated using a numerical model developed to simulate the transport and consumption of dissolved organic carbon (DOC) and multiple TEAs. This model employs the partial equilibrium (PE) approach developed by Jakobsen and Postma (1999) and demonstrated by Curtis (2003). This approach assumes that the rate-limiting step is fermentation of DOC (i.e., releasing electron equivalents) and that other TEA reactions occur close to equilibrium. This model implementation is equivalent to organic carbon fully fermenting to H_2 and CO_2 at a determined rate, and then H_2 becoming consumed by multiple aqueous and mineral phase TEA processes controlled by their equilibrium constants. As shown by Curtis (2003), the PE approach has the advantage of avoiding thermodynamically unfavorable reactions and large errors in pH while allowing concomitant redox processes using multiple TEAs (Postma and Jakobsen, 1996; Jakobsen and Postma, 1999; Jakobsen et al., 1998).

4.1 MODEL SETUP

The model was used to simulate the fate of the added organic carbon and how the reduced products affected the aquifer over a period of 40 years following addition of EVO to form a PRB. The model domain is a two-dimensional cross-section of a water table aquifer extending 12 m vertically and 520 m horizontally. The active reaction zone examined with the model extends 260 m in the direction of flow. The barrier was represented as a 6 m deep by 15 m long by 65 m wide zone containing a total of 4,800 kiloequivalents (keq) of soybean oil ($C_{56}H_{100}O_6$) evenly distributed in the treatment zone (206 kg per meter barrier width). Soybean oil dissolution was simulated as a first-order process so that 77% of the residual soybean oil was released to groundwater as DOC in 6.9 years. This scenario results in essentially all of the soybean oil being dissolved in 22 years.

DOC degrades by releasing electrons that react with TCE and also with other TEAs including O_2, sediment Mn(IV), sediment Fe(III), SO_4^{2-}, and CO_2, producing CH_4. The reaction between released electrons and TEAs was simulated as an equilibrium reaction. The rate of DOC consumption (r_1) was simulated as

$$r_1 = -k_1 * C_{DOC} - k_2 * C_{DOC} * C_{TCE}$$

where

C_{DOC} = DOC concentration (mM)
C_{TCE} = TCE concentration (mM)
k_1 = 1st order DOC decay rate
k_2 = 2nd order DOC and TCE decay rate

In the partial equilibrium framework, Fe[III] is treated as an equilibrium phase mineral. Dissolution of amorphous $Fe(OH)_3$ and goethite (FeOOH) occur by the reactions:

$$Fe(OH)_3 + 3H^+ \leftrightarrow Fe^{3+} + 3H_2O \qquad pK_{SP} = 4.9$$

and

$$FeOOH + 3H^+ \leftrightarrow Fe^{3+} + 2\,H_2O \qquad pK_{SP} = -1.0$$

At many sites, Fe(III) will be present as mixtures of amorphous $Fe(OH)_3$, goethite, and other minerals. As a result, the effective solubility product (pK_{SP}) for Fe(III) in any aquifer is unknown, but is expected to be somewhere between 4.9 and -1.0, values representative of readily dissolved and more stable Fe oxide forms respectively. A pK_{SP} value of 0.239 was used in this simulation based on model calibration results from the Bemidji site and evidence from numerous ERB sites of simultaneous iron reduction and methanogenesis, which does not occur when higher dissolution pK_{SP} values are applied. Dissolved Fe(II) and Mn(II) were assumed to undergo cation exchange with sediments and precipitation as siderite ($FeCO_3$) and rhodochrosite ($MnCO_3$). Magnetite precipitation was not considered in these simulations based on limited magnetite production at Bemidji.

CH_4 produced by fermentation coupled to methanogenic degradation initially enters the dissolved phase. Once the sum of partial pressures of all dissolved gasses ($P_{CH4} + P_{CO2} + P_{N2}$) reaches hydrostatic pressure, CH_4 and other gases are assumed to degas to the vadose zone. In the field, degassing is expected to occur in relatively coarse grained sediments where the gas bubbles can migrate upward through the sediment pores. In finer grained sediment, CH_4 bubbles can remain trapped within the pores by capillary forces. Once methane production slows, the CH_4 in these trapped bubbles could potentially dissolve back into groundwater and be carried downgradient with ambient groundwater flow. In the simulations presented here, all excess CH_4 is degassed and there are no trapped bubbles that redissolve or limit flow.

The model was run for a total of 40 years. The added soybean oil is depleted in 22 years so most of the SWQIs are produced during the 0–22 year period and then during the 22–40 year period the aquifer plume continues to evolve and slowly recover. The initial water and aquifer chemistry for the model is based roughly on that of the Bemidji crude oil spill site (**Table 4.1**). The model is homogeneous and isotropic with the groundwater flow velocity set to 0.06 m/day.

Table 4.1. Initial Condition and Background Concentrations [mM] of Inorganic Aqueous Species and Sediment Electron Acceptors.

	Concentration (mM)		**Concentration (mM)**
DIC (1 mM = 12 mg/L)	3.65	CH_4 (1 mM = 16 mg/L)	0.0
Ca^{2+} (1 mM Ca = 40 mg/L)	1.24	Cl^- (1 mM = 35 mg/L)	0.31
Fe^{2+} (1 mM = 56 mg/L)	5.1E-21	Mg^{2+} (1 mM = 24 mg/L)	0.59
Na^+ (1 mM = 23 mg/L)	0.077	O_2 (1 mM = 32 mg/L)	0.25
Mn^{2+} (1 mM = 55 mg/L)	0	SO_4^{2-} (1 mM = 96 mg/L)	1.56
pH	7.6	N_2 (inert) (1 mM = 28 mg/L)	0.45
Sediment Fe[III] (bioavailable)	0.98 g/kg	pe	14.3
Cation Exchange Capacity (CEC)	47.5 mM/L aquifer volume	Sediment Mn[IV]	0.03 g/kg

4.2 MODEL RESULTS

The model results are displayed in **Figures 4.1** and **4.2** as snapshots of the plume after 5, 15, and 30 years. The time point at 5 years was chosen to display the SWQI plume that develops as a result of the ERB emplacement. The 15-year figure displays conditions when the soybean oil is almost exhausted. At this time, the migration of the SWQI plume is apparent, but the waning of the soybean oil source is also clear, especially near the treatment zone. The final time point of 30 years is used to convey the progress of the recovery of the aquifer from the reduced conditions created by the remediation.

Figure 4.1 shows the spatial distribution of DOC, dissolved oxygen (DO), pH, SO_4, and CH_4 at 5, 15 and 30 years. The assumed first order dissolution rate for residual soybean oil results in 65% being dissolved by 5 years and consumption of all the soybean oil after 22 years. Significant concentrations of DOC are restricted to the area containing residual soybean oil, so CH_4 production is also restricted to this area.

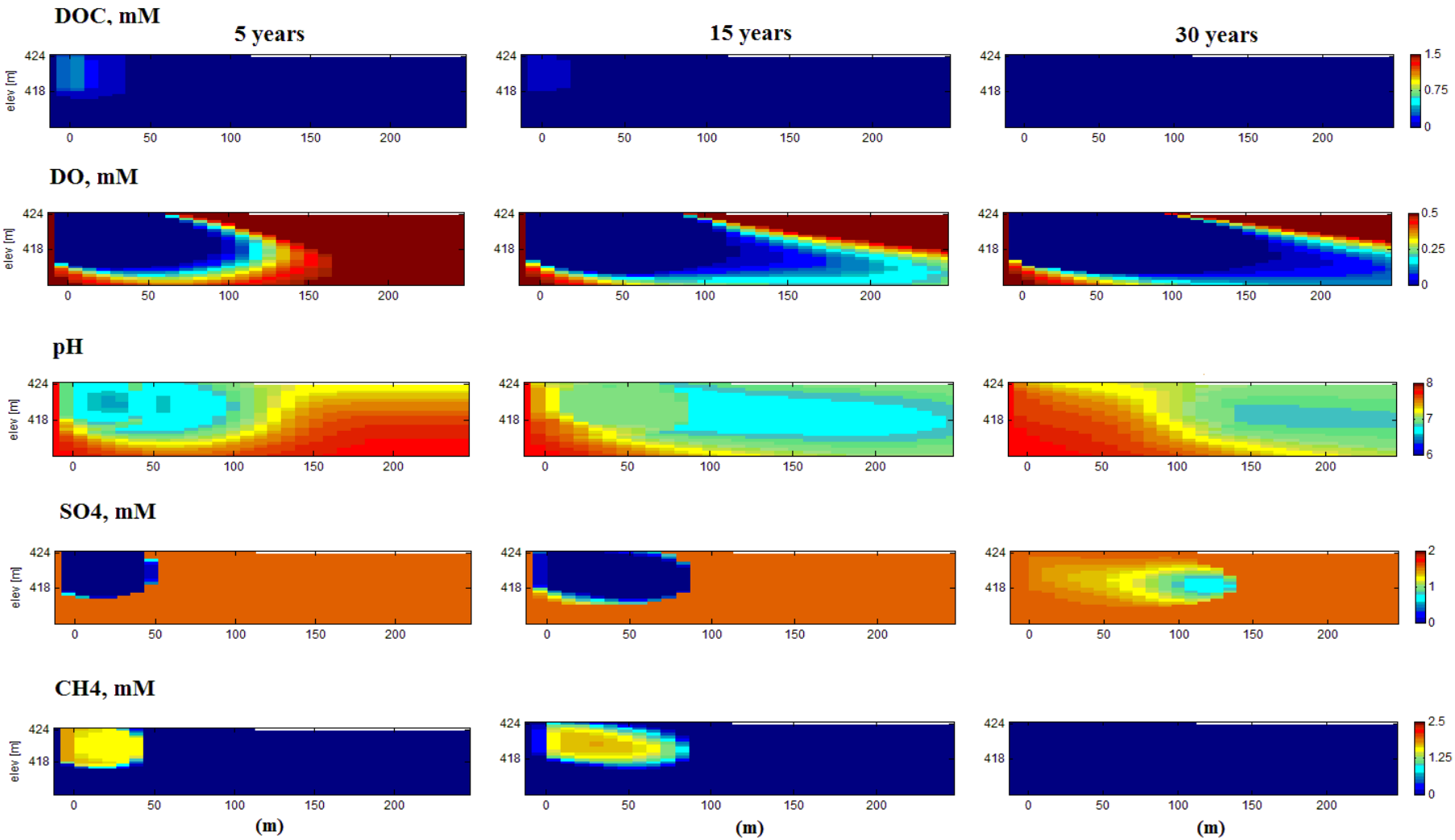

Figure 4.1. Simulated Dissolved Organic Carbon (DOC), Dissolved Oxygen (DO), pH, Sulfate (SO_4^{2-}) and Dissolved Methane (CH_4) Concentrations at 5, 15, and 30 Years after Substrate Addition.

DOC, DO, SO_4^{2-}, and CH_4 concentrations are in units of mM.

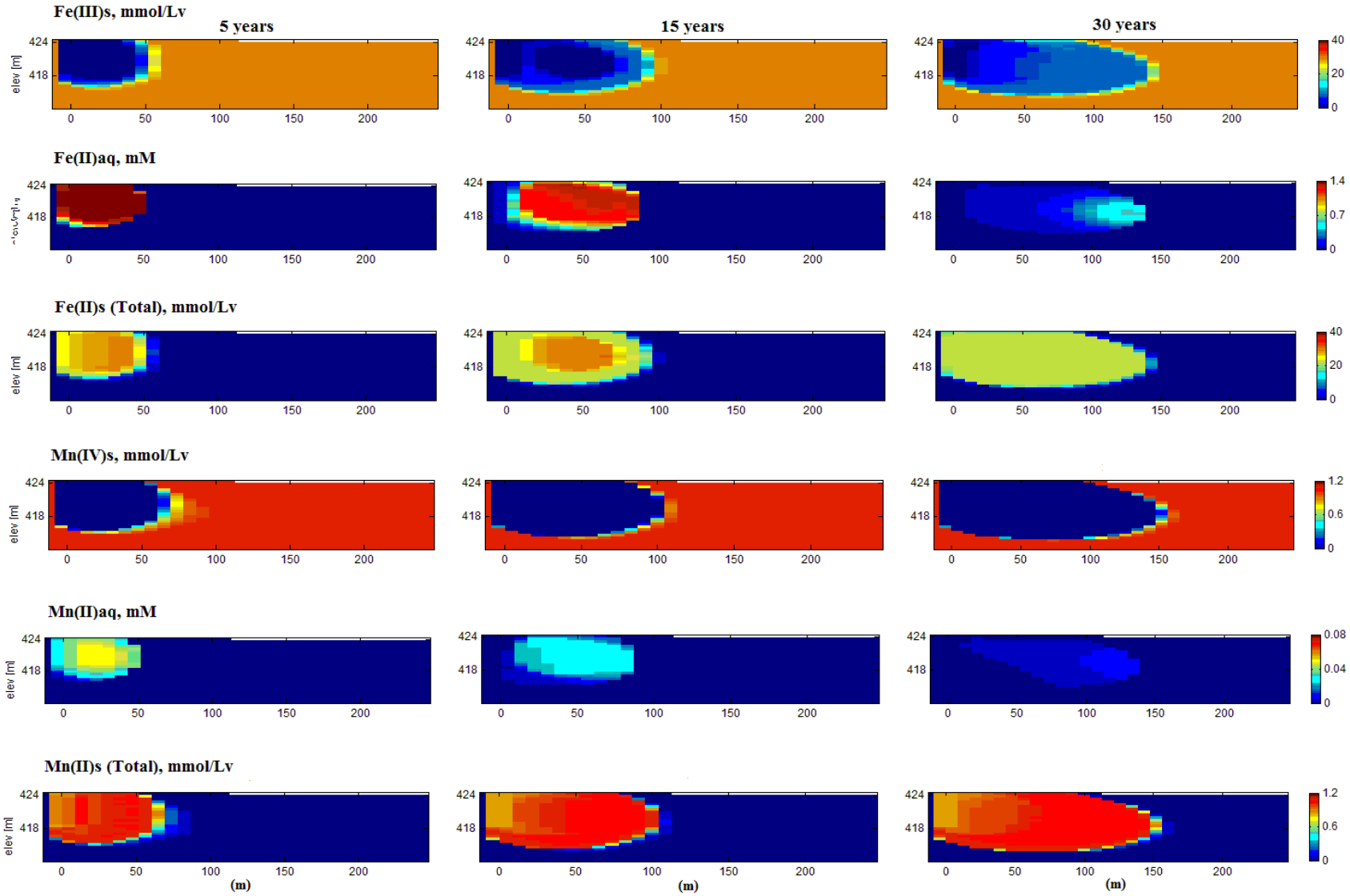

Figure 4.2. Simulated Sediment Fe[III], Dissolved Fe^{2+}, Sediment Fe(II), Sediment Mn(IV), Dissolved Mn^{2+}, and Sediment Mn(II) at 5, 15, and 30 years after Substrate Addition.

Fe^{2+} and Mn^{2+} concentrations are in units of mM. Sediment Fe(III), Fe(II), Mn(IV), and Mn(II) concentrations are in units of mmol per liter aquifer volume.

A plume of depleted O_2 extends over 100 m from the treatment zone by 5 years and at 15 years extends beyond 250 m. Although recovery of the aquifer begins at 22 years, increased O_2 is visible only at the base and top of the model plume at 30 years. The slow recovery of O_2 is due to the large reservoir of sorbed Fe(II) on the sediments that consumes O_2 transported from upgradient. In sulfate-rich aquifers FeS may form but is not expected to slow recovery because the mineral surface becomes oxidized restricts further oxidation of the underlying FeS. A similar slow recovery of an aquifer has been observed at the Cape Cod research site where treated wastewater entered the aquifer through infiltration beds for 56 years (Repert et al., 2006). While NO_3^- was not included in the model simulation, NO_3^- is expected to behave similarly to O_2 with slow recovery until the soybean oil and Fe(II) are depleted.

A plume of slightly lower pH water migrates from the source zone. After 5 years the pH plume extends over 100 m from the source, and at 15 years it extends beyond 250 m. Slightly higher pH values can be seen in the iron-reducing zone due to consumption of protons by the reaction of DOC oxidation coupled to iron reduction. The 30-year time point shows that once the soybean oil source is exhausted, pH in the aquifer recovers as clean groundwater moves in from upgradient. Note that the simulated pH changes are less than one unit and may not be detectable in typical monitoring programs because of the sparse coverage of monitoring wells. The pH is buffered by excess calcite and cation exchange of H^+ with aquifer minerals. More details on the reactions controlling pH can be found in Ng et al. (2015).

Immediately after addition of the soybean oil, SO_4^{2-} is depleted within the source zone. The zone of depleted SO_4 extends approximately 50 m from the source zone after 5 years and approximately 75 m from the source zone after 15 years. Lower SO_4^{2-} concentrations are observed up to approximately 140 m downgradient after 30 years; however, these levels are not as depleted as those closer to the injection area in earlier time periods. In addition, after 30 years, SO_4^{2-} concentrations in and around the source area began to recover as upgradient, sulfate-rich groundwater fluxes into the area. Recovery of SO_4^{2-} is much faster than O_2 since much more strongly reducing conditions are required for sulfate reduction.

Methane production begins immediately after emplacement of the soybean oil and by 5 years a methane plume extends over 50 m from the source. By this time, the total gas pressure in the treatment zone has exceeded hydrostatic pressure and outgassing has started. By 15 years, the dissolved methane plume extends almost 100 m from the source. The early establishment of anaerobic conditions in the aquifer after the start of treatment restricts aerobic methane oxidation to small areas on the fringe of the plume. Even after all the soybean oil has been depleted, CH_4 consumption with oxygen is limited to a zone of low O_2 and low CH_4 that separates these two plumes.

In this simulation, methane is assumed to be capable of driving reduction of sediment Fe(III) based on field monitoring results at the Bemidji site. If this occurs, then iron reduction will be the main process limiting the growth of the dissolved CH_4 plume. However, if adapted microorganisms capable of reducing Fe(III) using CH_4 are not present, dissolved CH_4 will migrate downgradient with little attenuation beyond dispersive mixing. Once the primary organic substrate (soybean oil) is exhausted, CH_4 production stops. If essentially all of the gaseous CH_4 has been released to the vadose zone, dissolved CH_4 concentrations are expected to decline relatively quickly.

However, if significant amounts of gaseous CH_4 are trapped below the water table, dissolution of these trapped bubbles could maintain the dissolved CH_4 plume for some time.

Dissolved Fe^{2+} and Mn^{2+} and sediment Fe(III), Fe(II), Mn(IV) and Mn(II) are shown in **Figure 4.2**. Sediment Fe(II) and Mn(II) includes both material attached to cation exchange sites on the sediment surfaces and material precipitated as carbonate minerals (siderite and rhodochrosite).

After 5 years, much of the sediment Fe(III) is depleted in the source zone, releasing dissolved Fe^{2+} to the aqueous phase. However, downgradient migration of dissolved Fe^{2+} is delayed behind the low O_2 plume by cation exchange to the sediments. Dissolved Fe^{2+} concentrations reach 1 mM while sediment Fe(II) reaches ~ 30 mM showing that most of the reduced iron is bound to the sediment. Over time, the simulated zone of depleted sediment Fe(III) grows since the model assumes these minerals can be reduced by dissolved CH_4. After all of the DOC has degraded, the large reservoir of sorbed Fe(II) remains steady and does not readily desorb. At 30 years, the recovery of the aquifer is apparent as the dissolved Fe(II) plume disperses and siderite redissolves, but these two forms make up a relatively small fraction of the total reduced Fe. As clean aerobic groundwater enters from upgradient, Fe(II) desorbs from the sediment, mixes with O_2, and re-precipitates as Fe(III). During the 40-year simulation, about 25% of bioavailable Fe(III) in the 520-m model domain is reduced, but the percentage is far higher in the injection zone (~90%).

Overall, Mn behaves similarly to Fe with Mn(IV) reduced to dissolved Mn^{2+} in the source area, and downgradient migration of Mn^{2+} limited by cation exchange on the sediments. The total amount of Mn(II) produced is much lower than Fe(II) due to the much lower amount of Mn(IV) originally present in the sediment. This is consistent with results from the SWQI database which show Mn^{2+} levels are often significantly lower than Fe^{2+}. The zone of depleted Mn(IV) is projected to grow more rapidly than the Fe(III) depleted zone because Mn can be reduced under relatively more oxidizing conditions than Fe. Similar to Fe, downgradient migration of dissolved Mn^{2+} is limited by cation exchange to the sediments and the dissolved Mn^{2+} dissipates once the soybean oil is depleted.

Figure 4.3 shows the distribution of electron (e^-) equivalents released over time in the entire model domain as soybean oil dissolves releasing DOC, which is then fermented reducing TCE, O_2, Mn, Fe, SO_4^{2-}, and producing CH_4. Over the first 15 years, the very large majority of e^- equivalents are used to reduce Fe(III) to Fe(II), SO_4^{2-} to S^{2-}, and CO_2 to CH_4. Overall, electrons consumed in O_2, Mn, and TCE reduction are minor contributors to the electron balance. After 22 years, the fraction of e^- equivalents associated with CH_4 reduction declines slightly with a tiny increase in Fe(II) as CH_4 reduces Fe(III) in the downgradient aquifer. As discussed above, reduction of Fe(III) by CH_4 depends on the presence of specialized microorganisms that facilitate this process and probably does not occur at some sites.

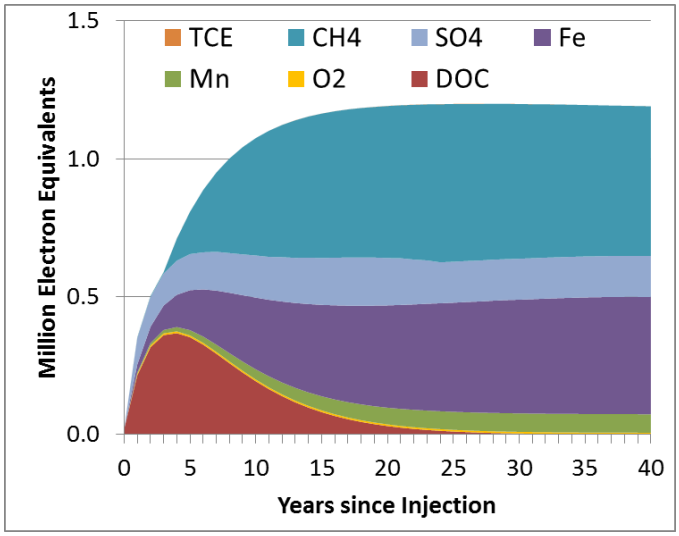

Figure 4.3. Simulated Distribution of Cumulative Electron Equivalents over Time Following Soybean Oil Addition to Stimulate ERB.

The contributions of the electron acceptors are represented by the vertical heights of their color bands at each time. Electron equivalents are calculated over the first 250 m downgradient of the injection point. Although TCE is present, the electron equivalents are too low to be visible on the scale of the plot.

In summary, iron reduction and methanogenesis are expected to be major electron sinks in many aquifers. In aquifers with high levels of SO_4^{2-}, sulfate reduction will also be a major sink. Much of the Fe(II) and Mn(II) produced is expected to remain immobilized on the aquifer material and is not expected to migrate long distances downgradient. Similarly, essentially all of the sulfide will precipitate with available metals with little to no sulfide migration downgradient. If appropriate microorganisms are present, reduction of Fe(III) can limit the downgradient migration of dissolved CH_4. However, these organisms may not be present, resulting in dissolved CH_4 migrating substantial distances downgradient. Once the fermentable organic carbon is depleted, CH_4 production will stop and the dissolved CH_4 plume is expected to dissipate.

However, the data mining and numerical modeling performed during this project make it clear that recovery of the aquifer to fully aerobic conditions is likely to be a very slow process. The aquifer impacted by an injected electron donor is expected to have secondary impacts that can restrict its use as drinking water for many years, due primarily to the large amount of reduced Fe(II) retained on the aquifer material.

5.0 REFERENCES

AFCEE (Air Force Center for Engineering and the Environment), NFESC (Naval Facilities Engineering Service Center), ESTCP (Environmental Security Technology Certification Program), 2004. Principles and Practices of Enhanced Anaerobic Bioremediation of Chlorinated Solvents. Prepared by Parsons Infrastructure & Technology Group, Inc., Denver, CO, USA.

Air Force Center for Environmental Excellence (AFCEE), 2008. Workshop on *In Situ* Biogeochemical Transformation of Chlorinated Solvents, February 2008.

Albrechtsen, H.-J., Heron, G. and Christensen, T. H., 1995. Limiting factors for microbial Fe(III)-reduction in a landfill leachate polluted aquifer (Vejen, Denmark). FEMS Microbiology Ecology 16: 233-248.

Amirbahman A., Kent, D. B., Curtis, G. P. and Davis, J. A., 2006. Kinetics of Sorption and Abiotic Oxidation of Arsenic(III) by Aquifer Materials. Geochim et Cosmochim Acta 70(3): 533-547.

Amos, R. T., Mayer, K. U., Bekins, B. A., Delin, G. N. and Williams, R. L., 2005. Use of dissolved and vapor-phase gases to investigate methanogenic degradation of petroleum hydrocarbon contamination in the subsurface. Water Resources Research, v. 41, no. 2.

Amos, R. T., Bekins, B. A., Cozzarelli, I. M., Voytek, M. A., Kirshtein, J. D., Jones, E. J. P. and Blowes, D.W., 2012. Evidence for iron-mediated anaerobic methane oxidation in a crude oil-contaminated aquifer. Geobiology 10(6): 506-517.

ATSDR, 2007. Toxicological Profile for Arsenic. Agency for Toxic Substances and Disease Registry (ATSDR), Atlanta, GA.

Baeyans, B. and Bradbury, M. H., 1997. A mechansitic description of Ni and Zn sorption on Na-montmorillonite Part I: Titration and sorption measurements. J. Contam. Hydrol. 27: 199-122.

Beal, E. J., House, C. H. and Orphan, V. J., 2009. Manganese- and iron-dependent marine methane oxidation. Science 325(5937): 184-187.

Bjerg, P.L., 1995. Distribution of redox-sensitive groundwater quality parameters downgradient of a landfill (Grindsted, Denmark). Environ. Sci. & Technol. 29: 1387–1394.

Bethke C. M., Sanford R. A., Kirk M. F., Jin Q. and Flynn T. M., 2011. The thermodynamic ladder in geomicrobiology. Am. J. Sci. 311: 183-210.

Boetius, A., Ravenschlag, K., Schubert, C. J., Rickert, D., Widdel, F., Gieseke, A., Amann, R., Jorgensen, B. B., Witte, U. and Pfannkuche, O., 2000. A marine microbial consortium apparently mediating anaerobic oxidation of methane. Nature 407(6804): 623-626.

Bose, P. and Sharma, A., 2002. Role of Iron in Controlling Speciation and Mobilization of Arsenic in Subsurface Environment. Water Research 36: 4916-4926.

Boyd, S. A., Shelton, D. R., Berry, D. and Tiedje, J. M., 1983. Anaerobic biodegradation of phenolic compounds in digested sludge. Appl. Environ. Microbiol. 36:50-53.

Bradbury, M. H. and Baeyans, B., 1997. A mechansitic description of Ni and Zn sorption on Na-montmorillonite Part II: modelling. J. Contam. Hydrol. 27: 223-248.

Butler, E. C. and Hayes, K. F., 1998. Effects of solution composition and pH on the reductive dechlorination of hexachloroethane by iron sulfide. Environ. Sci. Technol. 32: 1276-1284.

Caldwell, S. L., Laidler, J. R., Brewer, E. ., Eberly, J. O., Sandborgh, S. C., and Colwell, F. S., 2008. Anaerobic oxidation of methane: Mechanisms, bioenergetics, and the ecology of associated microorganisms. Environ. Sci. Technol. 42(18): 6791-6799.

Chen, M., Ma, L. Q. and Harris, W. G., 1999. Baseline Concentrations of 15 Trace Elements in Florida Surface Soils. J. Environ. Qual. 4: 1173-1181.

Colberg, P.J., 1988. Anaerobic microbial degradation of cellulose, lignin, oligolignols, and monoaromatic lignin derivatives. *In:* A. J. B. Zehnder (ed.), Biology of Anaerobic Microorganisms. John Wiley & Sons: New York, 1988; pp. 333-372.

Coward, M. F. and Jones, G. W., 1931. Limits of inflammability of gases and vapors. U.S. Bureau of Mines Bulletin, 279.

Cozzarelli, I. M., Herman, J. S., Baedecker, M. J. and Fischer, J. M., 1999. Geochemical heterogeneity of a gasoline-contaminated aquifer. J. Contam. Hydrol. 40(3): 261-284.

Crowe, S. A., Katsev, S., Leslie, K., Sturm, A., Magen, C., Nomosatryo, S., Pack, M. A., Kessler, J. D., Reeburgh, W. S., Roberts, J. A., Gonzalez, L., Haffner, G. D., Mucci, A., Sundby, B., and Fowle, D. A., 2011. The methane cycle in ferruginous Lake Matano. Geobiology 9(1): 61-78.

Curtis, G.P., 2003. Comparison of Approaches for Simulating Reactive Solute Transport Involving Organic Degradation Reactions by Multiple Terminal Electron Acceptors. Computers and Geosciences 29: 319-329.

Davis, J. A., Coston, J. A., Kent, D. B., and Fuller, C. C., 1998. Application of the surface complexation concept to complex mineral assemblages. Environ. Sci. Technol. 32(19), 2820-2828.

Davis, J. A. and Kent, D. B., 1990. Surface Complexation Modeling in Aqueous Geochemistry. *In:* M.F. Hochella and A.F. White (eds.), Mineral-Water Interface Geochemistry. Washington DC. Mineralogical Society of America, pp. 177-260.

Dixit S. and Hering J. G., 2003. Comparison of Arsenic(V) and Arsenic(III) Sorption onto Iron Oxide Minerals: Implications for Arsenic Mobility. Environ. Sci. Technol. 37: 4182-4189.

Dixit S. and Hering J. G., 2006. Sorption of Fe(II) and As(III) on goethite in single- and dual-sorbate systems. Chemical Geology 228: 6-15.

Dzombak, D.A., and Morel, F.M.M., 1990. Surface Complexation Modeling: Hydrous Ferric Oxide, Wiley, New York, 393 p.

Eaddy, A., 2008. Scale-Up and Characterization of an Enrichment Culture for Bioaugmentation of the P-Area Chlorinated Ethene Plume at the Savannah River Site; M.S. Thesis; Clemson University: Clemson, 2008.

Edwards, E. A., Wills, L. E., Reinhard, M. and Grbić –Galić, D., 1992. Anaerobic Degradation of Toluene and Xylene by Aquifer Microorganisms under Sulfate-Reducing Conditions. Appl. Environ. Microbiol. 58(3): 794-800.

Earth Science Services (ESS), 2004. Final Report, Field Test of Biogeochemical Reductive Dechlorination at Dover Air Force Base, Dover, Delaware.

ESTCP, 2006. Protocol for Enhanced *In Situ* Bioremediation Using Emulsified Edible Oil. Project ER-200221. ESTCP, Arlington, VA, USA. Prepared by Solutions-IES. http://www.serdp.org. Accessed September 14, 2013.

Ettwig K.F., Van Alen T., Van De Pas-Schoonen K.T., Jetten M.S.M., Strous M., 2009. Enrichment and molecular detection of denitrifying methanotrophic bacteria of the NC10 phylum. Applied Environ. Micro. 75: 3656–3662.

Ferry, M.L., R.T. Wilkin, R.G. Ford, J.T. Wilson, 2004. Nonbiological removal of *cis*-dichloroethylene in aquifer sediment containing magnetite. Environ. Sci. Technol. 38:1746-1752.

Fischer, M. L., Bentley, A. J., Dunkin, K. A., Hodgson, A. T., Nazaroff, W. W., Sextro, R. G. and Daisey, J. M., 1996. Factors affecting indoor air concentrations of volatile organic compounds at a site of subsurface gasoline contamination. Environ. Sci. Technol. 30: 2948–2957.

Ford, R. G., 2002. Rates of Hydrous Ferric Oxide Crystallization and the Influence on Coprecipitated Arsenate. Environ. Sci. Technol. 36: 2459-2463.

Ford, R. G., 2005. The Impact of Ground Water-Surface Water Interactions on Contaminant Transport with Application to an Arsenic Contaminated Site. EPA Environmental Research Brief, EPA/600/S-05/002. Cincinnati, OH: U.S. Environmental Protection Agency, (http://.epa.gov/ada/download/briefs/epa_600_s05_002.pdf).

Ford, F.G., Kent, D. B., and Wilkin, R. T., 2007. Arsenic. In: Monitored Natural Attenuation of Inorganic Contaminants in Ground Water, Volume 2: Assessment for Non-Radionuclides Including Arsenic, Cadmium, Chromium, Copper, Lead, Nickel, Nitrate, Perchlorate, and

Selenium, Ed.: Ford, R.G., Wilkin, R.T., and Puls, R. W., U.S. Environmental Protection Agency, Washington, DC, EPA/600/R-07/140

Fredrickson J. K., Zachara, J. M., Kennedy, D. W., Dong, H., Onstott, T. C., Hinman, N. W. and Li, S., 1998. Biogenic iron mineralization accompanying dissimilatory reduction of hydrous ferric oxide by a groundwater bacterium. Geochim. Cosmochim. Acta 62: 3239-3257.

Freedman, D., Lehmicke, L. and Verce, M. F., 2003. The Effect of Chemically Reducing Chromium(VI) with Polysulfides on Reductive Dechlorination of PCE. *In:* V.S. Magar and M.E. Kelley (eds.), *In Situ* and On-Site Bioremediation – 2003. Proceedings of the Seventh International *In Situ* and On-Site Bioremediation Symposium (Orlando, FL, June 2003). ISBN 1-57447-139-6, Battelle Press, Columbus, OH.

Fuller C. C., Davis J. A., Coston J. A. and Dixon E.,1996. Characterization of metal adsorption variability in a sand and gravel aquifer, Cape Cod, Massachusetts. U.S.A. J. Contam. Hydrol. 22, 165-187.

Gnabasik, B. J., Staeden, B. J., Wolfgram, D. J. and Van Neste, C. J., 2009. Enhancing Degradation in Addressing Dilute PCE Plumes. *In:* Proceedings of the Tenth International *In Situ* and On-Site Bioremediation Symposium (Baltimore, MD; May 2009), Battelle Press, Columbus, OH.

Grossman, E. L., Cifuentes, L. A. and Cozzarelli, I. M., 2002. Anaerobic methane oxidation in a landfill-leachate plume. Environ. Sci. Technol. 36(11): 2436-2442.

Hansel, C. M., Benner, S. G. and Fendorf, S., 2005. Competing Fe(II)-induced mineralization pathways of ferrihydrite. Environ. Sci. Technol. 39: 7147-7153.

Harkness, M. and Fisher, A., 2013. Use of emulsified vegetable oil to support bioremediation of TCE DNAPL in soil columns. J. Contam. Hydrol. 151: 16-33.

Harvey C. F., Swartz C. H., Badruzzaman, A. B. M., Keon-Blute, N., Yu, W., Ali, M. A., Jay, J., Beckie, R., Niedan, V., Brabander, D., Oates, P. M., Ashfaque, K. N., Islam, S., Hemond, H. F. and Ahmed, M. F., 2002. Arsenic mobility and groundwater extraction in Bangladesh. Sci. 298: 1602-1606.

He, Y., Su, C., Wilson, J., Wilkin, R., Adair, C., Lee, T., Bradley, P., Ferrey, M., 2009. Identification and Characterization Methods for Reactive Minerals Responsible for Natural Attenuation of Chlorinated Organic Compounds in Ground Water. EPA 600/R-09/115, December 2009.

He, Y. T., Fitzmaurice, A. G., Bilgin, A., Choi, S., O'Day, P., Horst, J, Harrington, J., Reisinger, H. J., Burris, D. R. and Hering, J. G., 2010. Geochemical Processes Controlling Arsenic Mobility in Groundwater: A Case Study of Arsenic Mobilization and Natural Attenuation. Appl. Geochem. 25: 69–80.

Hem, J. D., 1985. Study and Interpretation of the Chemical Characteristics of Natural Water, 3rd Ed., U.S Geological Survey Water-Supply Paper 2254, Alexandria, VA.

Hering, J. G., O'Day, P. A., Ford, R. G., He, Y. T., Bilgin, A., Reisinger, H. J. and Burris, D. R., 2009. MNA as a Remedy for Arsenic Mobilized by Anthropogenic Inputs of Organic Carbon. Ground Water Monit. Remed. 29(3): 84–92.

Hoelen, T. P. and Reinhard, M., 2004. Complete biological dehalogenation of chlorinated ethylenes in sulfate containing groundwater. Biodegradation 15(6): 395-403.

Höhn, R., Isenbeck-Schröter, M., Kent, D. B., Davis, J. A., Jakobsen, R., Jann, S., Niedan, V., Scholz, C., Stadler, S. and Tretner, A., 2006. Tracer test with As(V) under variable redox conditions controlling arsenic transport in the presence of elevated ferrous concentrations. J. Contam. Hydrol. 88(1-2): 36-54. doi:doi:10.1016/j.jconhyd.2006.06.001.

Hounslow, A.W., 1980. Ground-water Geochemistry: Arsenic in Landfills. Ground Water 18: 331-333.

HSDB, 2012. National Libraries of Medicine, Hazardous Substances Databank (74-82-8, methane), Available at: http://toxnet.nlm.nih.gov/cgi-bin/sis/search/a?dbs+hsdb:@term+@DOCNO+167.

Hunt, M. J., Shafer, M. B., Barlaz, M. A. and Borden, R. C., 1997. Anaerobic Biodegradation of Alkylbenzenes in Laboratory Microcosms Representing Ambient Conditions. Bioremed. J. 1: 53-64.

Islas-Lima, S., Thalasso, F., Gómez-Hernandez, J., 2004. Evidence of anoxic methane oxidation coupled to denitrification. Water Resour. Res. 38: 13–16.

Iversen, N., Oremland, R.S., Klug, M.J., 1987. Big Soda Lake (Nevada). 3. Pelagic methanogenesis and anaerobic methane oxidation. Limnol. Ocean. 32: 804–814.

Jacob, C., Weber, E. F., Bet, J. N. and Macnair, A. K., 2005. Full-Scale Enhanced Reductive Dechlorination using Sodium Lactate and Vegetable Oil. *In:* B.C. Alleman and M.E. Kelley (Conference Chairs), Proceedings of the Eighth International *In Situ* and On-Site Bioremediation Symposium (Baltimore, Maryland; June 6-9, 2005), ISBN 1-57477-152-3, Battelle Press, Columbus, OH.

Jakobsen, R., Albrechtsen, H. J., Rasmussen, M., Bay, H., Bjerg, P. L.and Christensen, T. H., 1998. H-2 concentrations in a landfill leachate plume (Grindsted, Denmark): *In situ* energetics of terminal electron acceptor processes. Environ. Sci. Technol. 32(14): 2142-2148.

Jakobsen, R., and Postma, D., 1999. Redox zoning, rates of sulfate reduction and interactions with Fe-reduction and methanogenesis in a shallow sandy aquifer, Romo, Denmark, Geochimica et Cosmochimica Acta 63(1): 137-151.

Jones, D. T. and Woods, D. R., 1986. Acetone-Butanol Fermentation Revisited. Microbiological Reviews 50(4): 484-524.

Kent, D. B., Abrams, R. H., Davis, J. A., Coston, J. A. and LeBlanc, D. R., 2000. Modeling the influence of variable pH on the transport of zinc in a contaminated aquifer using semiempirical surface complexation models. Water Resour. Res. 36(12): 3411-3425.

Kent, D. B., Davis, J. A., Anderson, L. C. D., Rea, B. A., and Coston, J. A., 2002. Effect of adsorbed metal contaminants on the transport of Zn- and Ni-EDTA complexes in a sand and gravel aquifer. Geochim. Cosmchim. Acta 66: 3017-3036.

Kent, D. B. and Fox, P. M., 2004. The influence of groundwater chemistry on arsenic concentrations and speciation in a quartz sand and gravel aquifer. Geochem. Trans. 5: 1-12.

Kent, D. B., Wilkie, J. A. and J. A. Davis, 2007. Modeling the movement of a pH perturbation and its impact on adsorbed zinc and phosphate in a wastewater-contaminated aquifer. Water Resour. Res. 43, W07440. doi:10.1029/2005WR004841.

Kelly, D., Cheng, J., Ault, T., Teo, J. and Eisen, D., 2009. Pilot Study to Evaluate the *In Situ* Reductive Dechlorination of Carbon Tetrachloride. *In:* Proceedings of the Tenth International *In Situ* and On-Site Bioremediation Symposium (Baltimore, MD; May 5-8, 2009), Battelle Press, Columbus, OH.

Komlos, J., Kukkadapu, R.K., Zachara, J.M., Jaffé, P.R., 2007. Biostimulation of iron reduction and subsequent oxidation of sediment containing Fe-silicates and Fe-oxides: Effect of redox cycling on Fe(III) bioreduction. Water Res. 41, 2996-3004.

Korte, N. E. and Fernando, Q., 1991. A Review of Arsenic (III) in Groundwater. Crit. Rev. Environ. Control 21: 1-39.

Kota, S., Barlaz, M. A., and Borden, R. C., 2004. Spatial heterogeneity of microbial and geochemical parameters in gasoline contaminated aquifers. Practice Periodical of Hazardous, Toxic, and Radioactive Waste Management 8: 105-118.

Kruczek, J. and B. Timmins, 2009. Field Study of *In Situ* Anaerobic Bioremediation of Pentachlorophenol in Groundwater. *In:* Proceedings of the Tenth International *In Situ* and On-Site Bioremediation Symposium (Baltimore, MD; May 2009), Battelle Press, Columbus, OH.

LaPat-Polasko, L., Bailiff, E. and Chow, S.W., 2009. Enhanced *In Situ* Bioremediation of Chlorinated Volatile Organic Compounds in Groundwater. *In:* Proceedings of the Tenth International *In Situ* and On-Site Bioremediation Symposium (Baltimore, MD; May 2009), Battelle Press, Columbus, OH.

Lee, W. and Batchelor, B., 2002. Abiotic Reductive Dechlorination of Chlorinated Ethylenes by Iron-Bearing Soil Minerals. 1. Pyrite and Magnetite. Environ. Sci. Technol. 36: 5147-5154.

Lee, W. and Batchelor, B., 2003. Reductive Capacity of Natural Reductants. Environ. Sci. Technol., 37: 535-541.

Li, L., Steefel, C.I., Williams, K.H., Wilkins, M.J., Hubbard, S.S., 2009. Mineral transformation and biomass accumulation associated with uranium bioremediation at Rifle, Colorado. Environ. Sci. Technol. 43, 5429-5435.

Liger, E., Charlet, L. and van Cappellen, P., 1999. Surface catalysis of uranium(VI) reduction by iron(II). Geochim. Cosmochim. Acta 63(19-20): 2939-2955.

Löffler, F.E., Sanford, R.A. and Ritalahti, K.M., 2005. Enrichment, cultivation, and detection of reductively dechlorinating bacteria. Methods in Enzymology 397: 77-111.

Lovley, D. R. and Phillips, E. J. P., 1986. Organic Matter Mineralization with Reduction of Ferric Iron in Anaerobic Sediments. Appl. Environ. Microbiol. 51: 683–689

Lovley, D. R. and Phillips, E. J. P., 1987. Rapid Assay for Microbially Reducible Ferric Iron in Aquatic Sediments. Appl. Environ. Microbiol. 53: 1536–1540.

Lovley, D. R., 1991. Dissimilatory Fe(III) and Mn(IV) Reduction. Microbiol. Rev. 55(2): 259-287.

Lovley, D. R., 1993. Dissimilatory Metal Reduction. Annu. Rev. Microbiol. 47: 263-290.

Lundegard, P. D., Johnson, P. C. and Dahlen, P., 2008. Oxygen transport from the atmosphere to soil gas beneath a slab-on-grade foundation overlying petroleum-impacted soil. Environ. Sci. Technol. 42: 5534–5540.

Ma, J., Rixey, W.G., DeVaull, G. E., Stafford, B. P. and Alvarez, P. J. J., 2012. Methane bioattenuation and implications for explosion risk reduction along the groundwater to soil surface pathway above a plume of dissolved ethanol. Environ. Sci. Technol. 46: 6013−6019.

Madison, A. S., Tebo, B. M., Mucci, A., Sundby, B. and Luther III, G. W., 2013. Abundant porewater Mn(III) is a major component of the sedimentary redox system. Science 341: 875-878.

Molin, J., Mueller, J., Hill, D., Hanson, D., Fowler, T. and Skrotzki, T., 2009. Direct Injection of ZVI and Organic Carbon Slurry for Treatment of PCE in Clayey Lithology. *In:* Proceedings of the Tenth International *In Situ* and On-Site Bioremediation Symposium (Baltimore, MD; May 2009), Battelle Press, Columbus, OH.

Morgan J. J., 2005. Kinetics of reaction between O_2 and Mn(II) species in aqueous solutions. Geochim. Cosmochim. Acta 69: 35-48.

Ng, G. H. C., Bekins, B. A., Cozzarelli, I. M., Baedecker, M. J., Bennett, P. C. and Amos, R. T., 2014. A mass balance approach to investigating geochemical controls on secondary water quality impacts at a crude oil spill site near Bemidji, MN. J. Contam. Hydrol. 164: 1-15.

Ng, G.-H.C., B.A. Bekins, I.M. Cozzarelli, M.J. Baedecker, P.C. Bennett, R.T. Amos, and W.N. Herkelrath, 2015, Reactive transport modeling of geochemical controls on secondary water quality impacts at a crude oil spill site near Bemidji, MN, Water Resour. Res., 51, 4156–4183, doi:10.1002/2015WR016964.

Nordstrom, D. K. and Wilde, F. D., 2005. Reduction-Oxidation Potential (Electrode Method), In: National Field Manual for the Collection of Water-Quality Data (TWRI Book 9)
Chapter A6. Field Measurements.

Oremland, R.S., Miller, L.G., Whiticar, M.J., 1987. Sources and flux of natural gases from Mono Lake, California. Geochimica et Cosmochimica Acta 51: 2915–2929.

Papanikolaou, S , Ruiz-Sanchez, P., Pariset, B., Blanchard, F. and Fick, M., 2000. High production of 1,3-propanediol from industrial glycerol by a newly isolated *Clostridium butyricum* strain. J. Biotechnol. 77: 191–208.

Parkhurst, D. L., Stollenwerk, K. G. and Colman, J. A., 2003. Reactive-transport simulation of phosphorus in the sewage plume at the Massachusetts Military Reservation, Cape Cod, Massachusetts, USGS Water Resour. Invest. Rept. 03-4017, 33 p.

Perkins, S. and Chui, G., 2008. *In Situ* Chemical Reduction of Hexavalent Chromium in Soil and Perched Groundwater Using Calcium Polysulfide. Remediation of Chlorinated and Recalcitrant Compounds – 2008. *In:* Proceedings of the Sixth International Conference on Remediation of Chlorinated and Recalcitrant Compounds (Monterey, CA, May 2008), Battelle Press, Columbus, OH.

Pierce, M. L. and Moore, C. B., 1982. Adsorption of Arsenite and Arsenate on Amorphous Iron Hydroxide. Water Res. 16: 1247-1253.

Polizzotto, M. L., Harvey, C. F., Li, G., Badruzzman, B., Ali, A., Newville, M., Sutton, S. and Fendorf. S., 2006. Solid-Phases and Desorption Processes of Arsenic within Bangladesh Sediments. Chemical Geology 228: 97-111.

Postma, D. and Appelo, C. A. J., 2000. Reduction of Mn-oxides by ferrous iron in a flow system: Column experiments and reactive transport modeling. Geochim. Cosmochim. Acta 64(7): 1237-1247.

Potsma, D. and Jakobsen, R., 1996. Redox Zonation: Equilibrium Constraints of the Fe(III)/SO4 Reduction Interface. Geochimica et Cosmochimica Acta 60: 3169-3175.

Qafoku, N. P., Kukkadapu, R. K., McKinley, J. P., Arey, B. W., Kelley, S. D., Wang, C., Resch, C. T. and Long, P. E., 2009. Uranium in framboidal pyrite from a naturally bioreduced alluvial sediment. Environ. Sci. Technol. 43: 8528-8534.

Raven, K. P., Jain, A. and Loeppert, R. H., 1998. Arsenite and Arsenate Adsorption on Ferrihydrite: Kinetics, Equilibrium, and Adsorption Envelopes. Environ. Sci. Technol. 32: 344-349.

Repert,D.A., Barber,L.B.; Hess,K.M., Keefe,S.H., Kent,D.B., Leblanc,D.R., Smith,R.L., 2006. Long-term natural attenuation of carbon and nitrogen within a groundwater plume after removal of the treated wastewater source. Environ. Sci. Technol. 40: 1154-1162.

Smith, R. L., D. B. Kent, and D. A. Repert, *In Revision*, Nitrate-Dependent, Anoxic Iron Oxidation and Associated Attenuation of Dissolved Arsenic and Phosphate in a Sand and Gravel Aquifer. Environ. Sci. Technol.

Riis, C., Christensen, A. G., Nielsen, H. H., Van Bemmel, M. and Ostergaard, 2007. Long-term Bioremediation of a Chlorinated Solvents Plume in a Fractured Limestone Aquifer Using a Dechlorinating Bioreactor. *In:* Proceedings of the Ninth International *In Situ* and On-Site Bioremediation Symposium (Baltimore, MD; May 2007), Battelle Press, Columbus, OH.

Robinson, C., Barry, D. A., McCarty, P. L., Gerhard, J. I. and Kouznetsova, I., 2009. pH control for enhanced reductive source zone bioremediation of chlorinated solvents. Sci. Total Environ. 407 (2009) 4560–4573.

Roden, E. E. and Zachara, J. M., 1996. Microbial reduction of crystalline iron(III) oxides: influence of oxide surface area and potential for cell growth. Environ. Sci. Technol. 30: 1618–1628.

Roden, E. E., Urrutia, M. M. and Mann, C. J., 2000. Bacterial Reductive Dissolution of Crystalline Fe(III) Oxide in Continuous-Flow Column Reactors. Appl. Environ. Microbiol. 66: 1062–1065.

Roden, E .E. and Urrutia, M. M., 2002. Influence of Biogenic Fe(II) on Bacterial Reduction of Crystalline Fe(III) Oxides. Geomicrobiology J. 19: 209–251.

Raghoebarsing, A. A., Pol, A., van de Pas-Schoonen, K. T., Smolders, A. J. P., Ettwig, K. F., Rijpstra, W. I. C., Schouten, S., Damste, J. S. S., Op den Camp, H. J. M., Jetten, M. S. M. and Strous, M., 2006. A microbial consortium couples anaerobic methane oxidation to denitrification. Nature 440(7086): 918-921.

Reeburgh, W.S., 2007. Oceanic methane biogeochemistry. Chemical Reviews 107: 486–513.

Ryker, S.J., 2001. Mapping arsenic in groundwater: Geotimes 46(11): 34-36.

Savoie, J. G., LeBlanc, D. R., Fairchild, G. M., Smith, R. L., Kent, D. B., Barber, L. B., Repert, D. A., Hart, C. P., Keefe, S. H. and Parsons, L. A., 2012. Groundwater-Quality Data for a Treated-Wastewater Plume near the Massachusetts Military Reservation, Ashumet Valley, Cape Cod, Massachusetts, 2006–08. USGS Data Series 648, http://pubs.usgs.gov/ds/648/.

Sawyer, C. N., McCarty, P. L. and Parkin, G. F., 1994. Chemistry for Environmental Engineering. McGraw-Hill Inc.

Serrano, S., Vlassopoulos, D., Garrido, F., and O'Day, P. A., 2013. A combined site-specific metals sorption and transport model for intact soil columns. Vadose Zone J. 12. doi:10.2136/vzj2012.0152.

Shelton, D. R. and Tiedje, J. M., 1983. General method for determining anaerobic biodegradation potential. Appl. Environ. Microbiol. 37: 850-857.

Sihota, N. J., Mayer, K. U., Toso, M. A. and Atwater, J. F., 2013. Methane emissions and contaminant degradation rates at sites affected by accidental releases of denatured fuel-grade ethanol. J. Contam. Hydrol. 151: 1-15.

Sivan, O., Adler, M., Pearson, A., Gelman, F., Bar-Or, I., John, S.G., Eckert, W., 2011. Geochemical evidence for iron-mediated anaerobic oxidation of methane. Limnol. Ocean. 56: 1536–1544, DOI: 10.4319/lo.2011.56.4.1536.

Smith, R.L., Howes, B.L., Garabedian, S.P., 1991. In situ measurement of methane oxidation in groundwater by using natural-gradient tracer tests. Applied Environ. Micro. 57: 1997– 2004.

Smedley, P. L. and Kinniburgh, D. G., 2002. A Review of the Source, Behaviour and Distribution of Arsenic in Natural Waters. Appl. Geochem. 17: 517-568.

Snoeyink, V. L. and Jenkins, D., 1980. Water Chemistry. New York: John Wiley & Sons, 1980. pp 328-329.

Stollenwerk, K., 2003. Geochemical processes controlling transport of arsenic in groundwater: A review of adsorption, in Arsenic in Groundwater. *In:* A.H. Welch and K.G. Stollenwerk (eds.), Luwer, Norwell, MA, USA, pp. 67-100.

Sung, Y., 2005. Isolation and ecology of bacterial populations involved in reductive dechlorination of chlorinated solvents. Ph.D. Dissertation, Georgia Institute of Technology, Atlanta, GA.

Swartz, C. H., Blute, N. K., Badruzzman, B., Ali, A., Brabander, D., Jay, J., Besancon, J., Islam, S., Hemond, H. F. and Harvey, C. F., 2004. Mobility of Arsenic in a Bangladesh Aquifer: Inferences from Geochemical Profiles, Leaching Data, and Mineralogical Characterization. Geochim. et Cosmochim. Acta 68: 4539-4557.

Tabak, H. H., Quave, S. A., Mashni, C. I., and Barth, E. F., 1981. Biodegradability Studies with Organic Priority Pollutant Compounds. Journal WPCF 53(10): 1503-1518.

Tang, G., Wu, W.-M., Watson, D. B., Parker, J. C., Schadt, C., Shi, X. and Brooks, S. C., 2013. U(VI) bioreduction with emulsified vegetable oil as the electron donor − microcosm tests and model development. Environ. Sci. Technol. 47: 3209-3217.

Tebo, B. M., Bargar, J. R., Clement, B. G., Dick, G. J., Murray, K. J., Parker, D., Verity, R. and Webb, S. M., 2004. Biogenic manganese oxides: properties and mechanisms of formation. Ann. Rev. Earth Planet. Sci. 32: 287-328.

Tillotson, J. M., and R. C. Borden, 2015. Secondary Water Quality Impacts Due to Enhanced Reductive Bioremediation: A Statistical Summary of 47 Sites, Ground Water Monitoring & Remediation, In Preparation.

TSI and Solutions-IES, 2003. Interim Report: Technology Application of Low Cost Emplacement of Insoluble Organic Substrate for Enhanced *In Situ* Reductive Dechlorination of Halogenated Aliphatic Hydrocarbons, Dover Air Force Base. Prepared for the Air Force Center for Environmental Excellence, Brooks City-Base, TX, March 2003.

USEPA, 1999. Final Directive. Use of Monitored Natural Attenuation at Superfund, RCRA Corrective Action, and Underground Storage Tank Sites. (http://www.epa.gov/swerust1/directiv/d9200417.htm)

USEPA, 1997. Technology Alternatives for the Remediation of Soils Contaminated with As, Cd, Cr, Hg, and Pb. Office of Emergency and Remedial Response , U.S. Environmental Protection Agency, Washington DC, EPA/540/S-97/500.

USEPA, 2009. List of Drinking Water Contaminants and Their MCLs. U.S. Environmental Protection Agency, Washington DC (http://www.epa.gov/safewater/contaminants/index.html).

Vainberg, S., Condee, C. W. and Steffan, R. J., 2009. Large scale production of *Dehalococcoides sp*. containing cultures for bioaugmentation. J. Indust. Microbiol. Biotechnol. 36: 1189-1197.

Vanbroekhoven, K., Satyawali, Y., Van Roy, S., Vangeel, S., Gemoets, J., Muguet, S., Zeuwts, L., Gommers, K. and Feyaerts, K., 2009. Stability of Metal Precipitates Formed after *In Situ* Bioprecipitation Induced by Sulfidogenesis. *In:* Proceedings of the Tenth International *In Situ* and On-Site Bioremediation Symposium (Baltimore, MD; May 5-8, 2009), Battelle Press, Columbus, OH.

van Breukelen, B.M., Griffioen J., 2004. Biogeochemical processes at the fringe of a landfill leachate pollution plume: potential for dissolved organic carbon, Fe(II), Mn(II), NH_4, and CH_4 oxidation. J. Contam. Hydrol. 73: 181–205.

van Breukelen, B.M., Roling, W.F.M., Groen, J., Griffioen, J., Van Verseveld, H.W., 2003. Biogeochemistry and isotope geochemistry of a landfill leachate plume. J. Contam. Hydrol. 65: 245–268.

Vanysek, P., 2014. Electrochemical Series. *In:* CRC Handbook of Chemistry and Physics 95th Edition. W.M. Haynes (ed.). Boca Raton, FL: CRC Press. pp 5-80 – 5-89.

Villalobos, M., Toner, B., Bargar, J. and Sposito, G., 2003. Characterization of the manganese oxide produced by *Pseudomonas putida* strain MnB1. Geochim. Cosmochim. Acta 67: 2649-2662.

Wang, X., Padgett, J. M., De la Cruz, F. B. and Barlaz, M. A., 2011. Wood Biodegradation in Laboratory-Scale Landfills. Environ. Sci. Technol. 45: 6864–6871.

Warren, E., Sihota, N. J., Hosterrler, F. D. and Bekins, B. A., 2014. Comparison of surficial CO_2 efflux to other measures of subsurface crude oil degradation. J. Contam. Hydrol. 164: 275-284.

Whiting, K., Evans, P., Henry, B., Wilson, J., Olsen, R., Becvar, E. and Lebrón, C., 2008. *In situ* biogeochemical transformation of chlorinated ethenes using engineered treatment systems. CDM.

Wielinga, B., Bostick, B., Hansel, C. M., Rosenzweig, R. F. and Fendorf, S., 2000. Inhibition of Bacterially Promotoed Uranium Reduction: Ferric (Hydr)oxides as Competitive Electron Acceptors. Environ. Sci. Technol. 34 (11): 2190-2195.

Wilkin, R. T., McNeil, M. S., Adair, C. J. and Wilson, J. T., 2001. Field Measurement of Dissolved Oxygen: A Comparison of Methods. Groundwater Monitoring and Remediation, Fall: 124-132.

Woods, D.R., 1995. The Genetic Engineering of Microbial Solvent Production, Trends in Biotechnology 13 (7): 259-264.

Yurovsky, M., Cacciatore, D., Hudson, L., Leigh, D. P., Bhullar, C. and Shaheen, W., 2009. Operation of *In Situ* System for Treatment of Hexavalent Chromium at the Selma Pressure Treating Superfund Site. *In:* Proceedings of the Tenth International *In Situ* and On-Site Bioremediation Symposium (Baltimore, MD; May 2009), Battelle Press, Columbus, OH.

van der Zee, C., Roberts, D. R., Rancourt, D. G. and Slomp, C. P., 2003. Nanogoethite is the dominant reactive oxyhydroxide phase in lake and marine sediments. Geology 31: 993-996.

Zhang, S., Kent, D. B., Elbert, D. C., Shi, Z., Davis, J. A. and Veblen, D. R., 2011. Mineralogy, morphology, and textural relationships in coatings on quartz grains in sediments in a quartz-sand aquifer. J. Contam. Hydrol. 124(1-4): 57-67.

APPENDIX A
DATABASE TABLES

Table A.1. Table A-1. Characteristics of ERB Sites Included in SWQI Database.

Site ID	Location	Injection Type	Organic Substrate	Data Source	No. of wells	Record (months)
Aerojet General Corporation	Rancho Cordova, CA	Horizontal Wells	Citric Acid	ESTCP Project Report	18	24
Aiea Laundry	Pearl Harbor, HI	Source	EOS, Lactate	Personal Correspondence	2	6
Altus AFB OU1 - Biowall	Altus, OK	Biowall	Mulch and compost	AFCEE Project Report	44	88
Altus AFB OU1 - Injections	Altus, OK	Source	EVO	Monitoring Report	5	20
Altus AFB SS-17	Altus, OK	PRB	EVO	Monitoring Report	14	20
Altus AFB SS-18	Altus, OK	Source	EOS	Monitoring Report	22	21
Altus AFB SS-22	Altus, OK	Source	EOS	Monitoring Report	52	21
Avon Park AFB	Avon Park, FL	Recirc	Lactate, ethanol	SERDP Project Report	5	5
Beale AFB Site 39 Building 2145	Marysville, CA	Source	EOS	Monitoring Report	9	15
Beale AFB Site 39 Source Area 1	Marysville, CA	Source	EOS	Monitoring Report	18	10
Boeing Former Compton Site	Compton, CA	Source	Newman Zone	Monitoring Report	14	36
Cape Canaveral Hangar K	Cape Canaveral, FL	Source	Soybean oil	AFCEE Project Report	19	68
Charleston NWS SWMU 17	Charleston, SC	Source	EOS	ESTCP Project Report	26	41
Cornhusker AAP OU1	Grand Island, NE	PRB	Newman Zone, Wesblend 66	Monitoring Report	47	48
Crown Cork & Seal Facility	Pittsburg, CA	Source	HRC	Monitoring Report	2	66
Dover AFB Area 5	Dover, DE	PRB	Lactate, Newman Zone	Monitoring Report	43	77
Dover AFB Area 6	Dover, DE	PRB	Lactate, Newman Zone	Monitoring Report	136	77
Dover AFB Site WP14	Dover, DE	Biowall	Mulch	AFCEE Project Report	14	39
East Charleston Business Park	Mountain View, CA	PRB	HRC	Monitoring Report	9	64
Fort Devens AOC 50	Devens, MA	PRB	Molasses	Monitoring Report	9	30
Fort Dix MAG-1	Fort Dix, NJ	Recirc	Lactate	ESTCP Project Report	22	12
Fort Worth Joint Reserve Base AOC-2	Fort Worth, TX	PRB	Soybean oil and HF corn syrup	AFCEE Project Report	14	26
Hickam AFB Site LF05 - Southeast Area	Honolulu, HI	Recirc	Lactic acid	Monitoring Report	37	4
Hickam AFB Site LF05 - TCRA Area	Honolulu, HI	PRB	Soybean oil	AFCEE Project Report	11	26
Indian Head Naval Surface Warfare Center	Indian Head, MD	Recirc	Lactic acid	Literature Report	14	5
JEB Little Creek Site 11	Virginia Beach, VA	PRB	SRS emulsified oil	Monitoring Report	26	12
JEB Little Creek Site 12	Virginia Beach, VA	PRB	EOS	Monitoring Report	17	13
JEB Little Creek Site 13	Virginia Beach, VA	PRB	LactOil, ethyl lactate	Monitoring Report	28	6

Table A-1 (continued). Characteristics of ERB Sites Included in SWQI Database.

Site ID	Location	Injection Type	Organic Substrate	Data Source	No. of wells	Data Record (months)
Maryland Perchlorate Site	Elkton, MD	PRB	EOS	ESTCP Project Report	8	42
McConnell AFB Site FT07	Wichita, KS	Biowall/Recirc	Mulch and soybean oil	Monitoring Report	18	8
Mercedes North Houston	Houston, TX	Source	HRC, Newman Zone, Cheese Whey	Monitoring Report	10	51
Moffett Field Site 26	Mountain View, CA	Source	EHC	Monitoring Report	14	22
Moffett Field Site 28 - Building 88	Mountain View, CA	Source	Lactate and lactic acid	Monitoring Report	7	10
Moffett Field Site 28 - Traffic Island	Mountain View, CA	Source	Lactoil	Monitoring Report	6	10
Moffett Field Site 28 - W9-18 Area	Mountain View, CA	Source	EHC	Monitoring Report	12	10
Naval Weapons Station Seal Beach - Site 40	Seal Beach, CA	Source	Sodium lactate, HRC	Monitoring Report	7	75
Oates Park	Mesquite, TX	Source	HRC	Monitoring Report	34	36
Pacific Scientific	Santa Barbara, CA	Source	HRC	Monitoring Report	4	110
Picatinny Arsenal Area 157	Dover, NJ	Recirc	Cheese whey	ESTCP Project Report	14	18
Renco Encoders	Goleta, CA	Source, PRB	HRC, HRC-X, Wilclear, Lactoil, EOS, EHC	Monitoring Report	14	117
Savannah River Site - F Area	Aiken, SC	Source	Molasses	Monitoring Report	27	19
Tinker AFB FTA-2	Oklahoma City, OK	Source	Soybean oil and HF corn syrup	AFCEE Project Report	20	23
Travis AFB Site DP039	Fairfield, CA	Biowall/Recirc	Mulch and soybean oil	Monitoring Report	10	11
Treasure Island Site 24	San Francisco, CA	Recirc	Sodium lactate	Monitoring Report	9	12
TRW Microwave	Santa Clara, CA	Source, PRB	HRC, Cheese Whey, EVO, EHC-L, ABC^{+}	Monitoring Report	20	132
Western Microwave	Sunnyvale, CA	PRB	HRC	Monitoring Report	33	68
Whittaker Bermite Facility Area	Santa Clarita, CA	Recirc	Citric Acid	Monitoring Report	13	7

Notes
PRB - Permeable reactive barrier
Recirc - Recirculation system
Source - Source area injections

Table A.2. Summary Statistics for Post-Injection Data Contained in SWQI Database.

	Well Location	Monitoring Points	Percentiles							% of wells >MCL
			Min	10th	25th	50th	75th	90th	Max	
Maximum Dissolved Manganese (mg/L)	Upgradient	61	0.002	0.0066	0.057	0.2	0.53	1.1	39	79%
	Injection Area	125	0.023	0.15	0.80	2.6	8.7	17	53	94%
	Downgradient - All	201	0.0015	0.016	0.054	0.53	2.6	11	86	76%
	0-10 m Downgradient	112	0.0065	0.018	0.087	1.1	4.5	12	86	77%
	10-25 m Downgradient	52	0.0015	0.020	0.13	0.44	1.7	7.1	59	83%
	25-50 m Downgradient	20	0.002	0.010	0.024	0.077	0.20	0.97	2.0	60%
	50+ m Downgradient	17	0.006	0.018	0.042	0.2	3.2	15	31	65%
Maximum Dissolved Iron (mg/L)	Upgradient	109	<0.04	<0.1	0.1	0.43	1.1	6.0	350	55%
	Injection Area	203	0.02	0.14	2.0	22	120	266	1,200	86%
	Downgradient - All	346	0.01	0.13	0.5	4.8	46	194	928	84%
	0-10 m Downgradient	180	0.02	0.16	1.2	8.2	78	251	928	87%
	10-25 m Downgradient	64	<0.1	0.17	0.50	6.9	50	218	470	86%
	25-50 m Downgradient	33	<0.1	0.38	1	8.9	75	167	404	93%
	50+ m Downgradient	69	0.01	0.1	0.2	0.74	5	21	200	56%
Maximum Dissolved Arsenic (mg/L)	Upgradient	39	<0.00031	0.00031	0.0016	0.0035	0.005	0.012	0.073	10%
	Injection Area	44	0.0011	<0.01	0.0088	0.033	0.11	0.49	1.2	70%
	Downgradient - All	94	0.0011	<0.005	<0.01	0.013	0.040	0.14	0.90	57%
	0-10 m Downgradient	60	0.0011	0.0028	<0.01	0.014	0.040	0.096	0.90	63%
	10-25 m Downgradient	18	0.0012	0.0040	<0.012	0.011	0.042	0.36	0.75	56%
	25-50 m Downgradient	6	<0.005	<0.0075	<0.01	0.0056	0.022	0.029	0.032	33%
	50+ m Downgradient	10	<0.005	<0.005	<0.005	0.0056	0.06768	0.111	0.12	40%
Maximum Sulfide (mg/L)	Upgradient	59	0.0215	<0.05	0.0745	<1	0.575	2.32	190	-
	Injection Area	119	<0.05	0.256	0.78	2	10	110.2	344	-
	Downgradient - All	160	0.01	0.0572	0.48	1	2	7.91	1300	-
	0-10 m Downgradient	86	0.01	0.086	0.39375	1.06	2.21	9.55	1300	-
	10-25 m Downgradient	38	<0.04	<0.1	0.4025	0.88	2.535	8.144	20	-
	25-50 m Downgradient	21	<0.05	<0.1	0.3	<1	0.9	1.3	1.6	-
	50+ m Downgradient	15	<0.1	<1	0.6	<2	1.75	2.54	2.9	-
Maximum Methane (mg/L)	Upgradient	107	0.0001	0.0015	0.0029	0.063	0.32	1.3	6.2	-
	Injection Area	261	<0.00031	0.050	1.2	9.0	15	23	120	-
	Downgradient - All	376	0.0002	0.0073	0.23	4.0	15	27	77	-
	0-10 m Downgradient	197	0.0028	0.20	0.91	7.6	17	31	77	-
	10-25 m Downgradient	69	0.00037	0.0056	<0.025	1.9	11	28	56	-
	25-50 m Downgradient	36	0.0002	0.0045	0.059	1.9	17	24	40	-
	50+ m Downgradient	74	0.00022	<0.002	0.013	0.25	4.9	17	35	-
Maximum Total Organic Carbon (mg/L)	Upgradient	113	<1	1.4	2.3	3.8	12	38	258	-
	Injection Area	303	0.3	3.1	12	230	1,038	3,548	33,000	-
	Downgradient - All	348	<1	2.2	4.5	16	114	506	7,890	-
	0-10 m Downgradient	174	<1	3.2	10	57	263	738	7,890	-
	10-25 m Downgradient	64	<1	1.9	2.8	7.0	81	385	5,080	-
	25-50 m Downgradient	35	<1	1.6	<5	9.6	20	125	885	-
	50+ m Downgradient	75	0.833	2.2	3.0	5.7	15	28	864	-

Notes

mg/L Milligrams per liter